NASA Technical Memorandum 102820

Dynamical Approach Study of Spurious Steady-State Numerical Solutions of Nonlinear Differential Equations

Part I -The ODE Connection and Its Implications for Algorithm Development in Computational Fluid Dynamics

H. C. Yee, Ames Research Center, Moffett Field, California
P. K. Sweby, University of Reading, Whiteknights, Reading, England
D. F. Griffiths, University of Dundee, Dundee, Scotland

April 1990

National Aeronautics and
Space Administration

Ames Research Center
Moffett Field, California 94035-1000

DYNAMICAL APPROACH STUDY OF SPURIOUS STEADY-STATE NUMERICAL SOLUTIONS OF NONLINEAR DIFFERENTIAL EQUATIONS

I. *The ODE Connection and Its Implications for Algorithm Development in Computational Fluid Dynamics*

H.C. Yee[1]
NASA Ames Research Center, Moffett Field, CA 94035, USA
P.K. Sweby[2]
University of Reading, Whiteknights, Reading RG6 2AX, England
and
D.F. Griffiths[3]
University of Dundee, Dundee, DD1 4HN, Scotland

ABSTRACT

The goal of this paper is to attempt to give some insight and guidelines on the application of nonlinear dynamic theory to the better understanding of steady-state numerical solutions and nonlinear instability in algorithm development for nonlinear differential equations that display genuinely nonlinear behavior in computational sciences and, in particular, computational fluid dynamics (CFD). This stems from the fact that, although the study of nonlinear dynamics and chaotic dynamics for nonlinear differential equations and for discrete maps have independently flourished rapidly for the last decade, there are very few investigators addressing the issue on the connection between the nonlinear dynamical behavior of the continuous systems and the corresponding discrete map resulting from finite-difference discretizations. This issue is especially vital for computational sciences since nonlinear differential equations in applied sciences can rarely be solved in closed form and it is often necessary to replace them by finite dimensional nonlinear discrete maps. In addition, it is also important to realize that these nonlinear discrete maps can exhibit a much richer range of dynamical behavior than their continuum counterparts.

Furthermore, it is also very important to identify some of the implications of what happens when linear stability breaks down for problems with genuinely nonlinear behavior. Studies indicate that for relatively simple nonlinear ordinary differential equations

[1] Research Scientist, Computational Fluid Dynamics Branch.
[2] Lecturer, Department of Mathematics.
[3] Senior Lecturer, Department of Mathematical Sciences.

(ODEs) and well-known time-discretization with modest step-sizes some schemes can converge to a spurious (false) steady-state solution in a deceptively "smooth" manner. In some instances, spurious steady states may appear below the linearized stability limit of the schemes, and consequently computation may lead to erroneous results. Our preliminary studies on partial differential equations (PDEs) also show that much of nonlinear dynamic (e.g. chaotic) phenomena have a direct relation for problems containing nonlinear source terms such as the reaction-diffusion, the reaction-convection or the reaction-convection-diffusion equations. Here our object is neither to provide theory nor to illustrate with realistic examples the connection of the dynamical behavior of practical PDEs with their discretized counterparts, but rather to give insight into the nonlinear features unconventional to this type of study and to concentrate on the fundamental ideas. Thus, in order to bring out the special properties, the illustrations center on simple scalar differential equation (DE) examples in which the exact solutions of the DEs are known.

I. INTRODUCTION

While the applied computational fluid dynamicists are busy developing numerical solver computer codes, grid generation codes, three-dimensional graphical stereo displays, and stretching the limits of the faster supercomputers in the world to numerically simulate the various 3-D complex aerodynamic configurations [1], there is a group of applied mathematicians, physicists, chemists, biologists, applied mechanicians, and meteorologists who are involved in a new science called "chaotic dynamics" (or nonlinear dynamics). The science of chaotic dynamics has cut across many traditional scientific disciplines for the last decade since chaotic dynamics is a science of the everyday world. It offers a way of seeing order and pattern where formerly only the random, the erratic, and the unpredictable were present. It explains much of the genuinely nonlinear phenomena that were once unexplainable. See references [2-10] for an introduction to this subject.

Nonlinear Dynamics & Chaotic Dynamics: Before the birth of chaotic dynamical theory, traditional study of nonlinear dynamics belonged to the applied mechanics disciplines of mechanical engineering. Modern nonlinear dynamics (since the late seventies) includes chaotic dynamics. Thus, unless otherwise stated, the term nonlinear dynamics and chaotic dynamics are used interchangeably. That is, nonlinear dynamics includes chaotic dynamics and vice versa.

Loosely speaking, the study of asymptotic behavior (steady-state solutions) of nonlinear differential equations (DEs) and nonlinear discrete maps (difference equations) and how the asymptotes change as parameters of the system are varied is most often referred to as nonlinear dynamic analysis and chaotic dynamic theory. Topics in this area include bifurcation theory, period doubling cascades resulting in chaos, etc. Stable chaotic solutions (chaotic attractors) may be defined loosely and simply as stable asymptotes that have infinite period and yet are still bounded. It is emphasized here that unless otherwise stated, all DEs and discrete maps are nonlinear and consist of system parameters, and the terms discrete maps and difference equations are used interchangeably.

Types of Dynamical Systems: Consider an ordinary differential equation (ODE) and a partial differential equation (PDE) of the forms

$$\frac{du}{dt} = \alpha S(u), \tag{1.1}$$

$$\frac{\partial u}{\partial t} + \frac{\partial f(u)}{\partial x} = \epsilon \frac{\partial^2 u}{\partial x^2} + \alpha S(u), \tag{1.2}$$

where α and ϵ are parameters and S is a nonlinear function in u and is independent of α (and ϵ). The function $f(u)$ can be linear or nonlinear in u. An ODE of this form in which t does not appear explicitly in S is called an autonomous dynamical

system. One can also consider a function S which is nonlinear in u and depends on t. ODEs of this type are called nonautonomous dynamical systems and they are more difficult to analyze; see references [5,8] for a discussion. The analysis would be more complicated if $S = S(u, \alpha)$ is nonlinear in both u and α. In this case, the DE is not only nonlinear in the dependent variable u (and independent variable t), but also nonlinear in the parameter space α. One can also consider systems that depend on more than one parameter and/or systems of equations of the above type.

Next consider nonlinear discrete maps (nonlinear difference equations) of the forms

$$u^{n+1} = u^n + D(u^n, u^{n-1}, r), \tag{1.3}$$

and

$$u_j^{n+1} = u_j^n + G(u_j^n, u_{j\pm1}^n, r). \tag{1.4}$$

Here r is a parameter, and D is nonlinear in u^n and u^{n-1} and linear or nonlinear in the parameter space r. The situation is similar for the function G. One can also consider discrete systems that depend on more than one parameter. A typical example is a discrete map arising from a finite-difference approximation of DEs such as (1.1) or (1.2). For the ODE, the resulting discrete maps might be nonlinear in α as well as the time step Δt, depending on the ODE solvers. For the PDE, again depending on the differencing scheme, the resulting discretized counterparts can be nonlinear in α, Δt, the grid spacing Δx and the numerical dissipation parameters even though the DEs consist of only one parameter or none.

One can also consider discrete maps (scalar or system) of the forms

$$u^{n+1} = u^n + D(u^{n+k}, ..., u^n, ..., u^{n-l}, r_1, r_2, ..., r_m), \tag{1.5}$$

where k, l, m are positive integers and $r_1, r_2, ..., r_m$ are parameters, and

$$u_j^{n+1} = u_j^n + G(u_{j\pm1}^{n+k}, ..., u_{j\pm1}^n, ..., u_{j\pm1}^{n-l}, u_j^{n+k}, ..., u_j^n, ..., u_j^{n-l}, r_1, r_2, ..., r_m). \tag{1.6}$$

Again, (1.6) can depend on more than the three indices $j, j \pm 1$. Systems (1.4) and (1.6) are sometimes referred to as a partial-difference equation. The dynamical behavior of (1.4) and (1.6) can be many orders of magnitude more difficult than (1.3) and (1.5). Any of the systems (1.1)-(1.6) are examples of dynamical systems.

Important Consideration: It is emphasized here that discrete maps, regardless of their origin, are dynamical systems on their own right. It is also important to distinguish the following five types of discrete maps:

1. Discrete maps arise naturally in physical sciences. They commonly arise through the inability to measure populations at all points in space and time [5,10,11] in population dynamics. They can also arise through the study of periodic excitation of dynamical systems [12,13] in applied mechanics.

2. Discrete maps arise from Poincaré sections in ODEs [2].

3. Discrete maps arise from discrete approximations of ODEs.

4. Discrete maps (partial-difference equations) arise from temporal and spatial finite difference approximations of PDEs.

5. Discrete models arise from the "Inverse Problems of Nonlinear Dynamics" in time series analysis of observable data or experiments [9].

Discrete maps of types 1 and 5 sometimes might not have any relationship with a specific continuum DE. As a matter of fact, there might be no concrete associated governing equations (continuum or otherwise) to start with for type 5 except the surrogated discrete map arising from the time series analysis. Type 2 arises naturally from the study of dynamical behavior of nonlinear ODEs. However, types 3 and 4 have an intimate link (but with a different tie than type 2) between the original governing continuum DEs and their discretized counterparts. Furthermore, it is important to distinguish the complexity involved in the analysis of types 3 and 4. Type 4 involves spatial as well as temporal dynamical behavior.

Note that for discrete maps of types 3 and 4, even though the DEs might be linear in the parameter space, depending on the numerical methods, the discretized counterparts might be linear or nonlinear in that parameter space. In addition, extra parameters which may be linear or nonlinear can also be introduced by the scheme as noted in the paragraph after equation (1.4). An important concept is that even though the DE does not depend on any parameter, its discretized counterpart does depend on at least one parameter. As can be seen in the subsequent sections, the nature of the dynamical behavior of these discrete maps is strongly influenced by properties of the numerical method and the types and forms of nonlinearity on the DEs. Furthermore, when dealing with nonlinear conservation laws of PDEs, the dynamical behavior of the discretized counterparts is also strongly influenced by elements such as conservation and nonlinearity of the schemes, and treatment of the source terms [14-18]. These issues are very crucial for the existence of spurious steady-state numerical solutions which will be explained in a later section. Here the term nonlinear scheme refers to a case where the resulting discrete maps are nonlinear when applied to scalar constant coefficient linear DEs.

Objectives: Our ultimate objective is to conduct long term basic research on the interdisciplinary field of integrating the theory of nonlinear dynamics with computational sciences and, in particular, with computational fluid dynamics (CFD). This new approach to CFD is extremely difficult and complex to analyze. A summary of the difficulty involved was discussed in Yee [14] and will be elaborated in sections IV and V. Our immediate goal is to study the behavior of spurious steady-state numerical solutions for nonlinear DEs and the dynamical behavior of this type of numerical solutions. Even within this frame work, the subject is still very young, board, difficult and unfamiliar to computational scientists as well as researchers working in nonlinear dynamics and

nonlinear physics.

The intent of this paper is to give a flavor of the subject, to familiarize the reader in computationl sciences with this new and exciting area, and most of all, to explain through simple illustrations why it is so important for computational scientists to learn about the subject. Some challenging topics for future research are also proposed.

Because of the complexity involved, there is a vast difference in the degree of difficulty on the study of the subject between the discretized counterparts of nonlinear ODEs and the discretized counterparts of nonlinear PDEs. In order to achieve our final goal of studying the dynamical behavior of numerical methods for nonlinear PDEs that arise from, e.g., computational fluid dynamics (CFD), we have to first fully understand this subject on the time discretization and later link this knowledge to the study of both the temporal and spatial nonlinear dynamical behavior of finite-difference methods for nonlinear PDEs of the nonhomogeneous hyperbolic and parabolic types.

Therefore, the content of this paper will concentrate on the dynamical behavior of time discretization for ODEs or systems of ODEs obtained from time-splitting [19] or method of lines [20] for PDEs, and emphasis will be placed on its implication for algorithm development in CFD and computational sciences in general. Hopefully this will be part I of a series of many future research papers to come under the same topic. Our companion paper [21] studies the dynamical behavior of the class of explicit Runge-Kutta methods in detail. The intent of this paper is to not only serve as a study of the state-of-the-art of nonlinear dynamical behavior of ODE solvers, but also more importantly to serve as an introduction and to present new results to motivate this vast, new yet unconventional concept. Thus the mission of this paper is not to provide the answer or theory or to illustrate the connection of dynamical behavior of practical PDEs to their discretized counterparts, but rather to gain insight into the nonlinear features unconventional to this type of study and concentrate on the fundamentals. In order to bring out the new features, the illustrations concentrate on the simple scalar DEs examples in which the exact solutions of the DEs are known.

Outline: The outline of the paper is as follows: First, a brief background, motivation and basic ideas will be given. Then some typical characteristics of dynamical systems with genuinely nonlinear behavior will be discussed. Next, the dynamical behavior of discrete maps arising from time discretization of ODEs will be studied and the main results and their implications for computational sciences will be described. Studies on discrete maps arising from finite-difference approximations of PDEs will not be elaborated. Rather, the level of complexity involved and state-of-the-art study on this subject will be briefly described. The paper will conclude with a few recommendations. Remarks will be given on the popular misconception of residual test for convergence in steady-state solution via the "time-dependent" approach and the popular misconception of the use of the "Inverse Problems of Nonlinear Dynamics" to analyze the dynamical behavior of time series data from a computer code in an attempt to learn about the true physical solution behavior of the governing PDEs. This application of time series analysis can be misleading and a wrong conclusion can be reached if the practitioner does not know by other means

other than the numerical solutions the exact solution behavior of the PDEs .

II. MOTIVATION & RELEVANCE

As discussed in the introduction, dynamical systems occur in the form of DEs and discrete maps. In order to motivate why the study of numerical analysis will not be complete without the utilization of the nonlinear dynamic approach, and to convey to practitioners in computational sciences the importance of distinguishing the difference between weakly nonlinear problems and genuinely nonlinear problems, this section is devoted to a discussion of the typical behavior of dynamical systems with genuinely nonlinear behavior and the basic characteristic difference in dynamical behavior between DEs and discrete maps in general. This discussion leads to the key elements of this paper, namely: (1) to establish the connection between the DEs and their discretized counterparts and (2) to convey to computational scientists how one should change the traditional way of thinking and practices when dealing with genuinely nonlinear problems.

2.1. Typical Characteristics of Dynamical Systems with Genuinely Nonlinear Behavior

The terms "nonlinear behavior" and "genuinely nonlinear behavior" are used quite often in the literature and there seems to be no unified exact definition or meaning [9]. Here these terms are used for nonlinear dynamical systems that exhibit mainly the following characteristics.

(1) The study of nonlinear dynamics most often emphasizes the importance of obtaining a global qualitative understanding of the character of the system's dynamics since local analysis is not sufficient to give the global behavior of genuinely nonlinear dynamical systems. As a matter fact, this is one of the major reasons why sometimes it required orders of magnitude more work than solving their linear counterparts.

(2) Unlike linear or weakly nonlinear problems, the solutions of genuinely nonlinear DEs and discrete maps are strongly dependent on initial data, boundary conditions and system parameters.

(3) Only genuinely nonlinear dynamical systems can have chaotic behavior and one of the striking characteristics of chaotic behavior is sensitivity of the solution to initial data. This characteristic is independent of whether the dynamical system is a continuum or a discrete map.

From here on, the terms "dynamical systems with genuinely nonlinear behavior" and "genuinely nonlinear dynamical systems" are used interchangeably. For convenience, the word "genuinely" is omitted in most parts of the paper.

2.2. Typical Difference in Dynamical Behavior of ODEs and Discrete Maps

The study of discrete maps is the discrete analog to the study of ODEs, as the study of recursion formulas is a discrete analog to the study of series expansions of functions. Much of the theory of ODEs can carry over to discrete maps with some slight modifications. However, there are new phenomena occurring in discrete maps which are absent in differential systems [22,23,12,13].

With repect to the topographical behavior, there are new kinds of behavior of trajectories in the neighborhood of equilibrium points of discrete maps. The behavior of separatrices associated with a saddle type of equilibrium point for a nonlinear difference system is far more complicated than the behavior of separatrices for a differential system. See Yee, Hsu and Hsu et al. [12,13,24,25] for details and examples.

With respect to similar equation types, the minimum number of first-order nonlinear autonomous ODEs is three for the existence of chaotic phenomena. However, a simple scalar first-order difference equation [26-30] like the logistic map

$$v^{n+1} = \mu v^n (1 - \frac{v^n}{4}), \qquad \mu \text{ a parameter}, \tag{2.1}$$

or its piecewise linear approximation [31]

$$\begin{aligned} v^{n+1} &= \mu v^n, \qquad v^n \leq 1 \\ &= \mu, \qquad 1 \leq v^n \leq 3 \\ &= \mu(4 - v^n) \qquad 3 \leq v^n. \end{aligned} \tag{2.2}$$

possesses very rich dynamical behavior such as period-doubling cascades resulting in chaos. Equation (2.2) has the same behavior as (2.1) except that simple closed form asymptotic solutions of all periods can be obtained. These characteristic trade differences between ODEs and discrete maps are very general. The discrete maps can arise from any of the five types as discussed in the introduction. It is in this spirit that we say that discrete maps can exhibit a much richer range of dynamical behavior than DEs. The next two sections focus on the typical difference and connection between the dynamical behavior of ODEs and their discretized counterparts.

2.3. Background and Motivation

Spurious asymptotic numerical solutions such as chaos were observed by Ushike [32] and Brezzi et al. [33] on the leapfrog method for the logistic ODE

$$\frac{du}{dt} = \alpha u(1 - u). \tag{2.3}$$

In reference [34], Schreiber and Keller discussed the existence of spurious asymptotic numerical solutions for a driven cavity problem. Some related studies are reported in [35].

Spurious solutions of Burgers' equation and channel flows have been studied and computed in [36-38]. Many other investigators in the computational sciences (e.g. [39-43]) have observed some kind of strange or chaotic behavior introduced by the numerical methods but were not able to explain systematically the source, the cause of their results, or most of all the implication and impact in practical applications in computational sciences. Due to the popularity of searching for chaotic phenomena, it is very trendy to relate inaccuracy in numerical methods with the onset of chaos. It is emphasized here that inaccuracy in long time integration of discrete maps resulting from finite discretization of nonlinear DEs comes in other forms prior to the onset of chaotic phenomena. Stable and unstable spurious steady states and spurious periodic numerical solutions set in before chaotic behavior occurs. These spurious asymptotes of finite period are just as inaccurate as chaotic phenomena as far as numerical integration is concerned. In other words, the prelude to chaotic behavior is the key element that we want to stress (i.e., before the the onset of chaos or a divergent solution) since the result of operating the time step beyond the linearized stability limit is not always a divergent solution in genuinely nonlinear behavior; spurious steady-state solutions can occur. As can be seen at a later section, this behavior is more difficult to detect than chaotic phenomena in practical computations.

Recently, it has been realized by numerical analysts that numerical methods for ODEs and PDEs can be considered as dynamical systems. Several papers [44,45] on numerical methods as dynamical systems have appeared in recent years. These investigators studied the dynamical behavior of the different ODE solvers per se without relating its close tie with the ODEs themselves. Although the study of chaotic dynamics for nonlinear differential equations and for discrete maps have independently flourished rapidly for the last decade, there are very few investigators addressing the issue of the connection between the nonlinear dynamical behavior of the continuous systems and the corresponding discrete map resulting from finite difference discretizations. This issue is especially vital for computational sciences since nonlinear differential equations in applied sciences can rarely be solved in closed form and it is often necessary to replace them by finite dimensional nonlinear discrete maps. Most often, typical applied scientists rely on numerical methods to give insight into the solution behavior of nonlinear DEs. It is not always clear how well a numerical solution can mimic the true physics of problems that possess genuinely nonlinear types of behavior.

Why is there such a need to study the connection between the continuum and its discretized counterparts for CFD applications? This stems from the fact that current supercomputer power can perform numerical simulations on virtually any simple 3-D aerodynamic configuration and, due to the limited available experimental data, the applied engineers are relying on or trusting the numerical simulations whole heartedly to help design our next generation aircraft and spacecraft. However, many of these

applied scientists are still using linear analysis as their guide to study highly nonlinear equations, and most often they are not aware of the limitations and pitfalls of many of the numerical procedures. Furthermore, most of the numerical algorithms in use operate under the accuracy and stability limit guidelines of the linearized model equation. It is only appropriate to analyze nonlinear problems with the nonlinear approach; i.e., by the nonlinear dynamic approach.

The unique dynamical property of the separate dependence of solutions on initial data for the individual nonlinear DE and its discretized counterpart is especially important for employing a "time-dependent" approach to the steady state with given initial data in hypersonic CFD. In many CFD computations, the steady-state equations are PDEs of the mixed type and a time-dependent approach to the steady state can avoid the complication of dealing with elliptic-parabolic or elliptic-hyperbolic types of PDEs. However, this time-dependent approach has created a new dimension of uncertainty. This uncertainty stems from the fact that in practical computations, the initial data are not known and a freestream condition or an intelligent guess for the initial conditions is used. In particular the controversy of the "existence of multiple steady-state solutions" through numerical experiments will not be exactly resolved until there is a better understanding of the separate dependence on initial data for both the PDEs and the discretized equations.

2.4. Connection Between the Dynamical Behavior of the Continuum and Its Discretized Counterpart

Aside from truncation error and machine round-off error, a more fundamental distinction between the continuum and its discretized counterparts is new behavior in the form of spurious stable and unstable asymptotes created by the numerical methods. This is due to the fact that nonlinear discrete maps can exhibit a much richer range of dynamical behavior than their continuum counterparts as discussed in section 2.2. Some instructive examples will be given in section III. These new phenomena were partially explored by the University of Dundee group [46-54], Sanz Serna [55], Iserles [56,57] and Stuart [58-62]. Their main emphasis was on phenomena beyond the linearized stability limit. The main contribution of our current study is (1) the occurrence of spurious steady-state numerical solutions below the linearized stability limit of the scheme for genuinely nonlinear problems, (2) the strong dependence of numerical solutions on the initial data, as well as other system parameters of the DEs such as boundary conditions and numerical dissipations terms, and (3) the implications for practical computations in hypersonic CFD.

Before discussing the numerical examples, the next two subsections will give an overall summary of our current findings (integrating with other relevant recent results). The discussion is divided into steady-state solutions and asymptotes of any period, and transient solutions.

2.4.1. Steady-state Solutions and Asympotes of Period Higher Than One:

Table 2.1 shows the possible stable asymptotic solution behavior between DEs (ODEs or PDEs) and their discretized counterparts. Some of the phenomena will be supported by simple examples in section III. The main connection between the DEs and their discretized counterparts is that steady-state solutions of the continuum are solutions of the discretized counterparts but not the reverse. Their main difference is that new phenomena are introduced by the numerical methods in the form of spurious stable and unstable asymptotic solutions of any period. In the past, the phenomena of spurious asymptotes were observed largely beyond the linearized stability of the schemes. Some numerical analysts and applied computational scientists were not alarmed and were skeptical about these phenomena since, theoretically, one is always guided by the linearized stability limit of the scheme. However, this resaoning is only valid if one is solving a scalar nonlinear ODE and the initial data are known. Another important concept is that the result of operating with time steps beyond the linearized stability limit is not always a divergent solution; spurious steady-state solutions and spurious asymptotes of higher period can occur.

Our current study also indicated that depending on the form of the nonlinear DEs, all ODE solvers can introduce spurious asymptotic solutions of some period or all periods. However, the most striking result is that for certain schemes and depending on the form of the nonlinear DEs, spurious steady states can occur below the linearized stability limit. See section III and our companion paper [21] for more details.

Another important factor is that associated with the same (common) steady-state solution, the basin of attraction (domain of attraction) of the continuum might be vastly different from the discretized counterparts. This is due entirely to the separate dependence and sensitivity on initial and boundary conditions for the individual system. The situation is compounded by the existence of spurious steady states and asymptotes of period higher than one and possibly chaotic attractors.

Here the basin of attraction of a dynamical system is the domain for which the set of initial conditions time asymptotically approaches a specific asymptote. Figures 2.1 and 2.2 show the basins of attraction of two popular ODE dynamical systems. Figure 2.1 shows the multiple stable steady states and their basins of attraction for the damped pendulum equation

$$\frac{du}{dt} = v, \tag{2.4a}$$

$$\frac{dv}{dt} = -\epsilon v - \sin(u) \tag{2.4b}$$

for $\epsilon = 0.4$. Figure 2.2 shows the multiple steady states and their basins of attraction for the simple predator-prey equation

$$\frac{du}{dt} = -3u + 4u^2 - uv/2 - u^3, \tag{2.5a}$$

$$\frac{dv}{dt} = -2.1v + uv. \tag{2.5b}$$

where u is the population of the prey and v is the population of the predator. These figures are taken from Parker and Chua [8] and were generated by the use of a variable time step Runge-Kutta-Fehlberg method with built in accuracy check (if the numerical solutions are approximating the true solution of the ODE). See reference [8] for details. These figures, although generated numerically, with the built in accuracy check the fixed points and basins of attraction coincide with the ODEs. The stable fixed points of the damped pendulum equation are $2n\pi$, $n = 0, 1, ...$ The unstable fixed points (saddles) are $(2n + 1)\pi$. The separatrices of the saddle points divide the phase plane into the different basins of attraction for the corresponding stable fixed points. The fixed points of the predator and prey equation are slightly less regular than the damped pendulum equation. Figure 2.2 shows two saddle points at $u = 1$, $v = 0$ and $u = 3$, $v = 0$, one stable focal point at $u = 2.1$, $v = 2$ and one stable nodal point at $u = 0$, $v = 0$. Again the separatrices of the saddle points divide the phase plane into the basins of attraction for the corresponding stable fixed points.

Intuitively, in the presence of spurious asymptotes, the basin of the true steady states (steady states of the DEs) can be separated by the basins of attraction of the spurious asymptotes and interwoven by unstable asymptotes, whether due to the physics (i.e., present in both the DEs and the discretized counterparts) or spurious in nature (i.e., introduced by the numerical methods).

For PDEs, another added dimension is that even with the same time discretization but different spatial discretizations or vice versa, the basins of attraction can also be extremely different. However, mapping out the basins of attraction for any nonlinear continuum dynamical system other than the very simple scalar equations relies on numerical methods. The type of nonlinear behavior and the dependence and sensitivity to initial conditions for both the PDEs and their discretized counterparts make the understanding of the true physics extremely difficult when numerical methods are the sole source. Under this situation, how can one delineate the numerical solutions that approximate the true physics from the numerical solutions that are spurious in nature? Hopefully, with our simple illustrations in section III, we can demonstrate the importance of the current subject and, most of all, stress the importance of knowing the general dynamical behavior of asymptotes of the schemes for genuinely nonlinear scalar DEs before applying these schemes in practical calculations.

2.4.2. Transient or Time-Accurate Solutions:

It is a common misconception that inaccuracy in long time behavior poses no consequences on transient or time-accuate solutions. This is not the case when one is dealing with genuinely nonlinear DEs. For genuinely nonlinear problems, due to the possible existence of spurious solutions, larger numerical errors can be introduced by the nu-

merical methods than one can expect from local linearized analysis or weakly nonlinear behavior. The situation will get more intensified if the initial data of the DE is in the basin of attraction of a chaotic transient [63-65] of the discretized counterpart. This is due to the fact that existence of spurious asymptotes transact wrong behavior in finite time. In fact, it is possible the whole solution trajectory is likely to be erroneous.

We'd like to end this section with a direct quote from Sanz-Serna and Vadillo's paper [55]. This quote indicates the danger of relying on linearized stability and convergence theory in analyzing nonlinear dynamical problems. Reference [55] is one of the few papers trying to convey to numerical analysts the flavor of the powerful "nonlinear dynamic approach". Hopefully, with the current discussion, we can convey to computational fluid dynamicists the flavor of the importance of the "nonlinear dynamic approach" in CFD analysis.

"Assume that the convergence of a numerical method has been established; it is still possible that for a given choice of Δt, or even for any such a choice, the qualitative behaviour of the numerical sequence u^0, u^1, ..., u^n, ... be competely different from that of the theoretical sequence $u(t_0)$, $u(t_1)$, ... $u(t_n)$, ... This discrepancy which refers to n tending to ∞, Δt fixed cannot be ruled out by the convergence requirement, as this involves a different limit process (namely Δt tending to 0). ——————————————————————————————————————. The fact that analyses based on linearization cannot accurately predict the qualitative behaviour of u^n for fixed Δt should not be surprising: there is a host of nonlinear phenomena (chaos, bifurcations, limit cycles ...) which cannot possibly be mimicked by a linear model."

III. THE ODE CONNECTION

In this section, we review some of the fundamentals and available theory and discuss our major results. The discussion will have some overlap with our companion paper [21].

3.1. Preliminaries

Consider an autonomous nonlinear ODE of the form

$$\frac{du}{dt} = \alpha S(u), \tag{3.1}$$

where α is a parameter and $S(u)$ is nonlinear in u. For simplicity of discussion, we consider only autonomous ODEs where α is linear in (3.1); i.e., α does not appear explicitly in S.

A fixed point u^* of an autonomous system (3.1) is a constant solution of (3.1); that is

$$S(u^*) = 0. \tag{3.2}$$

Note that the terms "equilibrium points", "critical points", "stationary points", "asymptotic solutions" (exclude periodic solutions for the current definition), "steady-state solutions" and "fixed points" are sometimes used with slightly different meanings in the literature, e.g., in bifurcation theory. For the current discussion and for the majority of nonlinear dynamic literature, these terms are used interchangeably. We might want to mention that certain researchers reserve the term "fixed point" for discrete maps only.

Consider a nonlinear discrete map from finite discretization of (3.1)

$$u^{n+1} = u^n + D(u^n, r), \tag{3.3}$$

where $r = \alpha \Delta t$ and $D(u^n, r)$ is linear or nonlinear in r depending on the ODE solvers. Here the analysis is similar if D is a nonlinear function of u^{n+p}, $p = 0, 1, ..., m$. Examples to illustrate the dependence on the numerical schemes for cases where D is linear or nonlinear in the parameter space will be given in the subsequent section.

A fixed point u^* of (3.3) (or fixed point of period 1) is defined by $u^{n+1} = u^n$, or

$$u^* = u^* + D(u^*, r) \tag{3.4a}$$

or

$$D(u^*, r) = 0. \tag{3.4b}$$

One can also define a fixed point of period p, where p is a positive integer by requiring that $u^{n+p} = u^n$ or

$$u^* = E^p(u^*, r) \quad \text{but} \quad u^* \neq E^k(u^*, r) \quad \text{for } 0 < k < p. \tag{3.5}$$

Here, $E^p(u^*, r)$ means that we apply the difference operator E p times, where $E(u^n, r) = u^n + D(u^n, r)$. For example, a fixed point of period 2 means $u^{n+2} = u^n$ or

$$u^* = E\big(E(u^*, r)\big). \tag{3.6}$$

In this context, when dealing with discrete systems, the term "fixed point" without indicating the period means "fixed point of period 1" or the steady-state solution of (3.3).

In order to illustrate the basic idea, the simplest form of the Ricatti ODE, i.e., the logistic ODE (2.3) with

$$S(u) = u(1 - u) \tag{3.7}$$

is considered. For this ODE, the exact solution is

$$u(t) = \frac{u^0}{u^0 + (1 - u^0)e^{-\alpha t}}, \tag{3.8}$$

where u^0 is the initial condition. The fixed points of the logistic equation are roots of $u^*(1 - u^*) = 0$; it has two fixed points $u^* = 1$ and $u^* = 0$.

To study the stability of these fixed points, we perturb the fixed point with a disturbance ξ, and obtain the perturbed equation

$$\frac{d\xi}{dt} = \alpha S(u^* + \xi). \tag{3.9}$$

Next, $S(u^* + \xi)$ can be expanded in a Taylor series around u^*, so that

$$\frac{d\xi}{dt} = \alpha \left[S(u^*) + S_u(u^*)\xi + \frac{1}{2} S_{uu}(u^*)\xi^2 + \cdots \right], \tag{3.10}$$

where $S_u(u^*) = \frac{dS}{du}\big|_{u^*}$. Stability can be detected by examining a small neighborhood of the fixed point provided if for given α, u^* is not a hyperbolic point [3,7,9] (i.e., if the real part of $\alpha S_u(u^*) \neq 0$). Under this condition ξ can be assumed small, its successive powers $\xi^2, \xi^3, \ldots$ can normally be neglected and the following linear perturbed equation is obtained

$$\frac{d\xi}{dt} = \alpha S_u(u^*)\xi. \tag{3.11}$$

The fixed point u^* is asymptotically stable if $\alpha S_u(u^*) < 0$ whereas u^* is unstable if $\alpha S_u(u^*) > 0$. If $\alpha S_u(u^*) = 0$, a higher order perturbation is necessary.

If we perturb the logistic equation around the fixed point with $\alpha > 0$, one can find that $u^* = 1$ is stable and $u^* = 0$ is unstable. It is well known that the general asymptotic solution behavior of the logistic ODE is that for any $u^0 > 0$, the solution will eventually tend to $u^* = 1$. Figure 3.1 shows the solution behavior of the logistic ODE.

Now, let us look at three of the well known ODE solvers. These are explicit Euler (Euler, forward Euler), leapfrog and Adam-Bashforth. For the ODE (3.1) with $S(u) = u(1-u)$, the dynamical behavior of their corresponding discrete maps is well established. The explicit Euler is given by

$$u^{n+1} = u^n + rS(u^n), \tag{3.12}$$

and it is after a linear transformation, the well known logistic map [26-30]. The leapfrog scheme can be written as

$$u^{n+1} = u^{n-1} + 2rS(u^n), \tag{3.13}$$

and it is a form of the Hénon map [32]. The Adam-Bashforth method given by

$$u^{n+1} = u^n + \frac{r}{2}\Big[3S(u^n) - S(u^{n-1})\Big], \tag{3.14}$$

is again a variant of the Hénon map and has been discussed by Prüffer [44] in detail.

We can determine fixed points of the discrete maps (3.12)-(3.14) and their stability properties in a similar manner as for the ODE. It turns out that all three of the discrete maps have the same fixed points as the ODE (3.1) — a desired property which is important for obtaining asymptotes of nonlinear DE numerically. Here we use asymptotes to mean fixed points of any period.

The corresponding linear perturbed equation for the discrete map (3.3), found by substituting $u^n = u^* + \xi^n$ in (3.3) and ignoring terms higher than ξ^n is

$$\xi^{n+1} = \xi^n\big[1 + \Delta t D_u(u^*, \Delta t)\big]. \tag{3.15}$$

Here the parameter α of the ODE has been absorbed in the parameter Δt due to the assumption that α does not appear explicitly in $S(u)$. For stability we require

$$|1 + \Delta t D_u(u^*, \Delta t)| < 1. \tag{3.16}$$

Again, for $|1 + \Delta t D_u(u^*, \Delta t)| = 1$, higher order perturbation is necessary. For a fixed point of period p the corresponding linear perturbed equation and stability criterion are

$$\xi^{n+p} = \xi^n E_u^p(u^*, \Delta t). \tag{3.17}$$

and

$$|E_u^p(u^*, \Delta t)| < 1, \tag{3.18a}$$

with

$$E_u^p(u^n, \Delta t) = \frac{d}{du} E(u^{n+p-1}, \Delta t) ... \frac{d}{du} E(u^n, \Delta t) \tag{3.18b}$$

For $S(u) = u(1-u)$, the stability of the stable fixed points of period 1 and 2 for discrete maps (3.12)-(3.14) with $r = \alpha \Delta t$ are

Explicit Euler:

$u^* = 1$ stable if $0 < r < 2$

period 2 stable if $2 < r < \sqrt{6}$.

Leapfrog:

$u^* = 1$ unstable for all $r \geq 0$

chaotic solution exist for all r no matter how small

Adam-Bashforth:

$u^* = 1$ stable if $0 < r < 1$

period 2 stable if $1 < r < \sqrt{2}$.

Figure 3.2 shows the stable fixed point diagram of period $1, 2, 4, 8$ by solving numerically the roots of (3.12) for $S(u) = u(1-u)$. The r axis is divided into 1,000 equal intervals. The numeric labelling of the branches denotes their period. The subscript E on the period 1 branch indicates the stable fixed point of the DE.

Two of these three examples serve to illustrate that the result of operating with a time step beyond the linearized stability limit of the stable fixed points of the nonlinear ODEs is not always a divergent solution; spurious asymptotes of higher period can occur. This is in contrast to the ODE solution, where only a single stable asymptotic value $u^* = 1$ exists for any $\alpha > 0$ and any initial data $u^0 > 0$. It is emphasized here that these spurious asymptotes, regardless of the period, stable or unstable, are solutions in their own right of the discrete maps resulting from a finite discretization of the ODE.

3.2. Spurious Steady-State Numerical Solutions

For the previous three ODE solvers, we purposely picked the type of schemes that do not exhibit spurious fixed points [56] but allow spurious fixed point of period higher than 1. In this section, we discuss the existence of spurious steady-state numerical solutions. Again, it is emphasized here that these spurious steady states, stable or unstable, are solutions in their own right of the resulting discrete maps. Consider two second-order Runge-Kutta schemes, namely, the modified Euler (R-K 2) and the improved Euler (R-K 2), the fourth-order Runge-Kutta method (R-K 4), and the second and third-order predictor-corrector method [66-68] of the forms

Modified Euler (R-K 2) method:

$$u^{n+1} = u^n + rS\left(u^n + \frac{1}{2}rS^n\right) \quad S^n = S(u^n) \tag{3.18}$$

Improved Euler (R-K 2) method:

$$u^{n+1} = u^n + \frac{r}{2}\left\{S\left[u^n + S(u^n + rS^n)\right]\right\} \tag{3.19}$$

R-K 4 method:

$$\begin{aligned} u^{n+1} &= u^n + \frac{r}{6}\left(k_1 + 2k_2 + 2k_3 + k_4\right) \\ k_1 &= S^n \\ k_2 &= S\left(u^n + \frac{1}{2}rk_1\right) \\ k_3 &= S\left(u^n + \frac{1}{2}rk_2\right) \\ k_4 &= S\left(u^n + \frac{1}{2}rk_3\right) \end{aligned} \tag{3.21}$$

Predictor-corrector method of order m:

$$\begin{aligned} u^{(0)} &= u^n + rS^n \\ u^{(k+1)} &= u^n + \frac{r}{2}\left[S^n + S^{(k)}\right], \qquad k = 0, 1, ..., m-1 \\ u^{n+1} &= u^n + \frac{r}{2}\left[S^n + S^{(m-1)}\right]. \end{aligned} \tag{3.22}$$

Using the same procedures, one can obtain the fixed points for each of the above schemes (3.18) - (3.22). Figures 3.3 - 3.7 show the stable fixed point diagrams of period 1,2,4 and 8 for these five schemes for $S(u) = u(1-u)$. Some of the fixed points of lower period were obtained by closed form analytic solution and/or by a symbolic manipulator such as MAPLE [69] to check against the computed fixed point. The majority are computed numerically [2,8]. The stability of these fixed points was examined by checking the discretized form of the appropriate stability conditions. Again the axis is divided into 1,000 equal intervals. The numeric labelling of the branches denotes their period, although some labels for period 4 and 8 are omitted due to the size of the labelling areas. The subscript E on the main period one branch indicates the stable fixed point of the DE while the subscript S indicates the spurious fixed points introduced by the numerical scheme. Spurious fixed points of period higher than one are obvious and are not labeled

except for special cases. Note that these diagrams, which appear in most parts as solid lines are actually points, which are only apparent in areas with high gradients.

To contrast the results, similar stable fixed point diagrams are also computed for $S(u) = u(1-u)(b-u)$, $0 < b < 1$. See figures 3.8 - 3.14. The stable fixed point for the ODE in this case is $u^* = b$ and the unstable ones are $u^* = 0$ and $u^* = 1$. For any $0 < u^0 < 1$ and any $\alpha > 0$, the solution will asymptotically approach the only stable asymptote of the ODE $u^* = b$.

Note that contrary to the DE, the maximum number of stable and unstable fixed points (real and complex) for each scheme varied between 4 to 16 for $S(u) = u(1-u)$ and 9 to 81 for $S(u) = u(1-u)(b-u)$, depending on the numerical methods and the r value. The domains of all of the fixed point diagrams are chosen so that they cover the most interesting part of the scheme and ODE combinations. Notice that asymptotes might occur in other parts of the domain as well.

Aside from the striking difference in topography in the stable fixed point diagrams of the various methods and ODE combinations, all of these diagrams have one similar feature; i.e., they all exhibit spurious stable fixed points, as well as spurious stable fixed points of period higher than one. Although in the majority of cases, these occur for values of r above the linearized stability limit, this not always the case, as in the modified Euler scheme applied to the logistic ODE and $du/dt = \alpha u(1-u)(b-u)$, $0 < b < .5$, and the R-K 4 applied to the logistic DE. For these two methods and ODE combinations, stable spurious fixed points occur below the linearzed stability limit. In some of the instances, these spurious fixed points are outside the interval of the stable and unstable fixed points of the ODEs. Others not only lie below the linearized stability limit but also in the region between the fixed points of the DEs and so could be very easily achieved in practice.

One might argue that for the ODEs that we are considering, it is trivial to check whether an asymptote is spurious or not. For example, if $\overline{u}$ is a spurious asymptote of period one, then $S(\overline{u}) \neq 0$. The main purpose of the current illustration is to set the baseline dynamical behavior of the scheme so that one can use it wisely in other more complicated settings such as when nonlinear PDEs are encountered in which the exact solutions are not known. Under this situation, spurious asymptotes could be computed and mistaken for the correct steady-state solutions.

Note that for the modified Euler method, spurious fixed points of higher periods and chaotic attractors as well as spurious steady states occur below the linearized stability limit. Let Ω be the basin of attraction of the fixed point of the ODE and let r^* be the corresponding linearized stability limit value of the scheme. Then there exists a portion of the basin Ω denoted by Ω^c in which $\Omega^c \subset \Omega$ and an interval of r with $0 < r < r^*$ which actually belongs to the basin of attraction of the chaotic attractor of the discretized counterparts. There also exist some other $\Omega^p \subset \Omega$ and an interval of r with $0 < r < r^*$ and $p \geq 1$ an integer, which actually belongs to the basin of attraction of a stable asymptote of period p of the corresponding discrete map. This leads to the

issue of the dependence of solutions on initial data which will be a subject of the next subsection.

3.3. Strong Dependence of Solutions on Initial Data

For simple nonlinear ODEs that we are considering, the fixed point diagram is extremely useful for the understanding of the dynamics of the DEs and their discretized counterparts. However, when fixed points of higher periods and/or complex nonlinear equations are sought, searching for the roots and testing for stability of highly complicated nonlinear algebraic equations can be expensive and might lead to inaccuracy.

Equally useful for understanding the dynamics are the bifurcation diagram and basin of attraction of fixed points for both the DEs and the difference schemes. The bifurcation diagram for the one-dimensional discrete maps displays the iterated solution u^n vs. r after iterating the discrete map for a given number of iterations with a chosen initial condition (or multiple initial conditions) for each of the r parameter values.

Bifurcation is broadly used to describe significant qualitative changes that occur in the orbit structure of a dynamical system as the system parameters are varied. In general, bifurcation theory can be divided into two general classes, namely, local and global. Local bifurcation theory is concerned with the bifurcation of fixed points of nonlinear equations and discrete maps. Global bifurcation studies phenomena away from the fixed points. It studies the interaction between different types of fixed points. One might define a bifurcation point as being any dynamical system which is structually unstable [3,8,9]. A fixed point is structurally stable if nearby solutions have qualitatively the same dynamics. The linearized stability limit of a fixed point of a scheme is the same as the bifurcation point in the corresponding bifurcation diagram of the resulting discrete map.

For the numerical computations of the bifurcation diagrams with a given interval of r and a chosen initial condition (or multiple initial conditions), the r axis is divided into 500 equal spaces. In each of the computations, the discrete maps were iterated with 600 preiterations and the next 200 iterations were plotted for each of the 500 r values. The domains of the r and u^n axes are chosen to coincide with the stable fixed point diagrams shown previously. For our current interest, it is not necessary to distinguish the difference between a stable fixed point of period 200 and a chaotic attractor.

Figure 3.15 shows the bifurcation diagram of the Euler scheme applied to the logistic DE with an initial condition $u^0 > 0$. It is of interest to know that in this case the bifurcation diagram looks practically the same for any $u^0 > 0$. This is due to the fact that no spurious fixed points or spurious asymptotes of low periods exist for $r < 2.627$. Comparing the bifurcation diagram with figure 3.2, one can see that if we computed all of the fixed points of period up to 200 for figure 3.2, the resulting fixed point diagram would look the same as the corresponding bifurcation diagram (assuming 800 iterations

of the logistic map are sufficient to obtain the converged stable asymptotes of period upto 200 and a proper set of initial data are chosen to cover the basins of all of the periods in question). The numeric labelling of the branches in the bifurcation diagram denote their period, with only the essential ones labelled for identification purposes.

In order to interpret the bifurcation diagram for other ODE and scheme combinations, some knowledge of the fixed point diagram is necessary, at least for the lower order periods. Otherwise, one cannot identify the exact periodicity of the asymptotes easily. As can be seen later, a "full" bifurcation diagram cannot be obtained efficiently without the aid of the stable and unstable fixed point diagram for schemes that exhibit spurious fixed points of any period, especially lower periods. In most cases, the unstable asymptotes divide the domain into the proper basins of attraction for the stable asymptotes (spurious or otherwise), and at least one initial data point is used from each of the basins of attraction before a full bifurcation diagram can be obtained.

In all of the fixed point diagrams 3.3 - 3.14, the bifurcation phenomena can be divided into three kinds. For the first kind, the paths (spurious or otherwise) resemble period doubling bifurcations (flip bifurcation) [2-5] similar to the logistic map. See figures 3.2, 3.6 and 3.8 for examples. The second kind occurs, most often, at the main branch 1_E, with the spurious paths branching from the correct fixed point as it reaches the linearized stability limit, and quite often even bifurcating more than once (pitchfork bifurcation or supercritical bifurcation [70,7]), as r increases still further before the onset of period doubling bifurcations. See figures 3.4, 3.7, 3.9 - 3.11 and 3.13 for examples. The third kind again occurs most often at the main branch 1_E. The spurious paths near the linearized stability limit of 1_E would experience a transcritical bifurcation [3,7,9,70]. See figures 3.3, 3.5, 3.7 and 3.14 for examples. Notice that the occurrence of transcritical and supercritical bifurcations are not limited to the main branch 1_E. See figures 3.11 - 3.14 for examples. The other commonly occurring bifurcation phenomenon is the subcritical bifurcation which was not observed in our two chosen $S(u)$ functions. With a slight change in the form of our cubic function $S(u)$, a subcritical bifurcation can be achieved [70,3,7,9]. The consequence of the latter three bifurcation behaviors is that bifurcation diagrams calculated from a single initial condition u^0 will appear to have missing sections of spurious branches, or even seem to jump between branches. This is entirely due to the existence of spurious asymptotes of some period or more than one period, and its dependence on the initial data. This occurs even for the Euler scheme as depicted in figure 3.8. See section 3.4 for further discussion of these four types of bifurcation phenomena.

Figures 3.16 - 3.18 show the bifurcation diagram by the modified Euler method for the logistic ODE with three different starting initial conditions. In contrast to the explict Euler method, none of these diagrams look alike. One can see the influence and the strong dependence of the asymptotic solutions on the initial data. Figure 3.19 shows the corresponding "full" bifurcation diagram, their earlier stages resembling the fixed point diagram 3.3. Figures 3.20 - 3.22 illustrate similar bifurcation behavior for the corresponding R-K 4 method. Figure 3.12 serves as an example to illustrate that the effect of overplotting a number of initial data, but not the appropriate ones, would not

be sufficient to cover all of the essential spurious branches. Figures 3.23 - 3.25 show a similar illustration for $S(u) = u(1-u)(b-u)$, $0 < b \leq .5$ by the improved Euler, R-K 4 and the modified Euler method. The strong dependence of solutions on initial data is evident from the various examples in which this type of behavior is very common for genuinely nonlinear problems.

In order to compute a "full" bifurcation diagram, we must overplot a number of diagrams obtained by the guide of the stable and unstable fixed point diagram as an appropriate set of starting initial data. In the case where the fixed point diagrams are extremely difficult to compute, a brute force method of simply dividing the domain of interest of the u^n axis into equal increments and using these u^n values as initial data is employed. The "full" bifurcation diagram is obtained by simply overplotting all of these individual diagrams on one.

For completeness, figures 3.26 - 3.38 show the "full" bifurcation diagrams for the corresponding fixed point diagrams shown previously. Figures 3.36 and 3.37 show a blow up section of figures 3.34 and 3.35. Notice that the exact values of the initial data are immaterial as long as these values cover all of the basins of attraction of the essential lower order periods (i.e., at least one initial data point is used from each of the basins). Here, we use the term "full" bifurcation diagram to mean just that. No attempt has been made to compute the true full bifurcation diagram since this is very costly and involves a complete picture of the basins of attraction for the domain of interest in question.

3.4. Classification of ODE solvers

(According to the Existence of Spurious Fixed Points)

In reference [56], Iserles studied the stability of ODE solvers for nonlinear autonomous ODE via the dynamical approach. He proved that linear multistep methods (LMM) [66-68] that give bounded values at infinity always produce correct asymptotic behavior, but it is not the case with Runge-Kutta methods and some predictor-corrector methods. He demonstrated that the Runge-Kutta and predictor-corrector methods may lead to false asymptotes. However, he did not discuss the possibility of these spurious asymptotes existing below the linearized stability limit.

For implicit LMM, he assumed the resulting nonlinear algebraic equations are solved exactly. He also showed the influence of nonlinear algebraic solvers on the size of stability regions for implicit LMM. His conclusion was that the standard nonlinear algebraic solver — the modified Newton-Raphson method

$$u_{n+1}^{(k+1)} = u_{n+1}^{(k)} - \frac{u_{n+1}^{(k)} - u_n - \frac{r}{2}\left[S(u_n) + S(u_n^{(k)})\right]}{1 - \frac{r}{2}S_u(u_n)}, \tag{3.23}$$

can drastically degrade the region of stability limit as compared to the Newton-Raphson method

$$u_{n+1}^{(k+1)} = u_{n+1}^{(k)} - \frac{u_{n+1}^{(k)} - u_n - \frac{r}{2}\left[S(u_n) + S(u_n^{(k)})\right]}{1 - \frac{r}{2}S_u(u_n^{(k)})}. \tag{3.24}$$

On the other hand, the direct iteration method

$$u_{n+1}^{(k+1)} = u_n + \frac{r}{2}\left[S(u_n) + S(u_{n+1}^{(k)})\right] \tag{3.25}$$

converges only if the step sizeis of the same order of magnitude as that required for an explicit method. Thus the advantage of using an implicit method to enhance stability is lost. Here for clarity of notation, when iteration procedures are involved, u_n is used in place of u^n of the previous section.

The implications of behavior detailed in Iserles' work [56] range far beyond pure ODE. For most CFD application, the use of implicit time discretization to "time" march the solution to steady state is very common. The resulting nonlinear algebraic systems are solved by either noniterative linearization [71,14] or by some kind of iterative or relaxation procedures. Very often, applied computational fluid dynamicists experience a non-convergent solution where the residual will decrease only so far before reaching a plateau with a time step larger than the explicit method. Therefore the behavior observed in Iserles' work could explain the degradation in the stability of the implicit scheme in practice. Indeed, even though the mechanisms involved are far more complicated than those studied here, elements such as spatial discretization dynamical behavior and nonlinear coupling effect for systems, could well be an explanation.

More recently, Iserles and Sanz-Serna [57] established conditions for using a variable step size analysis to avoid spurious fixed points in a class of Runge-Kutta methods.

Looking at the problem from another perspective, it is very useful to find the cause of the existence of spurious asymptotes by looking at the form and properties of the resulting discrete maps, regardless of the methods. We have the following two observations.

(1) Assume that the only parameter that was introduced by a numerical method is Δt. Then from Iserles results and our current investigation, one obvious necessary condition for the existence of spurious steady states of ODE solvers for (3.1) is the introduction of nonlinearity in the parameter space Δt. This is evident from our examples and general analysis. For example, if Δt (or r) is linear in (3.3), then (3.3) can be written as

$$u^{n+1} = u^n + crS(u^n), \quad c \text{ a constant of the scheme.} \tag{3.26}$$

Therefore any fixed point of (3.3) is a fixed point of (3.1). Without lost of generality, a similar proof applies to the resulting difference operator D from a p time level scheme.

(2) The second observation is that one can classify the types of spurious steady state in the form of bifurcation theory near a bifurcation point or a bifurcation limit

point. Figures 3.39 and 3.40 show the definition of the various types of branching points and the stability of solution in the neighborhood of branch points. In other words, the classification is according to the onset of spurious asymptotes of subcritical, supercritical or transcritical bifurcations. See figure 3.41 for the definition of the three types of phenomena.

Assume an ODE solver introduces nonlinearity in the parameter space Δt for (3.1). Then a necessary and sufficient condition for the occurrence of spurious steady states below the linearized stability limit on the main branch 1_E (stable fixed points of the DE) is that a transcritical or subcritical bifurcation of the types shown in figures 3.42 and 3.43 exist at the bifurcation point or near a bifurcation limit point. It is emphasized here that the existence of spurious fixed points of higher period can be independent of the existence of spurious steady states (fixed points of period 1).

A detailed analytical analysis on the existence of transcritical, subcritical and supercritical bifurcations for the class of Runge-Kutta methods can be found in our companion paper [21]. Figures 3.44 - 3.54 illustrate the onset of different types of spurious steady states by showing the stable and unstable fixed points of periods 1 and 2, and the types of bifurcation phenomena for the modified Euler, Improved Euler and R-K 4 and the predictor-corrector schemes of order 2 and 3 for $S(u) = u(1-u)$ and $S(u) = u(1-u)(b-u), \quad 0 < b \leq .5$. In order to illustrate the different behavior in an uncluster fashion, not all of the periods 1, 2 and branching points are labeled. It is interesting to see the manner in which the onset of the different types of bifurcations occur, in particular, the birth of the different types of bifurcations away from the 1_E branches.

3.5. Basins of Attraction

Due to the separate dependence and sensitivity on initial data for the individual DEs and the discretized counterparts, in conjunction with the existence of spurious steady states and asymptotes of higher periods, even associated with the same (common) steady-state solution, the basin of attraction of the continuum might be vastly different from the discretized counterparts.

Take for example, $S(u) = u(1-u)$. The only stable fixed point of the logistic ODE is $u = 1$. The entire domain of the real u^n-axis is divided into two basins of attraction for the ODE independent of any positive α. Now if one numerically integrates the ODE by the modified Euler method, extra stable and unstable fixed points can be introduced by the scheme depending on the value of r. That is for certain ranges of the r values, the u^n-axis is divided into four basins of attraction. But of course for other ranges of r, higher period spurious numerical solutions exist, more basins of attraction are created within the same u^n-axis range, etc. Stable and unstable fixed point diagrams such as figures 3.44 - 3.54 are very useful in the division of the u^n-axis into different basins of lower periods.

3.6. Systems of ODEs

As can be seen from the previous sections, the rich and complicated dynamical behavior of discrete maps resulting from finite discretization of simple nonlinear scalar autonomous ODEs is very enlightening, educational and useful in giving some indications of the strange behavior encountered in practice. One would naturally ask how highly coupled nonlinear first-order autonomous systems complicate the issue. After all, these types of systems occur naturally in physical science and engineering fields. Examples are

(1) second or higher order nonlinear scalar autonomous or nonautonomous ODEs arising from mechanical systems,

(2) meteorology,

(3) chemical reaction equations arising from chemistry,

(4) system of ODEs arising from the method of lines approach in reaction-diffusion, reaction-convection and reaction-convection-diffusion equations.

Future work will be directed towards investigation into the nonlinear dynamical effect of using ODE solvers for nonlinear system of ODEs. Here, we do not attempt to give a detailed discussion on this subject, but rather indicate some of the implications from our experience as well as what is availiable in the literature.

First, the coupling of first-order nonlinear systems arising from a higher-order scalar nonlinear ODE is very different from the truly nonlinear coupling on systems of first-order ODEs. This difference carries over to their discretized couterparts. Second, due to the nonlinear coupling effect, whatever is observed in the nonlinear scalar case will definitely exists in the coupled system case in a more complex manner. Even with the help of the center manifold theorem [2-5], nonlinear systems of higher than three first-order ODEs are still extremely difficult to analyze. One major factor in analyzing the associated discrete maps from finite discretization of the continuum is that when three or more time levels of ODE solvers are used, even though the continuum is a first-order scalar autonomous ODE, the resulting discrete maps are $(p-1)$th-order, where p is the time level. One can extrapolate the complexity involved if nonlinear coupled systems of higher-order ODEs were discretized by p-time levels of ODEs solvers. Some aspects and implications of numerical integration of second- and third-order ODEs are discussed in references [39,40,72]. Some of our preliminary numerical experiments agree with the above general conclusion.

3.7. Suitability to the Type of Computational Environment

The main approach that we use in this paper is to establish the necessary mathematical reasoning and then to support this reasoning with extensive numerical experiments.

Our current study on one-dimensional scalar nonlinear dynamical equations which consist of a single parameter indicates that the understanding of the nonlinear effects encountered when applying finite-difference schemes to nonlinear differential equations is greatly aided by the analysis of bifurcation diagrams which record the values of successive iterations for a range of parameters. Equally useful are diagrams showing the basins of attraction of equilibria, both those of the differential equations and the spurious attractors generated by the difference scheme. The generation of such diagrams, however, is computationally expensive, especially for the basins of attraction where each point on the diagram represents a different choice of parameters for which many iterations of the scheme must be performed to determine its significance.

In all the bifurcation diagrams, the computations were performed on the VMS VAX in double precision. Take for example, figure 3.34. Each dot on the plot represents a solution obtained by integrating the discretized equation 800 times with each of the 20 prescribed initial data and each of the 500 equally space values of $r = \alpha\Delta t$. In other words, we are integrating the same equation for 10,000 different values of r and initial data combinations, and also iterating the same equation for each of these combinations with 800 iterations. The task can therefore be greatly enhanced by parallel computation, since essentially the same process needs to be applied to each point in a fine two- or three-dimensional array, each element representing a pixel on a high resolution screen or plotter. It is therefore a task highly suited to machines, such as the Connection machine, which have large numbers of processors enabling the entire region or subregions of the problem to be analysed in one pass rather than in a sequential point-by-point approach. The intensity of (repetitive) computing involved is too great to gain major benefit from machines such as the CRAY.

For multidimensional systems consisting of several parameters, we envision that the intensity of repetitive computing to obtain a bifurcation diagram or a basin of attraction cannot be realized if it is not performed on a massively parallel computer such as the Connection machine.

IV. LEVEL OF COMPLEXITY FOR PDEs

In order to systematically approach the subject of studying spurious steady-state numerical solutions of nonlinear nonhomogeneous hyperbolic and parabolic PDEs via the nonlinear dynamic approach, we propose to pursue the subject in three stages. First, we will attempt to obtain a full understanding of the subject for time discretization of ODEs. The investigation can give insight into numerical methods employing the Strang type of operator splittings or methods of lines approach for nonhomogeneous hyperbolic and parabolic PDEs. The second stage will involve the study of the discrete travelling wave solutions of the reaction-convection and reaction-convection-diffusion equations. The third stage will involve the study of the complete temporal-spatial discretizations of the reaction-convection and reaction-convection-diffusion equations. The last stage of the proposed plan is extremely difficult to analyze. Some aspects of full discretizations and discrete travelling wave solutions were investigated by [46-54, 58-62,73,74,10].

The question now is in what specific area will this approach advance the state-of-the-art in CFD. Our preliminary study indicated that many existing results for nonlinear dynamical systems such as chaos, bifurcations, and limit cycles (closed periodic orbits [5]) have a direct application to problems containing nonlinear source terms such as the reaction-diffusion, reaction-convection or the reaction-convection-diffusion equations. Also they have a direct application to most of the nonlinear shock-capturing methods such as the total variation diminishing (TVD) schemes [14,75-78]. With the advent of increasing demand for numerical accuracy, stability, efficiency, and uniqueness of numerical solutions in modeling such equations, an interdisciplinary approach for the analysis of these systems and schemes is needed. Besides it is a common practice in CFD to employ a time-dependent approach to achieve steady state. The separate dependence of solutions on initial data and system parameters for the individual PDE and its finite-difference equations is the crucial element in determining how well a numerical solution can mimic the true physics of the problem.

The following is an attempt to give a flavor of the subject and at the same time provide a justification for the importance of this subject area in CFD algorithm development for our next generation aerodynamics needs.

4.1. Model Equations

One of the recent areas of emphasis in CFD has been the development of appropriate finite-difference methods for nonequilibrium gas dynamics in the hypersonic range [14,78-81]. A nonlinear scalar reaction-diffusion model equation would be of the form

$$\frac{\partial u}{\partial t} = \varepsilon \frac{\partial^2 u}{\partial x^2} + \alpha S(u), \qquad \varepsilon, \alpha \text{ system parameters,} \tag{4.1}$$

a nonlinear scalar reaction-convection model equation would be of the form

$$\frac{\partial u}{\partial t} + \frac{\partial f(u)}{\partial x} = \alpha S(u), \tag{4.2}$$

and a nonlinear scalar reaction-convection-diffusion model equation would be of the form

$$\frac{\partial u}{\partial t} + \frac{\partial f(u)}{\partial x} = \varepsilon \frac{\partial^2 u}{\partial x^2} + \alpha S(u). \tag{4.3}$$

Here $f(u)$ a linear or nonlinear function of u. The nonlinear source term (or the reaction term) $S(u)$ can be very stiff. Note that phenomena such as chaos, bifurcations and limit cycles only relate to source terms $S(u)$ which are nonlinear in u. Equation (4.3) can be viewed as a model equation in combustion or as one of the species continuity equations in nonequilibrium flows (except in this case, the source term is coupled with other species mass fractions).

The above model equations are good starting points in the investigation of correlation between the theory of chaotic dynamical systems and uniqueness, stability, accuracy and convergence rate of finite-difference methods for CFD.

4.2. Level of Complexity

The main interest is to investigate what types of new phenomena arise from the numerical methods that are not present in the original nonlinear PDE, as a function of the stiff coefficient α, the diffusion coefficient ε, and the time step Δt with a fixed (or variable) grid spacing Δx. The time step can vary greatly depending on whether the time discretization is explicit or implicit. More precisely, one wants to weed out all undesirable phenomena due to the numerical method (e.g., additional equilibrium points introduced by the time as well as spatial discretizations, degradation of the domain of attraction, etc.) and to identify whether the numerical method really describes the true solution of the PDE under prescribed initial and boundary conditions with α, ε, the time step Δt and the grid spacing Δx being parameters. The study can be divided into steady and unsteady behavior with or without *shock waves*.

The major stumbling block is that combustion-related and high speed hypersonic flow problems usually contain multiple equilibrium states and shock waves that are inherent in the governing equations. Furthermore, spurious equilibrium states can be introduced by the time differencing and/or the spatial differencing. In many instances the stable and unstable equilibrium states, whether due to the physics or spurious in nature, are interwoven over the domain of interest and are usually very sensitive to the initial conditions and the time steps (even when the chosen time step is within the linearized stability limit as indicated in our study) as well as variation of parameters such as angle of attack, Reynolds number and coefficients of physical and numerical dissipations and physical and numerical boundary conditions.

The sensitivity of numerical solutions to coefficients of physical and numerical dissipations is evident from the study of Mitchell and Bruch on the reaction-diffusion equation. Their main result is that diffusion, which is usually perceived as having a stabilizing effect, is able to produce chaotic as well as divergent numerical solutions. Another interesting result due to Mitchell and Bruch was the production of chaos by decreasing the space increment or increasing the time increment. They showed that the addition of diffusion poses severe problems unless waves of constant speed c are assumed, in which case it reverts to an ODE with $x + ct$ as the independent variable. The sensitivity of numerical solutions to numerical boundary condition procedures was discussed in [82,83].

On the subject of sensitivity and dependence of solutions on initial data, the basin of attraction might be very different between the PDE and the discretized counterpart. The basin of attraction might contract or be very different from the basin of attraction for the original PDEs depending on the numerical methods. In many instances, even with the same spatial discretization but different time discretizations, the basins of attraction can also be extremely different. One can extrapolate the complexity involved when the influence of the various temporal as well as spatial discretizations are sought on the basins of attractivity.

Table 4.1 summarizes the level of complexity for a systematic approach to these types of PDE. The check mark on each type of PDE and approach indicate the ones where some work has been done on this subject. The majority are credited to the University of Dundee group [46-54] and some related theory by A. Stuart [58-62].

4.3. Involvement in the Study of Full Discretization of PDE

Consider a three-level explicit time differencing and a three-point spatial differencing of the reaction-convection-diffusion equation (4.3) of the form

$$u_j^{n+1} = u_j^n + H\left(u_{j-1}^n, u_j^n, u_{j+1}^n, u_{j-1}^{n-1}, u_j^{n-1}, u_{j+1}^{n-1}, \alpha, \epsilon\Delta t, \Delta x\right), \tag{4.4}$$

where u_j^n is the numerical solution at $t = n\Delta t$ and $x = j\Delta x$. Then the study of the asymptotes of (4.4) amounts to the study of fixed point behavior of period p in time and period q in space, denoted by (p, q), where p and q are integers. Here the fixed point of the partial-difference equation (4.4) is defined in a slightly more complicated way than for the ODE.

For example, a fixed point of period (1,1) is defined as $u_{j+1}^{n+1} = u_j^n$ and a fixed point of period (2,1) is defined as $u_{j+1}^{n+2} = u_j^n$. However, a fixed point of period (1,2) is defined as $u_{j+2}^{n+1} = u_j^n$. Thus, in general a fixed point of period (p,q) is defined as $u_{j+q}^{n+p} = u_j^n$. One can see that for $p, q > 3$, solving the resulting nonlinear algebraic equation is very involved, especially when physical boundary conditions and physical dissipation terms as well as numerical boundary conditions [82,83,34] and numerical dissipation [47] are

additional dimensions of consideration. Current available work involved the studies beyond the linearized stability limit of the schemes, and assumed the nonexistence of spurious fixed points of period (1,1). See references [46-54] for details.

4.4. Influence in Dynamical Behavior by Property of the PDEs and Schemes, and Treatment of the Source Terms

Although the general study of the dynamical behavior of partial-difference equations for the conservation law [84,85] of (4.3) is an enormous task, if we can isolate certain restricted subsets of the PDEs and schemes in hand which are immune to the type of phenomena discussed in section III for time discretization as well as spatial discretization, then we can concentrate on the rest of the unknowns.

As can be seen in section III, the nature of the dynamical behavior of the discretized counterparts is strongly influenced by properties of the numerical method and the types and form of nonlinear DEs. Here we want to study the influence on the dynamical behavior of elements such as conservation and nonlinearity of the schemes, and treatment of the source terms [14-17,78-81] when nonlinear conservation laws of PDEs are sought.

First, take the convection equation (4.2) with $S(u) = 0$ and consider a conservative explicit scheme [76,14] which is consistent with the conservation law of the form

$$u_j^{n+1} = u_j^n - \lambda\left[h_{j+\frac{1}{2}}^n - h_{j-\frac{1}{2}}^n\right], \tag{4.5}$$

where $\lambda = \Delta t/\Delta x$ and $h_{j\pm\frac{1}{2}}^n$ are the numerical flux functions. For a two-time level and five-point spatial scheme, $h_{j\pm\frac{1}{2}}^n = h(u_j^n, u_{j\pm1}^n, u_{j\pm2}^n)$.

We also can consider a two-parameter family of scheme

$$u_j^{n+1} + \frac{\lambda\theta}{1+\omega}\left[h_{j+\frac{1}{2}}^{n+1} - h_{j-\frac{1}{2}}^{n+1}\right] = u_j^n - \frac{\lambda(1-\theta)}{1+\omega}\left[h_{j+\frac{1}{2}}^n - h_{j-\frac{1}{2}}^n\right]$$

$$+\frac{\omega}{1+\omega}(u_j^n - u_j^{n-1}). \tag{4.6}$$

where $0 \le \theta \le 1$. When $\theta = 0$, the scheme is explicit and when $\theta = \omega + 1/2$, the scheme is temporally second-order accurate. One can obtain (4.5) from (4.6) by setting $\theta = 0$ and $\omega = 0$. The time differencing belongs to the class of LMM. Under the assumption that this scheme is conservative and consistent with the conservation law, discrete map (4.6) will have no spurious steady-state numerical solution since consistency means

$$h(u^*, u^*, u^*) = f(u^*). \tag{4.7}$$

Thus any steady-state solutions of (4.6) are steady-state solutions of the original PDE.

Now the situation is different when $S(u) \neq 0$. Under this situation, even if the same time and spatial discretization are employed, one still has to evaluate $\overline{S}$ properly. Here $\overline{S}$ is the function S evaluated at some proper average state $\overline{u}$ [14-17] for the full discretization that is consistent with the scheme [18], and achieves conservation at jumps. For a discussion on this subject, see references [78, 15-17] for details. The other crucial aspect is that when $S(u) \neq 0$, a full investigation on the dynamical behavior of the temporal and spatial discretization is necessary. The knowledge gained from the finite-difference methods analysis for $S(u) = 0$ does not carry over to the $S(u) \neq 0$ case.

4.5. Discrete travelling Waves

Analysis of the dynamical behavior of the full discretization of nonlinear nonhomogeneous PDEs of the hyperbolic and parabolic types is very involved. In this section, we look at a more restricted class of solutions — the discrete travelling wave solutions.

Consider a reaction-diffusion equation

$$\frac{\partial u}{\partial t} = \frac{\partial^2 u}{\partial x^2} + \tilde{S}(u). \tag{4.8}$$

Solution $u(x,t)$ depend on the space variable x and on the time t. Every zero of $\tilde{S}(u)$ constitutes an equilibrium of the PDE. Then a travelling wave solution is a profile $U(x)$ that travels along the x-axis with propagation speed $\overline{\lambda}$. Neither the shape of the wave nor the speed of propagation changes. To find travelling waves, we seek solutions

$$u(x,t) = U(x - \overline{\lambda}t), \tag{4.9}$$

resulting in an ODE

$$U'' + \overline{\lambda}U' + \tilde{S}(U) = 0. \tag{4.10}$$

By solving this ODE, one can calculate asymptotic states for the PDE. Let U_1 and U_2 be roots of $\tilde{S}(u)$ and hence equilibrium solutions for both the PDE and ODE. The asymptotic behavior of solution U for $x \to \pm\infty$ determines the type of travelling wave. Every solution with

$$U(\infty) = u_1 \tag{4.11a}$$

$$U(-\infty) = u_2, \tag{4.11b}$$

with $u_1 \neq u_2$, is a front wave of the ODE. This corresponds to a heteroclinic orbit [3] of the ODE, connecting the two stationary points u_1 and u_2. Here for a second-order autonomous ODE (4.10), when distinct saddles are connected, one encounters a heteroclinic orbit; also a heteroclinic orbit may also join a saddle to a node or vice versa. Another type of special orbit is a homoclinic orbit. A homoclinic orbit connects a saddle point to itself and such orbits have an infinite period. Several heteroclinic orbits

may form a closed path called a homoclinic cycle. Both the heteroclinic and homoclinic orbits are of great interest in applications because they form the profiles of travelling wave solutions of many reaction-diffusion problems. See references [3,10,73,74] for a discussion.

Similarly, one can study discrete travelling wave solutions for the finite discretization of (4.8). See references [73,74] for a discussion. Understanding of the discrete traveling wave solutions of the corresponding PDEs only gives insight into a very small subset of the dynamics of the PDEs. In most cases, it provides no information at all for the fully discretized equation.

V. IMPLICATIONS & RECOMMENDATIONS

Due to the complexity of the large increase in system dimension and the involvement of multiple floating parameters for finite difference methods in PDEs, we are not certain that a similar systematic general result can be arrived at for more complex nonlinear systems. The main indication at this point is from our time discretization study.

5.1. Results Drawn from the ODE Connection Study

Our study illustrates a few very important implications which are very fundamental in explaining what happens when linear stability breaks down for truly nonlinear problems; i.e., equations that display genuinely nonlinear types of behavior. The important points are as follows:

(1) There is sensitivity to initial data and strong dependence on discretization parameters such as the time step and the grid spacing Δx. Dependence of solutions on initial condition is important for employing a time-dependent approach to the steady-state with a given initial condition and boundary conditions in hypersonic or combustion flows, especially when initial data of the governing PDE are not known.

(2) Associated with the same (common) steady-state solution the basin of attraction of the DEs might be vastly different from the discretized counterparts. This is mainly due to the dependence and sensitivity on initial conditions and boundary conditions for the individual systems. In the absence of the influence of the initial and boundary conditions, the difference in the basins of attraction between the continuum and its discretized counterparts occurs even when an implicit LMM type of method is used unless the resulting nonlinear algebraic equations are solved exactly.

(3) Nonunique steady-state solutions can be introduced by the spatial discretization even though the original PDEs might possess only an unique steady-state solution and a LMM type of time discretization is used so that no spurious steady-state exists in time. The tie between temporal and spatial dynamical behavior is more severe when one is dealing with the nonseparable temporal and spatial finite-difference discretization such as the Lax-Wendroff type, where the time and spatial difference cannot be separated from each other. The situation would be more complicated if the governing nonlinear PDE possesses more than one steady-state solution as well as the spurious ones that are purely due to the numerical method.

(4) For certain time discretizations, spurious steady-state solutions may occur below the linearized stability limit of the scheme.

(5) The result of operating with a time step beyond the linearized stability limit is not always a divergent solution; spurious steady-state solutions can occur.

(6) There is a misconception that computational instability or inaccuracy can often be cured simply by making Δt smaller. Other elements such as (1) - (5) above as well as the variation of the grid spacings, numerical dissipation terms and system parameters other than the time steps can interfere with the dynamical behavior.

(7) When linearized stability limits are used as a guide for a time step constraint for highly coupled nonlinear system problems, this time step might exceed the actual linearized stability limit of the coupled equations. Therefore all of the situations in (1) - (6) can occur. In particular, when one tries to stretch the maximum limit of the linearized allowable time step for highly coupled systems, most likely all of the different type of spurious branches of supercritical, subcritical and trancritical bifurcations can be achieved in practice depending on the initial conditions. That is why the occurrence of spurious steady-state solutions beyond the linearized stability limit is not just secondary but might be as important as the occurrence of spurious steady states below the linearized stability limit.

5.2. Recommendations

It is of utmost importance to know the nonlinear dynamical behavior of the various schemes before their actual use for practical applications. Otherwise, it might be very difficult to asses the accuracy (spurious or otherwise) of the solution when the numerical method is the sole source of the understanding of the physical solutions. When in doubt, it is always safer to use schemes that do not produce spurious steady-state solutions for the nonlinear scalar case. Some examples of methods of this type in time discretization can be listed:

(1) LMM [56] ODE solvers such as the explicit, implicit Euler, three-point backward differentation, etc. can be used.

(2) One can use the "Regular" Runge-Kutta methods [57].

(3) Solving the nonlinear algebraic systems arising from implicit LMM method exactly would avoid spurious steady state numerical solutions. Otherwise, the type of iteration method in solving nonlinear algebraic systems can degrade the basin of attractivity of implicit LMM [57].

The insight gained from time discretization will only give an indication in separable schemes or method of lines approaches. Also, the commonly used residual test [86-88] in the time-dependent approach to the steady state might be misleading. This is the direct consequence of what was indicated in section 5.1. The popular misconception of using the inverse problem of nonlinear dynamics to analyze a time series data from a finite difference method computer code in an attempt to learn about the true physical solution behavior of the continuum governing PDEs without knowing by other means the exact solution behavior of the PDEs other than the numerical solutions can also be misleading. These will be discussed in the next two sections.

5.3. Residual Test

Consider a quasilinear PDE of the form

$$\frac{\partial u}{\partial t} = G(u, u_x, u_{xx}, \alpha, \epsilon), \tag{5.1}$$

where G is nonlinear in u, u_x and u_{xx} and α and ϵ are system parameters. For simplicity, consider a two time level and a $(p+q)$ point grid stencil of the form

$$u_j^{n+1} = u_j^n - H(u_{j+q}^n, ..., u_j^n, ..., u_{j-p}^n, \alpha, \epsilon, \Delta t, \Delta x) \tag{5.2}$$

for the PDE (5.1). Let U^*, a vector representing $(u_{j+q}^*, ..., u_j^*, ..., u_{j-p}^*)$ be a steady-state numerical solution of (5.2). It is a common practice in CFD to use a time dependent approach such as (5.2) to solve the steady-state equation $G(u, u_x, u_{xx}, \alpha, \epsilon) = 0$. The iteration is stopped when the residual H or some L_2 norm of the dependent variable u between two successive iterates is less than a pre-selected level.

Aside from the various standard numerical error such as truncation error, machine round-off error, etc. [89], there is a more fundamental question on the validity of the residual test and/or L_2 norm test. If the scheme happens to produce spurious steady-state numerical solutions, these spurious solutions would still satisfy the residual and L_2 norm tests in a deceptively smooth manner. Moreover, aside from the spurious solutions issue, depending on the combination of time as well as spatial discretizations, it is not easy to check whether $G(u^*, u_x^*, u_{xx}^*, \alpha, \epsilon) \to 0$ even though $H(U^*, \alpha, \epsilon, \Delta t, \Delta x) \to 0$. This is contrary to the ODE case, where if u^* is spurious in (1.1) then $S(u^*) \neq 0$. Among other factors, this is one of the contributing factors in the increase in magnitude of difficulty for analyzing the dynamical behavior of numerical methods for hyperbolic and parabolic PDEs.

One might argue that one can judge the accuracy of the scheme by comparing the numerical solutions with more than one numerical methods and by doing a sequence of grid refinement and time step reductions. The latter approach might not be feasible at an acceptable cost. The former might not be foolproof if one does not know the dynamical behavior of the finite difference schemes being used. One important contributing factor on the use of the Lax-Wendroff types of schemes [90,91] is that these schemes are more accurate and sometimes more stable when operated on or near the linearized stability limit.

5.4. The Inverse Problems of Nonlinear Dynamics

The use of the inverse problem of nonlinear dynamics to analyze the dynamical behavior of time series data arising from experimental or observable data has received much attention in nonlinear physics as well as in many of the engineering disciplines. The approach is very useful for gaining some insights into the nonlinear dynamical behavior

in problems where experimental or observable data are the main source of information. Often the associated governing equations (continuum or otherwise) do not exist to start with. There has been an explosion of theory, numerical procedures and computer software addressing this rapidly growing direction [92-95]. There also has been much recent interest in forecasting algorithms that attempt to analyze a time series by fitting nonlinear models. The attractive feature of this approach is that when used correctly on the correct problems one can reduce the complexity of the problem from un-manageable higher dimensions to a very low dimension. It is therefore a natural tendency for practioners in computational sciences to apply this approach to analyze the dynamical behavior of time series data from a finite difference method computer code in an attempt to learn about the true physical solution behavior of the governing PDEs. This application of time series analysis can be misleading and can lead to a wrong conclusion if the practitioner does not know by other means the exact solution behavior of the PDEs other than from the numerical solutions. Examples of the use of this type of approach in CFD computations have been presented in references [96-98]. It can be seen from our study that the conclusions drawn from this type of time series analysis provide very little information, but rather can actually mislead one as to the true physics of the problem.

VI. CONCLUDING REMARKS

Spurious stable as well as unstable steady-state numerical solutions, spurious asymptotic numerical solutions of higher period, and even stable chaotic behavior can occur when finite-difference methods are used to solve nonlinear DEs numerically. The occurrence of spurious asymptotes is independent of whether the DE posseses a unique steady state or has additional periodic solutions and/or exhibits chaotic phenomena. The form of the nonlinear DEs and the type of numerical schemes are the determining factor. In addition, the occurrence of spurious steady states is not restricted to the time steps that are beyond the linearized stability limit of the scheme. In many instances, it can occur below the linearized stability limit. Therefore, it is essential for practitioners in computational sciences to be knowledgeable about the dynamical behavior of finite-difference methods for nonlinear scalar DEs before the actual application of these methods to practical computations. It is also important to change the traditional way of thinking and practices when dealing with genuinely nonlinear problems.

In the past, spurious asymptotes were observed in numerical computations but tended to be ignored because they all were assumed to lie beyond the linearized stability limits of the time step parameter Δt. As can be seen from our study, bifurcations to and from spurious asymptotic solutions and transitions to computational instability not only are highly scheme dependent and problem dependent, but also initial data and boundary condition dependent, and not limited to time steps that are beyond the linearized stability limit.

The symbiotic relation among all of these various factors makes this topic fascinating

and yet extremely complex. The main fundamental conclusion is that, in the absence of truncation and machine round-off errors, there are qualitative features of the nonlinear DE which cannot be adequately represented by the finite-difference methods and vice versa. The major feature is that convergence in practical calculations involved fixed Δt as $n \rightarrow \infty$ rather than $\Delta t \rightarrow 0$ as $n \rightarrow \infty$. It should be emphasized that the resulting discrete maps from finite discretizations can exhibit a much richer range of dynamical behavior than their continuum counterparts. A typical feature is the existence of spurious numerical asymptotes that can interfere with stability, accuracy and basins of attraction of the true physics of the continuum.

References

[1] NASA Computational Fluid Dynamics Conference, NASA Conference Publication 10038, Vol. 1 and 2, March 7-9, 1989.

[2] R.L. Devaney, *An Introduction to Chaotic Dynamical Systems*, Addison Wesley, New York, 1987.

[3] R. Seydel, *From Equilibrium to Chaos*, Elsevier, New York, 1988.

[4] J. Guchenheimer and P. Holmes, *Nonlinear Oscillations, Dynamical Systems, and Bifurcations of Vector Fields*, Springer-Verlag, New York, 1983.

[5] J.M.T. Thompson and H.B. Stewart, *Nonlinear Dynamics and Chaos*, John Wiley, New York, 1986.

[6] C.S. Hsu, *Cell-to-Cell Mapping*, Springer-Verlag, New York, 1987.

[7] M. Kubícek and M. Marek, *Computational Methods in Bifurcation Theory and Dissipative Structures*, Springer-Verlag, New York, 1983.

[8] T.S. Parker and L.O. Chua, *Practical Numerical Algorithms for Chaotic Systems*, Springer-Verlag, New York, 1989.

[9] E. A. Jackson, *Perspectives of Nonlinear Dynamics*, Cambridge, Cambridge, 1989.

[10] E. Beltrami, *Mathematics for Dynamic Modeling*, Academic Press, Orlando, 1987.

[11] R.M. May, "Biological Populations Obeying Difference Equations: Stable Points, Periodic Orbits and Chaos," J. Theoret. Biol., Vol. 51, 1975, pp. 511-524.

[12] H.C. Yee, "A Study of Two-Dimensional Nonlinear Difference Systems and Their Applications," Ph.D. Dissertation, University of Calif, Berkeley, Calif., USA, 1975.

[13] C.S. Hsu, "On Nonlinear Parameteric Excitation Problems," *Advances in Applied Mechanics*, Vol. 17, 1977, pp. 245-301, Academic Press, New York.

[14] H.C. Yee, "A Class of High-Resolution Explicit and Implicit Shock-Capturing Methods," NASA TM-101088, Feb. 1989.

[15] P.K. Sweby, " "TVD" Schemes for Inhomogeneous Conservation Laws," Proc. Nonlinear Hyperbolic Equations, Eds. J. Ballmann & R. Jeltsch, Notes on Numerical Fluid Machanics, 24, 1989, pp. 599-607.

[16] P.K. Sweby, "Source Terms and Conservation Laws: A Preliminary Discussion," Numerical Analysis Report 6/89, Department of Mathematics, University of Reading, England.

[17] B. Engquist and B. Sjögreen, "Numerical Approximation of Hyperbolic Conservation Laws with Stiff Terms," CAM Report 89-07, Department of Mathematics,

UCLA, Calif. USA, March 1989.

[18] K.W. Wallace, "Spurious Period Doubling Bifurcations in a Discretized Reaction-Advection Model," M.S. Thesis, Faculty of Science, University of Dundee, Scotland, Sept. 1989.

[19] G. Strang, "On the Construction and Comparison of Difference Schemes," SIAM J. Num. Anal. Vol. 5, 1968, pp. 506-517.

[20] R.D. Richtmyer and K.W. Morton, *Difference Methods for Initial-Value Problems*, Interscience-Wiley, New York, 1967.

[21] P.K. Sweby, H.C. Yee and D.F. Griffiths, "On Spurious Steady-State Solutions of Explicit Runge-Kutta Schemes," NASA TM, March 1990.

[22] A.M. Panov, "Behavior of the Trajectories of a System of Finite Difference Equations in the Neighbourhood of a Singular Point," Uch. Zap. Ural. Gos. Univ. vyp, Vol. 19, 1956, pp. 89-99.

[23] O. Perron, "Uber Stabilität und Asymtotisches Überhalten de Lösungen eines Systems endlicher Differenzengleichungen," J. Reine Angew. Math. Vol. 161, 1929, pp. 41-64.

[24] C.S. Hsu, H.C. Yee and W.H. Cheng, "Determination of Global Regions of Asymptotic Stability for Difference Dynamical Systems," J. Appl. Mech., Vol. 44, pp., 1977, pp. 147-153.

[25] C.S. Hsu, H.C. Yee and W.H. Cheng, "Steady-State Response of a Nonlinear System Under Impulsive Periodic Parametric Excitation," J. Sound Vib., Vol. 50, 1977, pp. 95-116.

[26] R.M. May, "Simple Mathematical Models with Very Complicated Dynamics," Nature, Vol. 261, 1976, pp. 459-467.

[27] R.M. May, "Biological Populations with Nonoverlaping Generations: Stable Points, Stable Cycles, and Chaos," Science, Vol. 186, No. 15, 1974, pp. 645-647.

[28] T.Y. Li and J.A. Yorke, "Period Three Implies Chaos," Am. Math. Monthly, Vol. 82, 1975, pp. 985-992.

[29] E.N. Lorenz, "The Problem of Deducing the Climate from the Governing Equations," Tellus, Vol. 16, 1964, pp. 1-11.

[30] M.J. Feigenbaum, "Quantitative Universality for a Class of Nonlinear Transformations," J. Stat. Phys., Vol. 19, 1978, pp. 25-52.

[31] C.S. Hsu and H.C. Yee, "Behavior of Dynamical Systems Governed by a Simple Nonlinear Difference Equation," J. Appl. Mech., Vol. 44, 1975, pp. 870-876.

[32] S. Ushiki, "Central Difference Scheme and Chaos," Physica 4D, 1982, pp. 407-424.

[33] F. Brezzi, S. Ushike and H. Fujii, "Real and Ghost Bifurcation Dynamics in Dif-

ference Schemes for Ordinary Differential Equations," *Numerical Methods for Bifurcation Problems*, T. Kupper, H.D. Mittleman and H. Weber eds., Birkhauser-Verlag, Boston, 1984.

[34] R. Schreiber and H.B. Keller, "Spurious Solution in Driven Cavity Calculations," J. Comput. Phys., Vol. 49, No. 1, 1983.

[35] W.J. Beyn and E.J. Doedel, "Stability and Multiplicity of Solutions to Discretizations of Nonlinear Ordinary Differential Equations," SIAM J. Sci. Statist. Comput., Vol. 2, 1981, pp. 107-120.

[36] R.B. Kellogg, G.R. Shubin, and A.B. Stephens, SIAM J. Numer. Anal. Vol. 17, No. 6, 1980, pp. 733-739.

[37] A.B. Stephens and G.R. Shubin, SIAM J. Sci. Statist Comput., Vol. 2, 1981, pp. 404-415.

[38] G.R. Shubin, A.B. Stephens and H.M. Glaz, "Steady Shock Tracking and Newton's Method Applied to One-Dimensional Duct Flow," J. Comput. Phys., Vol. 39, 1981, pp. 364-374.

[39] P.G. Reinhall, T.K. Caughey and D.W. Storti, "Order and Chaos in a Discrete Duffing Oscillator: Implications on Numerical Integration," Trans. of the ASME, J. Appl. Mech., 89-APM-6, 1989.

[40] E.N. Lorenz, "Computational Chaos – A Prelude to Computational Instability," Physica D, Vol. 35, 1989, pp. 299-317.

[41] A.J. Lichtenberg and M.A. Lieberman, *Regular and Stochastic Motion*, Appl. Math. Sci. Bd. 38, 1983, Springer-Verlag, New York.

[42] R.H. Miller, "A Horror Story about Integration Methods," to appear.

[43] W.A. Mulder and B. van Leer, "Implicit Upwind Methods for the Euler Equations," AIAA-83-1930, July 1983.

[44] M. Prüffer, "Turbulence in Multistep Methods for Initial Value Problems," SIAM J. Appl. Math. Vol. 45, 1985, pp. 32-69.

[45] W.-J. Beyn, "On the Numerical Approximation of Phase Portraits Near Stationary Points," SIAM J. Numer. Anal., Vol. 24, No. 5, 1987, pp. 1095-1113.

[46] A.R. Mitchell and D.F. Griffiths, "Beyond the Linearized Stability Limit in Non Linear Problems," Report NA/88 July 1985, Department of Mathematical Sciences, University of Dundee, Scotland U.K.

[47] A.R. Mitchell and J.C. Bruch, Jr., "A Numerical Study of Chaos in a Reaction-Diffusion Equation," Numerical Methods for PDEs, Vol. 1, 1985, pp. 13-23.

[48] A.R. Mitchell, P. John-Charles and B.D. Sleeman, "Long Time Calculations and Non Linear Maps," Numerical Analysis Report 93, May 1986, Department of Mathematical Sciences, University of Dundee, Scotland.

[49] V.S. Manoranjan, A.R. Mitchell, and B.D. Sleeman, "Bifurcation Studies in Reaction-Diffusion," J. Comput. App. Math., Vol. 11, 1984, pp. 27-37.

[50] B.D. Sleeman, D.F. Griffiths, A.R. Mitchell and P.D. Smith, "Stable Periodic Solutions in Nonlinear Difference Equations," SIAM J. Sci. Stat. Comput., Vol. 9, No. 3, May 1988, pp. 543-557.

[51] D.F. Griffiths and A.R. Mitchell, "Stable Periodic Solutions of a Nonlinear Partial Difference Equation in Reaction Diffusion," Report NA/113, Jan. 1988, Dept. Math. and Compt. Science, University of Dundee, Scotland.

[52] A.R. Mitchell, G. Stein and M. Maritz, "Periodic Structure Beyond a Hopf Bifurcation," Comm. Appl. Num. Meth., Vol. 4, 1988, pp. 263-272.

[53] D.F. Griffiths and A.R. Mitchell, "Stable Periodic Bifurcations of an Explicit Discretization of a Nonlinear Partial Differential Equation in Reaction diffusion," Inst. Math. Applics., J. Num. Analy., Vol. 8, 1988, pp. 435-454.

[54] A.R. Mitchell and S.W. Schoombie, "Nonlinear Diffusion and Stable Period 2 Solutions of a Discrete Reaction-Diffusion Model," J. Comp. Appl. Math., Vol 25, 1989, pp. 363-372.

[55] J.M. Sanz-Serna and F. Vadillo, "Nonlinear Instability, the Dynamic Approach," in Proceedings Dundee, 1985, G.A. Watson and D.F. Griffiths, eds., Pitman, London.

[56] A. Iserles, "Nonlinear Stability and Asymptotics of O.D.E. Solvers," International Conference on Numerical Mathematics, Singapore, R.P. Agarwal, ed., Birkhauser, Basel, 1989.

[57] A. Iserles and J.M. Sanz-Serna, "Equilibria of Runge-Kutta Methods," Numerical Analysis Reports, DAMTP 1989/NA4, May 1989, Univeristy of Cambridge, England.

[58] A.M. Stuart, "Linear Instability Implies Spurious Periodic Solutions," submitted to IMA J. Num. Anal., 1988.

[59] A. Stuart, "The Global Attractor Under Discretisation," to appear, Proc. NATO Conference on Continuation & Bifurcation, 1989.

[60] A. Stuart and A. Peplow, "The Dynamics of the Theta Method," to appear, SIAM J. Sci. Stat. Comput.

[61] A. Stuart, " Nonlinear Instability in Dissipative Finite Difference Schemes," SIAM Review, Vol. 31, No. 2, 1989, pp. 191-220.

[62] A. Stuart, "Linear Instability Implied Spurious Periodic Solutions," to appear, IMA J. Numer. Anal.

[63] C. Grebogi E. Ott and J. Yorke, "Chaos, Strange Attractors, and Fractal Basin Boundaries in Nonlinear Dynamics," Science, Vol. 238, 1987, pp. 585-718.

[64] S.W. McDonald, C. Grebogi E. Ott and J. Yorke, "Fractal Basin Boundaries,"

Physica 17D, 1985, pp. 125-153.

[65] C. Grebogi E. Ott and J. Yorke, "Crises, Sudden Changes in Chaotic Attractors, and Transient Chaos," Physics 7D, 1983, pp. 181-200.

[66] J.D. Lambert, *Computational Methods in Ordinary Differential Equations*, John Wiley, New York, 1973.

[67] C.W. Gear, *Numerical Initial Value Problems in Ordinary Differential Equations* (Prentice-Hall, 1971).

[68] J.C. Butcher, *The Numerical Analysis of Ordinary Differential Equations*, John Wiley, New York, 1987.

[69] MAPLE, algebraic manipulation package, University of Waterloo, Canada, 1988

[70] D. Whitley, "Discrete Dynamical Systems in Dimensions One and Two," Bull. London Math Soc. Vol. 15, 1983, pp. 177-217.

[71] R.M. Beam and R.F. Warming, "Implicit Numerical Methods for the Compressible Navier-Stokes and Euler Equations," Lecture Notes for Computational Fluid Dynamics, von Karman Institute for Fluid Dynamics, March 29 - April 2, 1982, Rohde-Saint-Genèse, Belgium.

[72] J. Maynard Smith, *Mathematical Ideas in Biology*, Cambridge University Press, Cambridge, 1968.

[73] H. Ikeda, M. Mimura and Y. Nishiura, "Global Bifurcation Phenomena of Travelling Wave Solutions for Some Bistable Reaction-Diffusion Systems," Nonlinear Analysis, Theory, Methods and Applications, Vol. 13, No. 5, 1989, pp. 507-526.

[74] T. Hagstrom and H.B. Keller, "The Numerical Calculation of travelling Wave Solutions of Nonlinear Parabolic Equations," SIAM J. Sci. Stat. Comput., Vol. 7, No. 3, 1986.

[75] A. Harten and S. Osher, "Uniformly High-Order Accurate Nonoscillatory Schemes I," SIAM J. Num. Analy. Vol. 24, No. 2, 1987, pp. 279-309.

[76] A. Harten, "On a Class of High Resolution Total-Variation-Stable Finite-Difference Schemes," SIAM J. Num. Anal., Vol. 21, 1984, pp. 1-23.

[77] P.L. Roe, "Some Contributions to the Modelling of Discontinuous Flows," Lectures in Applied Mathematics, Vol. 22 (Amer. Math. Soc., Providence, R.I., 1985).

[78] R.J. LeVeque and H.C. Yee, "A study of Numerical Methods for Hyperbolic Conservation Laws with Stiff Source Terms," NASA TM-100075, March 1988, J. Comput. Phys., Vol. 86, No. 1, Jan. 1990.

[79] M. Pandolfi, M. Germano and N. Botta, "Non-Equilibrium Reacting Hypersonic Flow About Blunt Bodies: Numerical Prediction, AIAA-88-0514, Jan. 1988.

[80] P. Colella, A. Majda, and V. Roytburd, "Theoretical and Numerical Structure for Reacting Shock Waves," SIAM J. Sci. Stat. Comput. Vol. 7, 1986, pp.

1059-1080.

[81] T.R. Young and J.P. Boris, "A Numerical Technique for Solving Stiff Ordinary Differential Equations Associated with the Chemical Kinetics of Reactive-Flow Problems," J. Phys. Chem. Vol. 81, 1977, pp. 2424-2427.

[82] H.C. Yee, "Numerical Approximation of Boundary Conditions with Applications to Inviscid Equations of Gas Dynamics," NASA TM-81265, 1981.

[83] H.C. Yee, R.M. Beam and R.F. Warming, "Boundary Approximations for Implicit Schemes for One-Dimensional Inviscid Equations of Gasdynamics," AIAA J., Vol. 20, No. 9, 1982, pp. 1203-1211.

[84] P.D. Lax and B. Wendroff, "Systems of Conservation Laws," Commun. Pure Appl. Math., Vol. 13, 1960, pp. 217-237.

[85] R.J. LeVeque, "Hyperbolic Conservation Laws and Numerical Methods," Lecture Series on Computational Fluid Dynamics, von Karman Institute for Fluid Dynamics, Rhode-St-Genèse, Belgium, March 5-9, 1990.

[86] A. Jameson, W. Schmidt and E. Turkel, "Numerical Solutions of the Euler Equations by Finite Volume Methods Using Runge-Kutta Time-Stepping Schemes," AIAA-81-1259, 1981.

[87] J.D. Anderson, Jr, "Introduction to Computational Fluid Dynamics," von Karman Institute for Fluid Dynamics, 1985 lecture series, Rhode-Saint-Genèse, Belgium.

[88] G.A. Sod, *Numerical Methods in Fluid Dynamics*, Cambridge University Press, Cambridge, 1985.

[89] J.H. Ferziger, "Estimation and Reduction of Numerical Error," Forum on Methods of Estimating Uncertainty Limits in Fluid Flow Computations, ASME Winter Annual Meeting, San Francisco, Dec. 1989.

[90] P.D. Lax and B. Wendroff, "Difference Schemes for Hyperbolic Equations with High Order of Accuracy," Commun. Pure Appl. Math., Vol. 17, 1964, pp. 381-398.

[91] R.W. MacCormack, "The Effect of Viscosity in Hypervelocity Impact Cratering," AIAA-69-354, Cincinnati, Ohio, 1969.

[92] N.H. Packard, J.P. Crutchfield, J.D. Farmer and R.S. Shaw, "Geometry from a Time Series," Physical Review Letters, Vol. 45, No. 9, 1980, pp. 712-716.

[93] J.P. Eckmann and D. Ruelle, "Ergodic Theory of Chaos and Strange Attractors," Rev. Mod. Phys., Vol. 57, No. 3, Part I, 1985, pp. 617-656.

[94] H. Froehling, J.P. Crutchfield, D. Farmer, N.H. Packard and R. Shaw, "On Determing the Dimension of Chaotic Flows," Physica 3D, 1981, pp. 605-617.

[95] E.J. Kostelich and J.A. Yorke, "The Analysis of Experimental Data Using Time-Delay Embedding Methods," Institute for Physical Science and Technology Technical Report, University of Maryland, College Park, Maryland, USA.

[96] T.H. Pulliam, "Low Reynolds Number Numerical Solutions of Chaotic Flows," AIAA-89-1023, Jan. 9-12, 1989.

[97] T.H. Pulliam, "Numerical Simulation of Chaotic Flows: Measures of Chaos," Forum on Chaotic Dynamics in Fluid Dynamics, ASME Fluids Engineering Spring Conference, La Jolla, Calif. July 1989.

[98] A. Fortin, M. Fortin and J.J. Gervais, "A numerical Simulational Flow," J. Comput. Phys., 70, 1987, pp. 295-310.

Figure Captions

Table 2.1 Possible stable asymptotic solution behavior for DEs and their discretized counterparts.

Fig. 2.1 Phase portrait and basins of attraction of the damped pendulum equation (this figure is taken from reference [8]).

Fig. 2.2 Phase portrait and basins of attraction of the predator-prey equation (this figure is taken from reference [8]).

Fig. 3.1 Asymptotic solution behavior of the logistic ODE $du/dt = \alpha u(1-u)$ for $\alpha > 0$.

Fig. 3.2 Stable fixed points of periods 1,2,4,8 of the explicit Euler scheme for the logistic ODE $du/dt = \alpha u(1-u)$.

Fig. 3.3 Stable fixed points of periods 1,2,4,8 of the modified Euler (R-K 2) scheme for the logistic ODE $du/dt = \alpha u(1-u)$.

Fig. 3.4 Stable fixed points of periods 1,2,4,8 of the improved Euler (R-K 2) scheme for the logistic ODE $du/dt = \alpha u(1-u)$.

Fig. 3.5 Stable fixed points of periods 1,2,4,8 of the Runge-Kutta 4th-order (R-K 4) scheme for the logistic ODE $du/dt = \alpha u(1-u)$.

Fig. 3.6 Stable fixed points of periods 1,2,4,8 of the predictor-corrector scheme of order 2 for the logistic ODE $du/dt = \alpha u(1-u)$.

Fig. 3.7 Stable fixed points of periods 1,2,4,8 of the predictor-corrector scheme of order 3 for the logistic ODE $du/dt = \alpha u(1-u)$.

Fig. 3.8 Stable fixed points of periods 1,2,4,8 of the explicit Euler scheme for the ODE $du/dt = \alpha u(1-u)(0.5-u)$.

Fig. 3.9 Stable fixed points of periods 1,2,4,8 of the modified Euler (R-K 2) scheme for the ODE $du/dt = \alpha u(1-u)(0.5-u)$.

Fig. 3.10 Stable fixed points of periods 1,2,4,8 of the improved Euler (R-K 2) scheme for the ODE $du/dt = \alpha u(1-u)(0.5-u)$.

Fig. 3.11 Stable fixed points of periods 1,2,4,8 of the Runge-Kutta 4th-order (R-K 4) scheme for the ODE $du/dt = \alpha u(1-u)(0.5-u)$.

Fig. 3.12 Stable fixed points of periods 1,2,4,8 of the predictor-corrector scheme of order 2 for the ODE $du/dt = \alpha u(1-u)(0.5-u)$.

Fig. 3.13 Stable fixed points of periods 1,2,4,8 of the predictor-corrector scheme of order 3 for the ODE $du/dt = \alpha u(1-u)(0.5-u)$.

Fig. 3.14 Stable fixed points of periods 1,2,4.8 of the modified Euler (R-K 2) scheme for the ODE $du/dt = \alpha u(1-u)(b-u)$, $b = 0.1,\ 0.2,\ 0.3,\ 0.4$.

Fig. 3.15 Bifurcation diagram of the explicit Euler scheme for the logistic ODE $du/dt = \alpha u(1-u)$.

Fig. 3.16 Bifurcation diagram of the modified Euler (R-K 2) scheme for the logistic ODE $du/dt = \alpha u(1-u)$ with $u^0 = 2.7$.

Fig. 3.17 Bifurcation diagram of the modified Euler (R-K 2) scheme for the logistic ODE $du/dt = \alpha u(1-u)$ with $u^0 = 1.5$.

Fig. 3.18 Bifurcation diagram of the modified Euler (R-K 2) scheme for the logistic ODE $du/dt = \alpha u(1-u)$ with $u^0 = 0.25$.

Fig. 3.19 "Full" bifurcation diagram of the modified Euler (R-K 2) scheme for the logistic ODE $du/dt = \alpha u(1-u)$.

Fig. 3.20 Bifurcation diagram of the Runge-Kutta 4th-order (R-K 4) scheme for the logistic ODE $du/dt = \alpha u(1-u)$ with $u^0 = 0.5$.

Fig. 3.21 Bifurcation diagram of the Runge-Kutta 4th-order (R-K 4) scheme for the logistic ODE $du/dt = \alpha u(1-u)$ with multiple initial data.

Fig. 3.22 "Full" bifurcation diagram of the Runge-Kutta 4th-order (R-K 4) scheme for the logistic ODE $du/dt = \alpha u(1-u)$.

Fig. 3.23 Bifurcation diagrams of the improved Euler (R-K 2) scheme for the ODE $du/dt = \alpha u(1-u)(0.5-u)$ for four different sets of initial input data.

Fig. 3.24 Bifurcation diagrams of the Runge-Kutta 4th-order (R-K 4) scheme for the ODE $du/dt = \alpha u(1-u)(0.5-u)$ for four different sets of initial input data.

Fig. 3.25 Bifurcation diagrams of the modified Euler (R-K 2) scheme for the ODE $du/dt = \alpha u(1-u)(0.4-u)$ for four different sets of initial input data.

Fig. 3.26 "Full" bifurcation diagram of the improved Euler (R-K 2) scheme for the logistic ODE $du/dt = \alpha u(1-u)$.

Fig. 3.27 "Full" bifurcation diagram of the Adam-Bashforth scheme for the logistic ODE $du/dt = \alpha u(1-u)$.

Fig. 3.28 "Full" bifurcation diagram of the predictor-corrector scheme of order 2 for the logistic ODE $du/dt = \alpha u(1-u)$.

Fig. 3.29 "Full" bifurcation diagram of the predictor-corrector scheme of order 3 for the logistic ODE $du/dt = \alpha u(1-u)$.

Fig. 3.30 "Full" bifurcation diagrams of the modified Euler (R-K 2) scheme for the ODE $du/dt = \alpha u(1-u)(b-u)$, $b = 0.1,\ 0.2,\ 0.3,\ 0.4$.

Fig. 3.31 "Full" bifurcation diagrams of the explict Euler scheme for the ODE $du/dt = \alpha u(1-u)(0.5-u)$.

Fig. 3.32 "Full" bifurcation diagram of the modified Euler (R-K 2) scheme for the ODE $du/dt = \alpha u(1-u)(0.5-u)$.

Fig. 3.33 "Full" bifurcation diagram of the Adam-Bashforth scheme for the ODE $du/dt = \alpha u(1-u)(0.5-u)$.

Fig. 3.34 "Full" bifurcation diagram of the improved Euler (R-K 2) scheme for the ODE $du/dt = \alpha u(1-u)(0.5-u)$.

Fig. 3.35 "Full" bifurcation diagram of the Runge-Kutta 4th-order (R-K 4) scheme for the ODE $du/dt = \alpha u(1-u)(0.5-u)$.

Fig. 3.36 "Full" bifurcation diagram of the improved Euler (R-K 2) scheme for the ODE $du/dt = \alpha u(1-u)(0.5-u)$ (enlarged).

Fig. 3.37 "Full" bifurcation diagram of the Runge-Kutta 4th-order (R-K 4) scheme for the ODE $du/dt = \alpha u(1-u)(0.5-u)$ (enlarged).

Fig. 3.38 "Full" bifurcation diagram of the predictor-corrector scheme of order 2 for the ODE $du/dt = \alpha u(1-u)(0.5-u)$.

Fig. 3.39 Types of branching points.

Fig. 3.40 Stability of solutions in the neighborhood of branch points, one-dimensional case. — stable, - - - unstable a,b,c,d: limit (regular turning) point; e,f,g,h: bifurcation (double) points; i,j,k,l: bifurcation-limit (singular turning) points; m,n,o,p,q: additional possible cases when the dimension of u is greater than one (this figure is taken from reference [7]).

SOLUTION TYPE	ODEs OR PDEs	DISCRETIZED COUNTERPARTS
# OF ASYMPTOTES OR STEADY-STATE SOLUTIONS	SINGLE	SINGLE
	SINGLE	MULTIPLE
	MULTIPLE	SAME # OF MULTIPLE
	MULTIPLE	ADDITIONAL # OF MULTIPLE
PERIODIC SOLUTIONS	NO	YES
	YES	YES (+ EXTRA)
CHAOS	NO	YES
	YES	YES (+ EXTRA)

Table 2.1 Possible stable asymptotic solution behavior for DEs and their discretized counterparts.

I. **ODE CONNECTION:** GAIN INSIGHT INTO TIME DISCRETIZATION OF PDEs

SCALAR
SYSTEM — TIME SPLITTING OR METHOD OF LINES

II. **DISCRETE TRAVELLING WAVE:** $\frac{\partial u}{\partial t} + C\frac{\partial u}{\partial X} = \varepsilon\frac{\partial^2 u}{\partial X^2} + \alpha S(u)$

SCALAR:
- REACTION-DIFFUSION ✓
- REACTION-CONVECTION
- REACTION-CONVECTION-DIFFUSION

III. **FULL DISCRETIZATION (TEMPORAL AND SPATIAL):**

SCALAR: (S≠0)	✓ ✓ ✓	LINEAR SCHEME FOR SPATIAL DISCRETIZATION
SCALAR: (S=0)		NONLINEAR SCHEME FOR SPATIAL DISCRETIZATION
SCALAR: (S≠0)		NONLINEAR SCHEME FOR SPATIAL DISCRETIZATION

Table 4.1 Systematic approach – level of complexity.

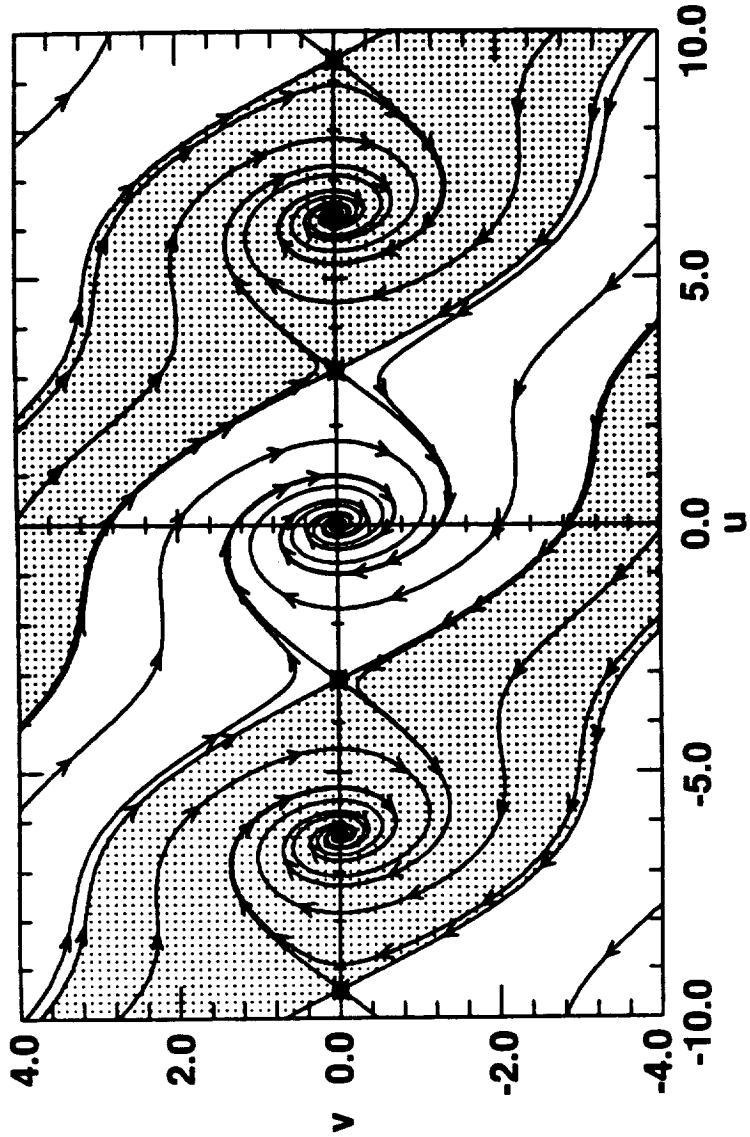

Fig. 2.1 Phase portrait and basins of attraction of the damped pendulum equation (this figure is taken from reference [8]).

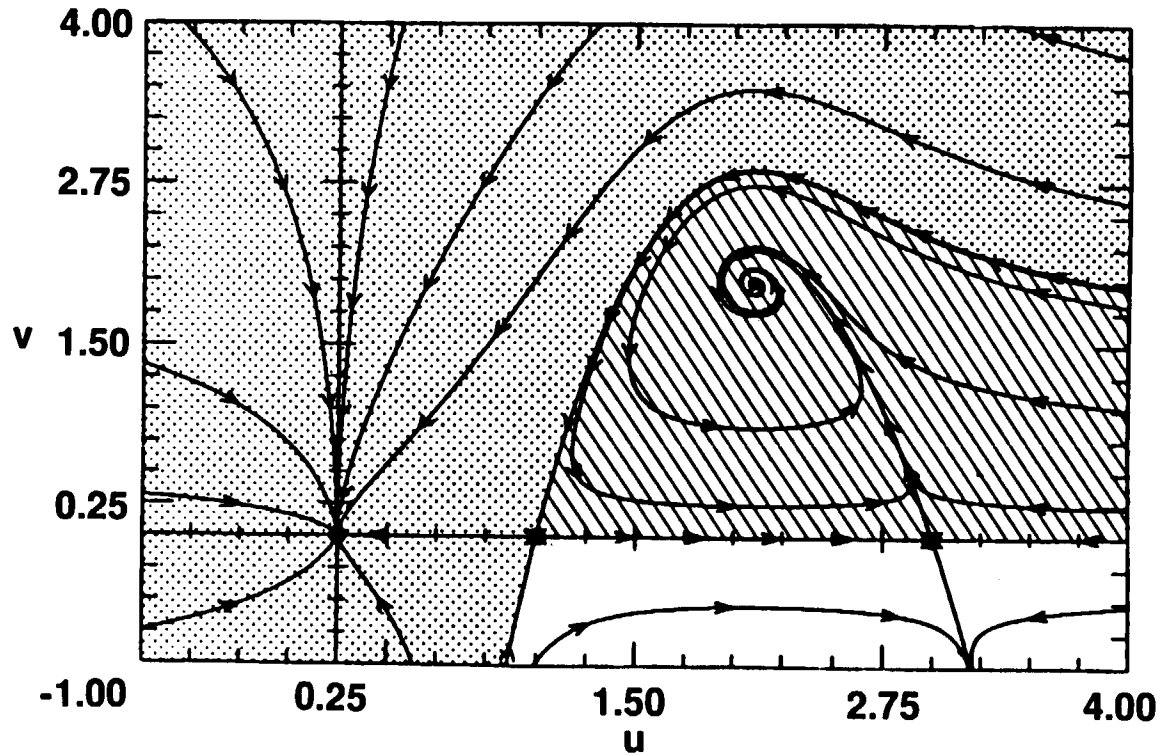

Fig. 2.2 Phase portrait and basins of attraction of the predator-prey equation (this figure is taken from reference [8]).

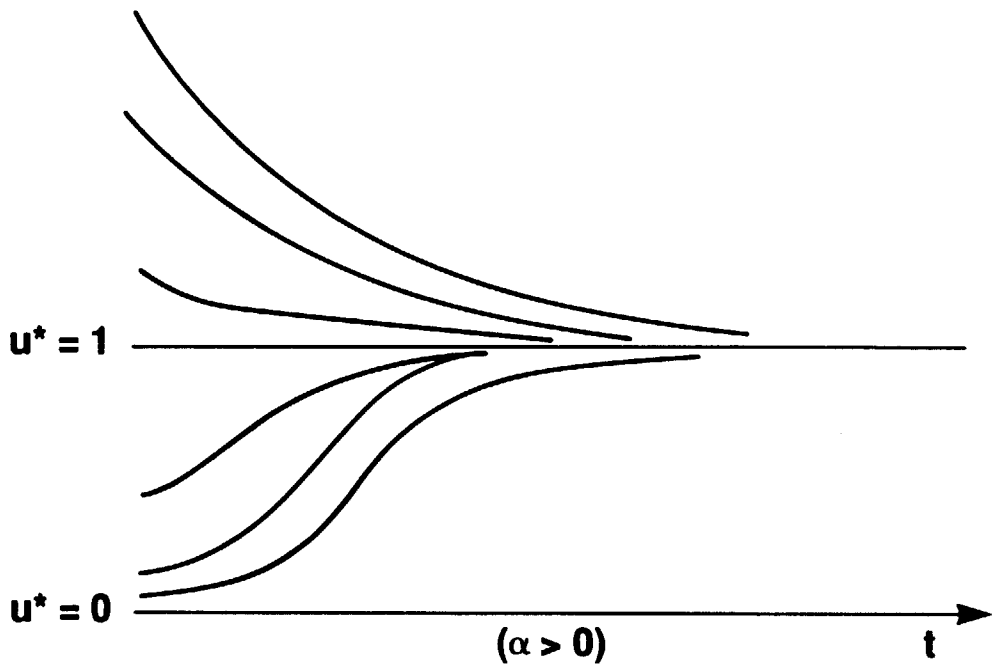

Fig. 3.1 Asymptotic solution behavior of the logistic ODE $du/dt = \alpha u(1-u)$ for $\alpha > 0$.

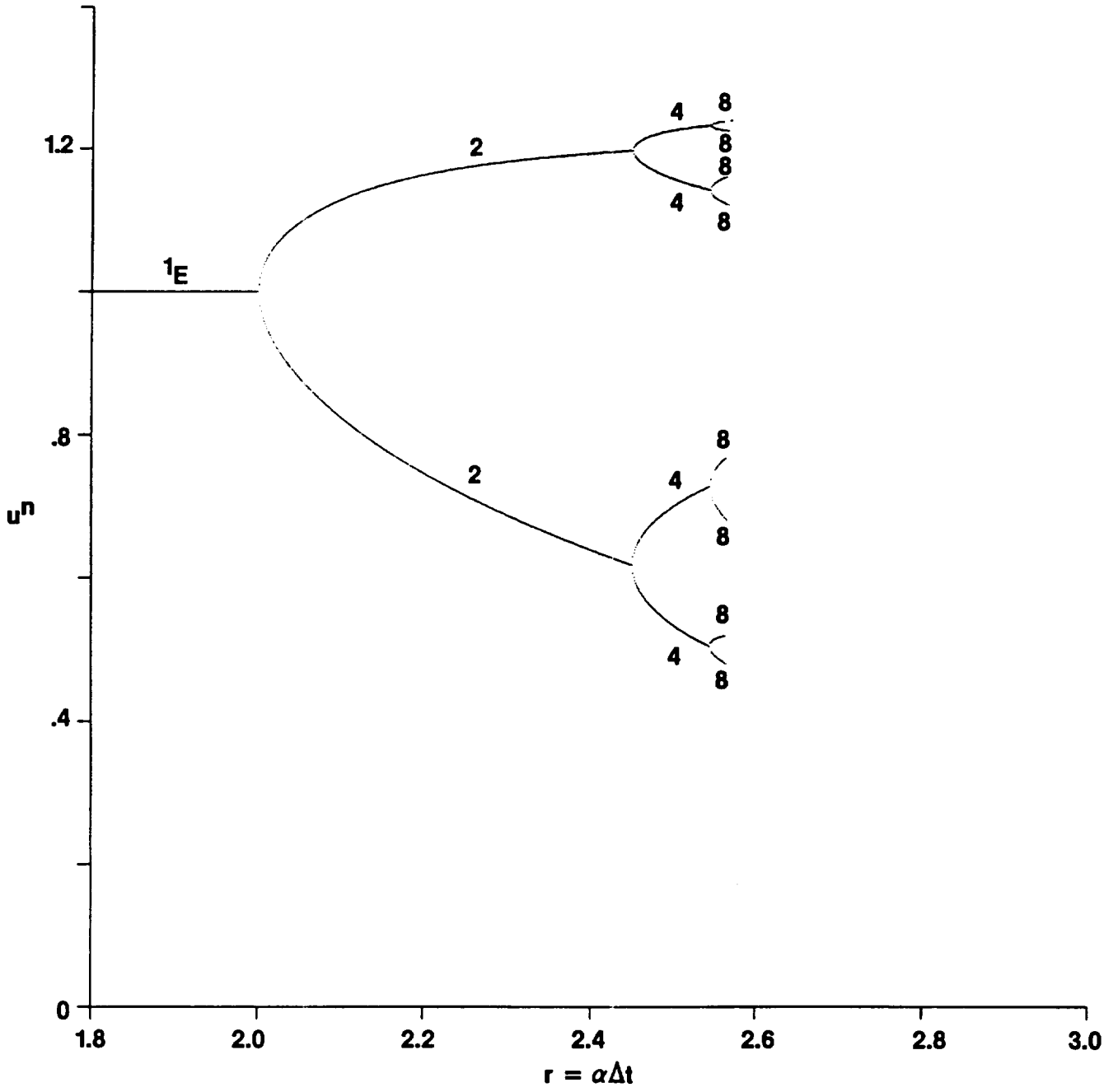

Fig. 3.2 Stable fixed points of periods 1,2,4,8 of the explicit Euler scheme for the logistic ODE $du/dt = \alpha u(1-u)$.

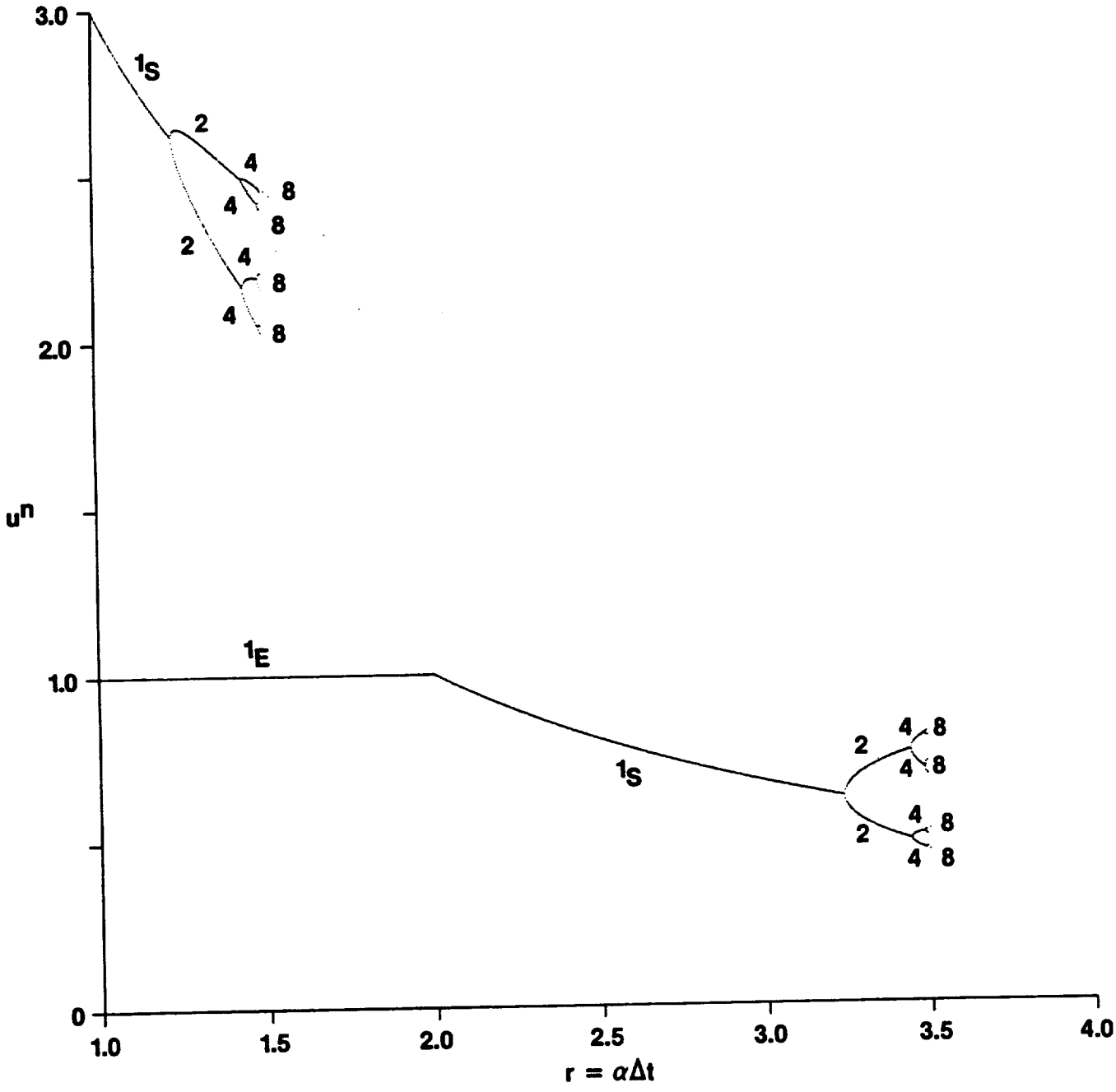

Fig. 3.3 Stable fixed points of periods 1,2,4,8 of the modified Euler (R-K 2) scheme for the logistic ODE $du/dt = \alpha u(1-u)$.

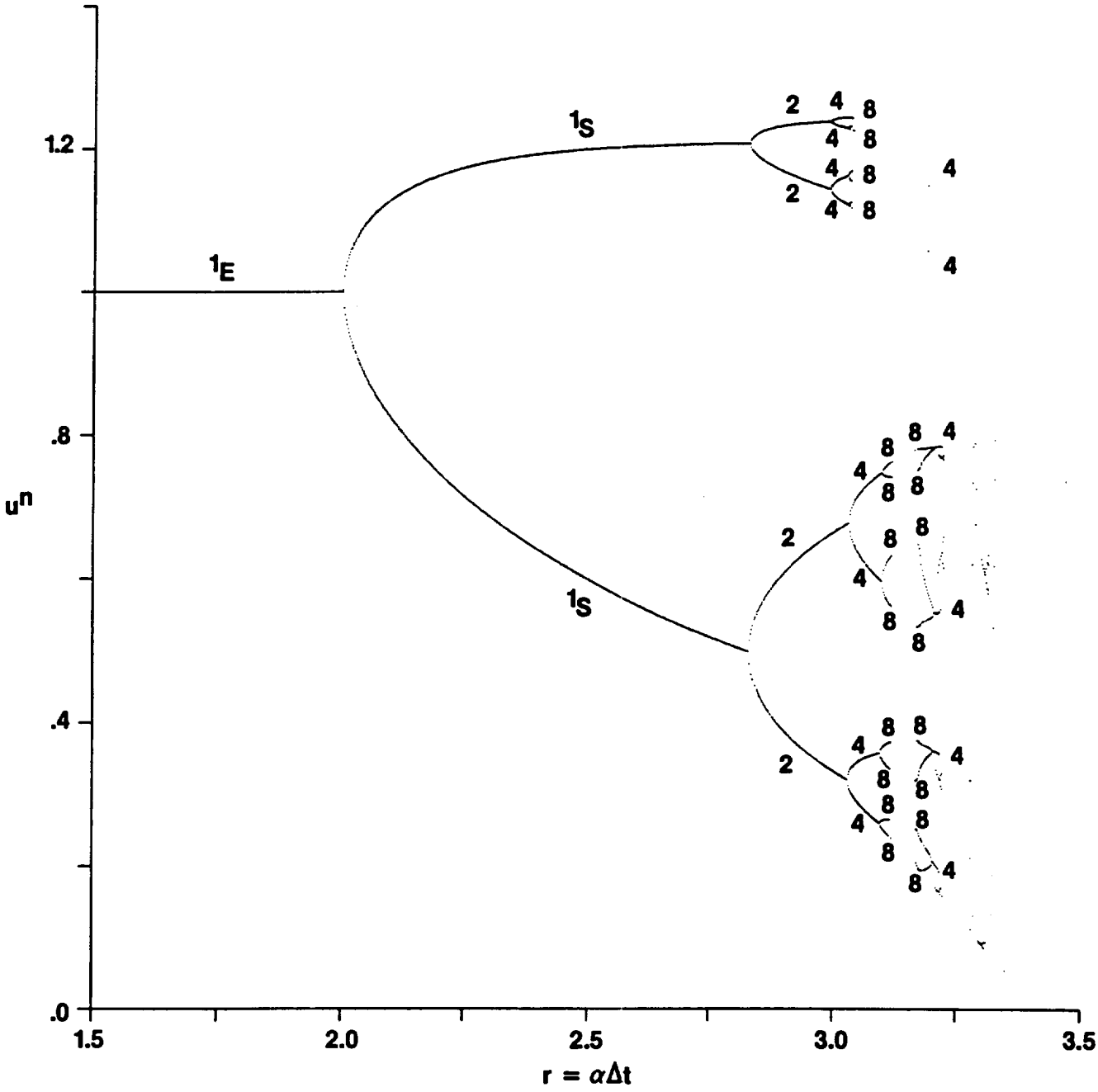

Fig. 3.4 Stable fixed points of periods 1,2,4,8 of the improved Euler (R-K 2) scheme for the logistic ODE $du/dt = \alpha u(1-u)$.

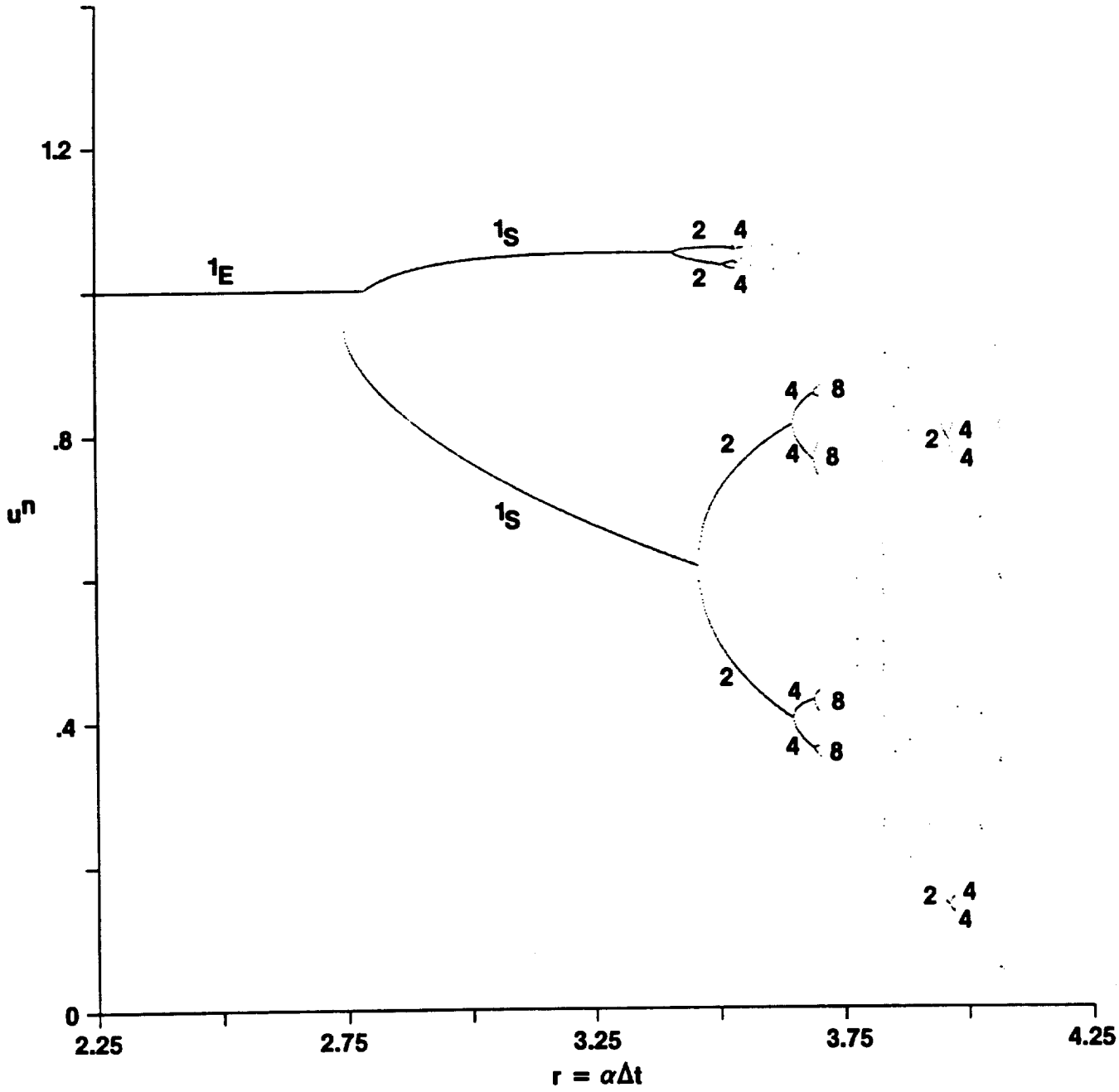

Fig. 3.5 Stable fixed points of periods 1,2,4,8 of the Runge-Kutta 4th-order (R-K 4) scheme for the logistic ODE $du/dt = \alpha u(1-u)$.

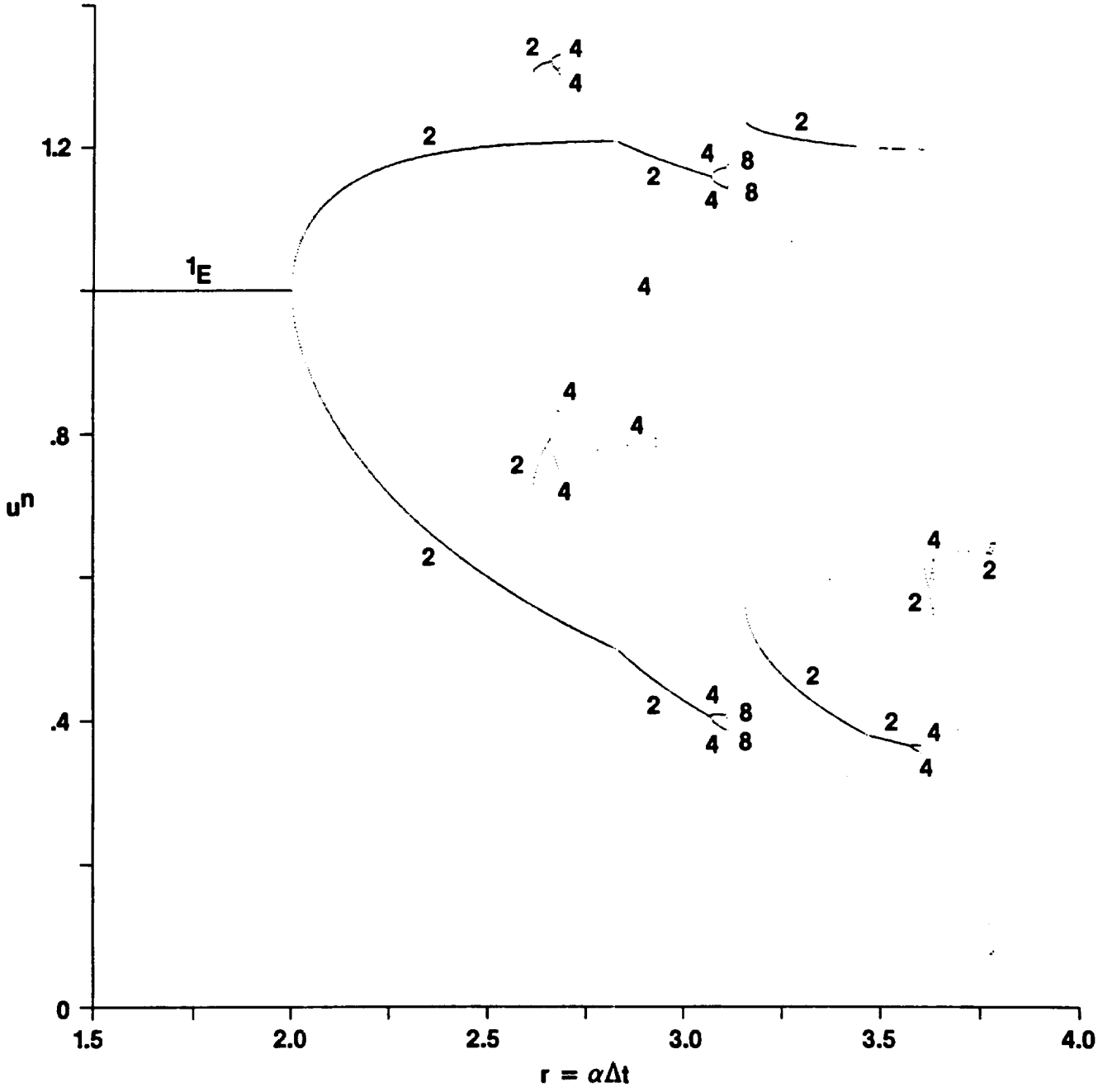

Fig. 3.6 Stable fixed points of periods 1,2,4,8 of the predictor-corrector scheme of order 2 for the logistic ODE $du/dt = \alpha u(1-u)$.

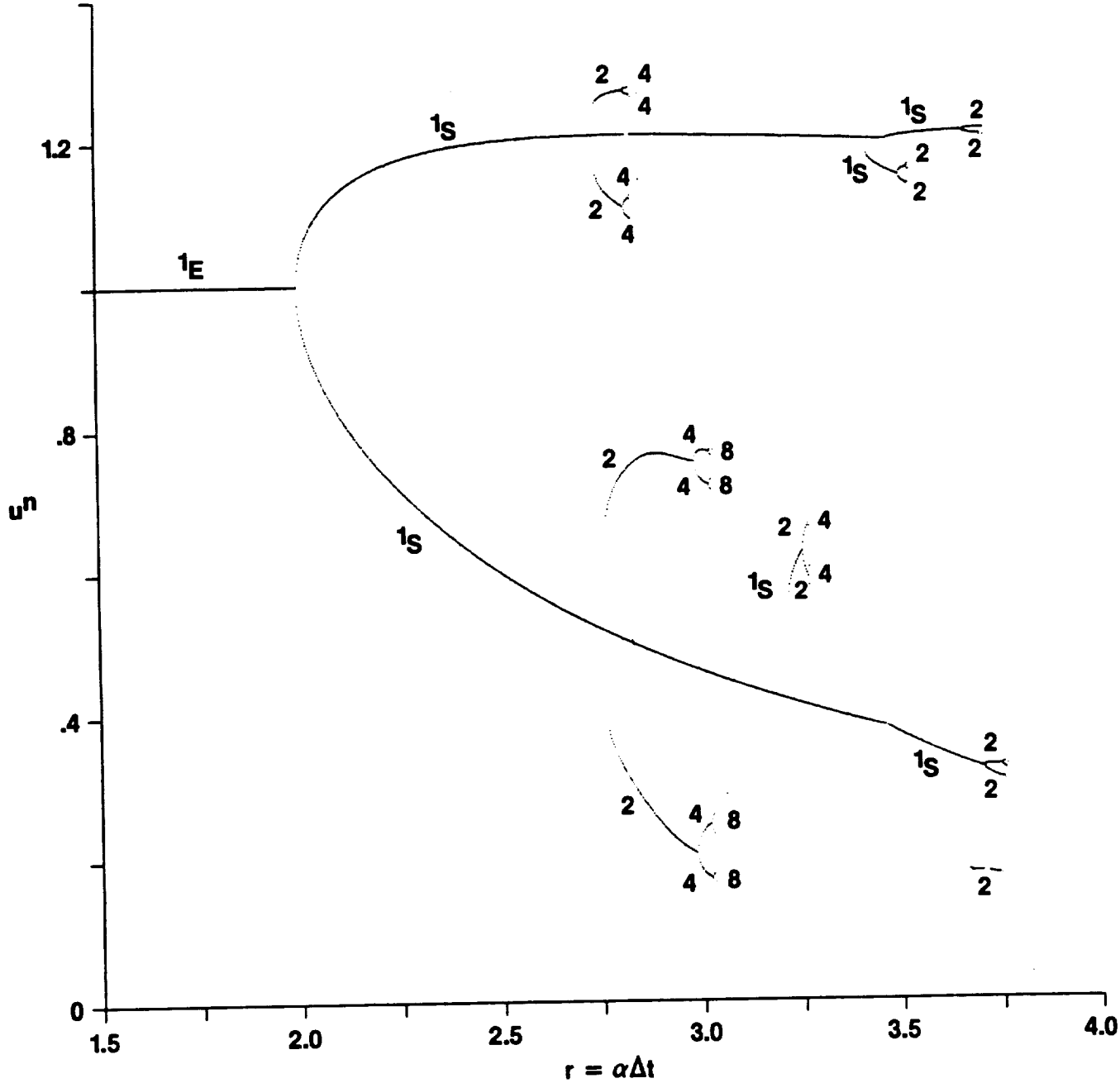

Fig. 3.7 Stable fixed points of periods 1,2,4,8 of the predictor-corrector scheme of order 3 for the logistic ODE $du/dt = \alpha u(1-u)$.

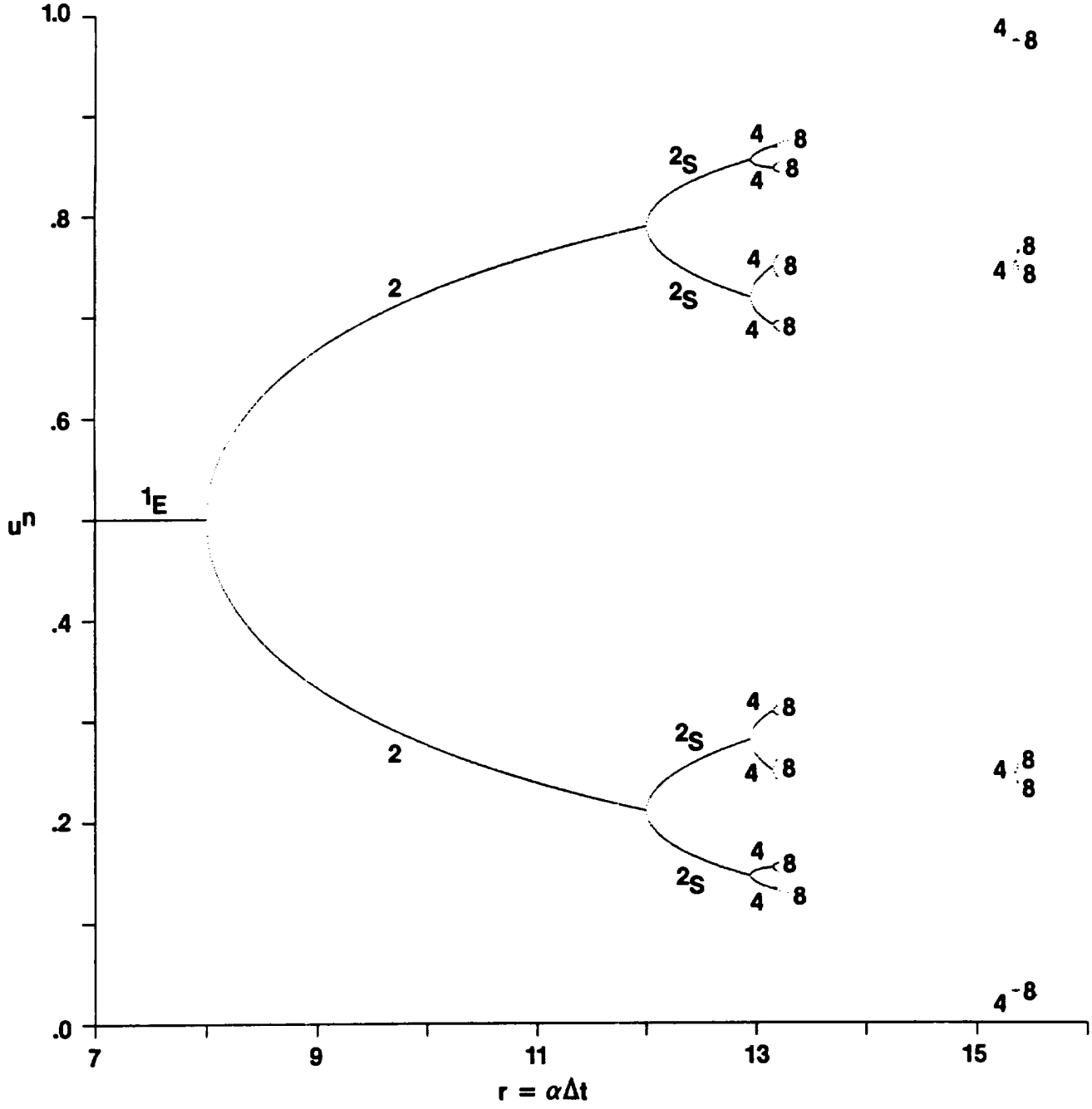

Fig. 3.8 Stable fixed points of periods 1,2,4,8 of the explicit Euler scheme for the ODE $du/dt = \alpha u(1-u)(0.5-u)$.

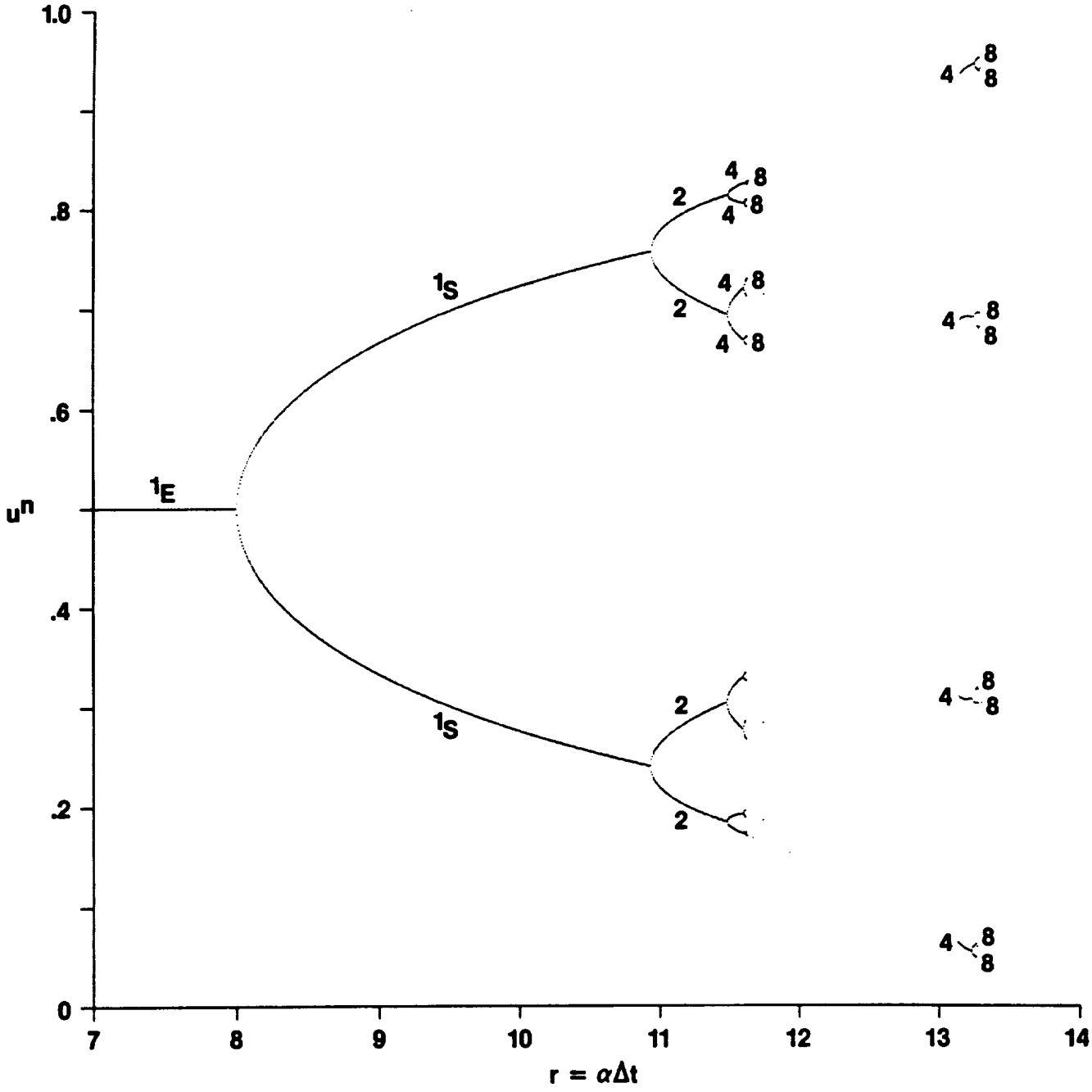

Fig. 3.9 Stable fixed points of periods 1,2,4,8 of the modified Euler (R-K 2) scheme for the ODE $du/dt = \alpha u(1-u)(0.5-u)$.

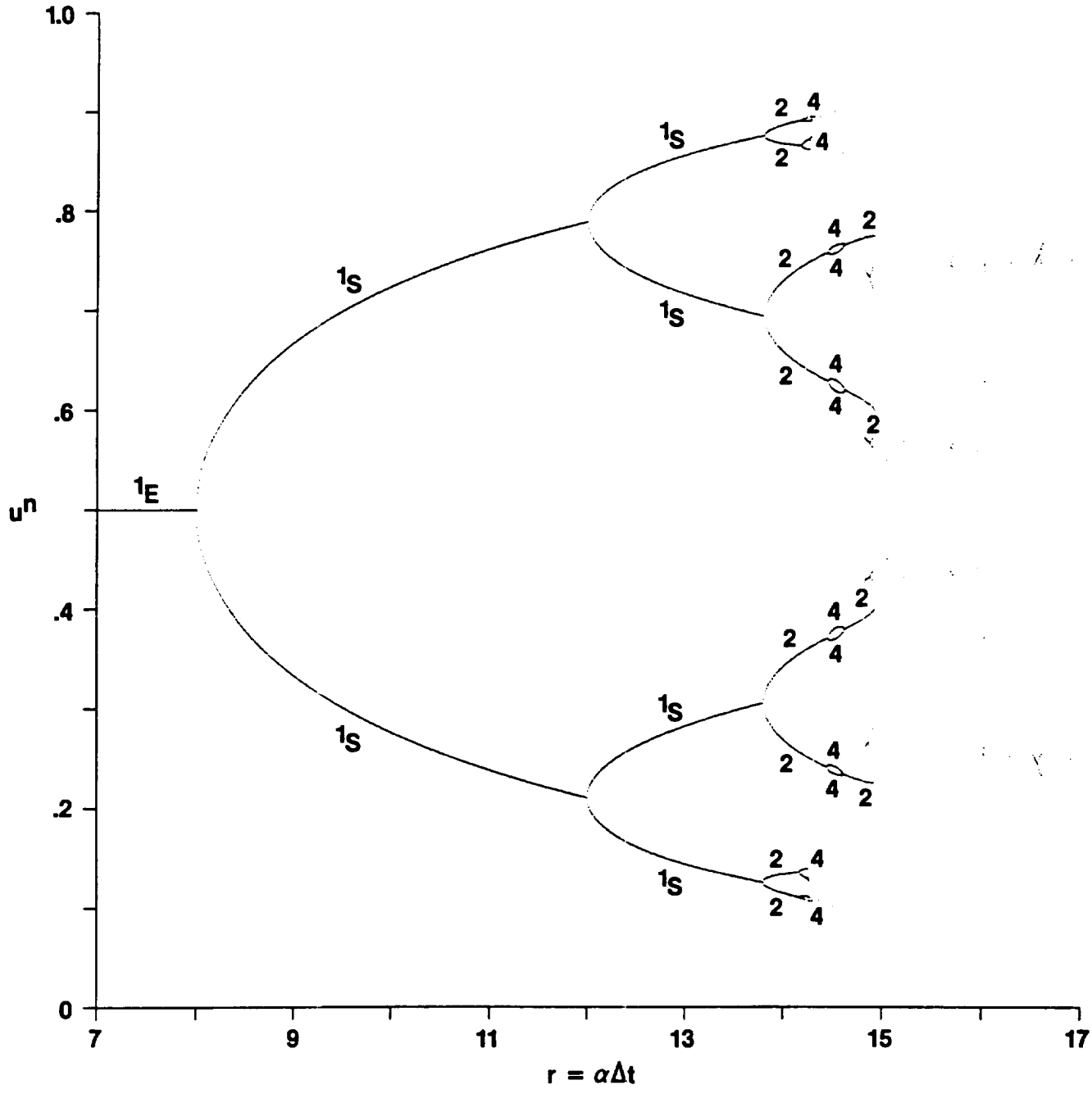

Fig. 3.10 Stable fixed points of periods 1,2,4,8 of the improved Euler (R-K 2) scheme for the ODE $du/dt = \alpha u(1-u)(0.5-u)$.

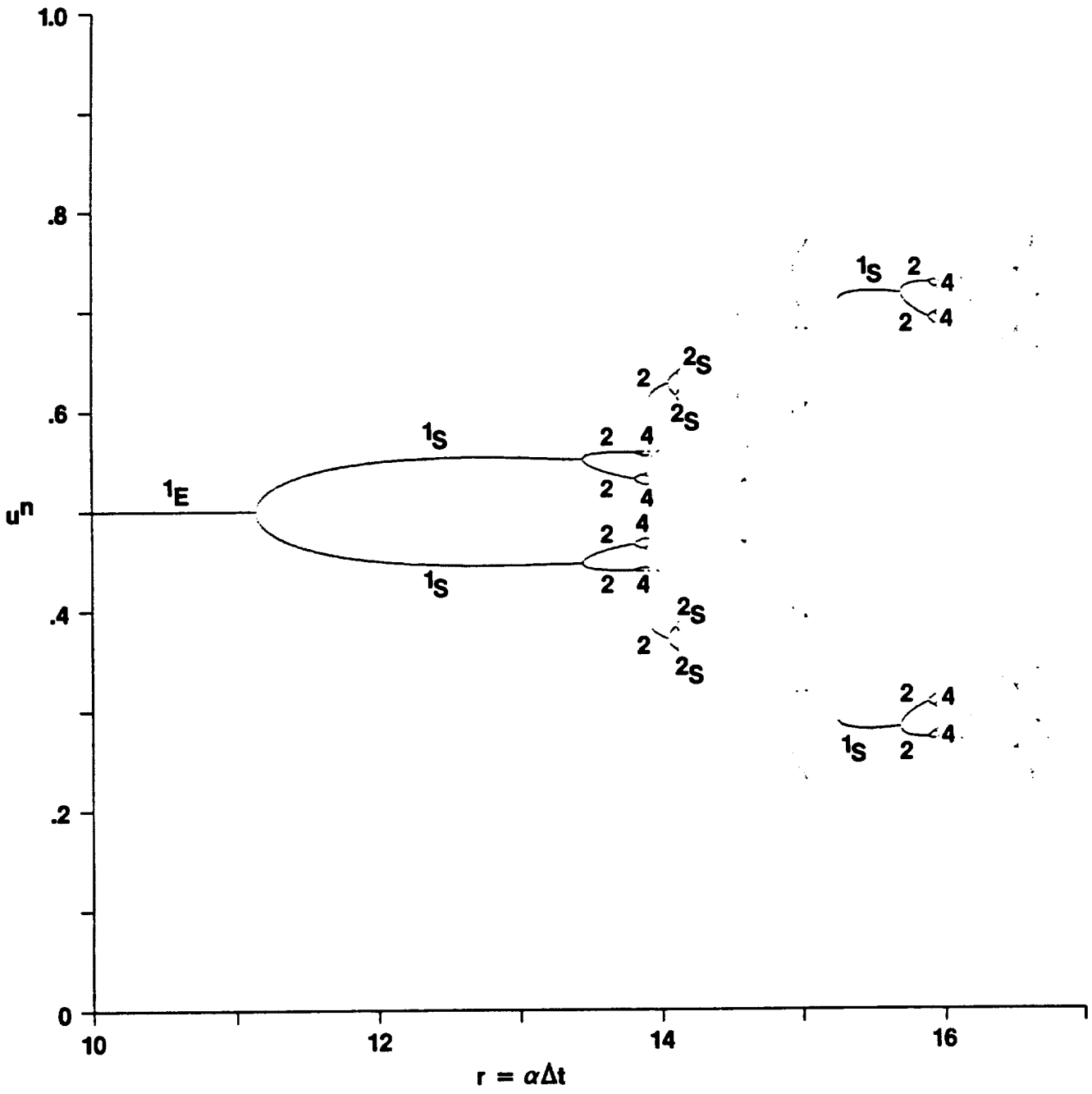

Fig. 3.11 Stable fixed points of periods 1,2,4,8 of the Runge-Kutta 4th-order (R-K 4) scheme for the ODE $du/dt = \alpha u(1-u)(0.5-u)$.

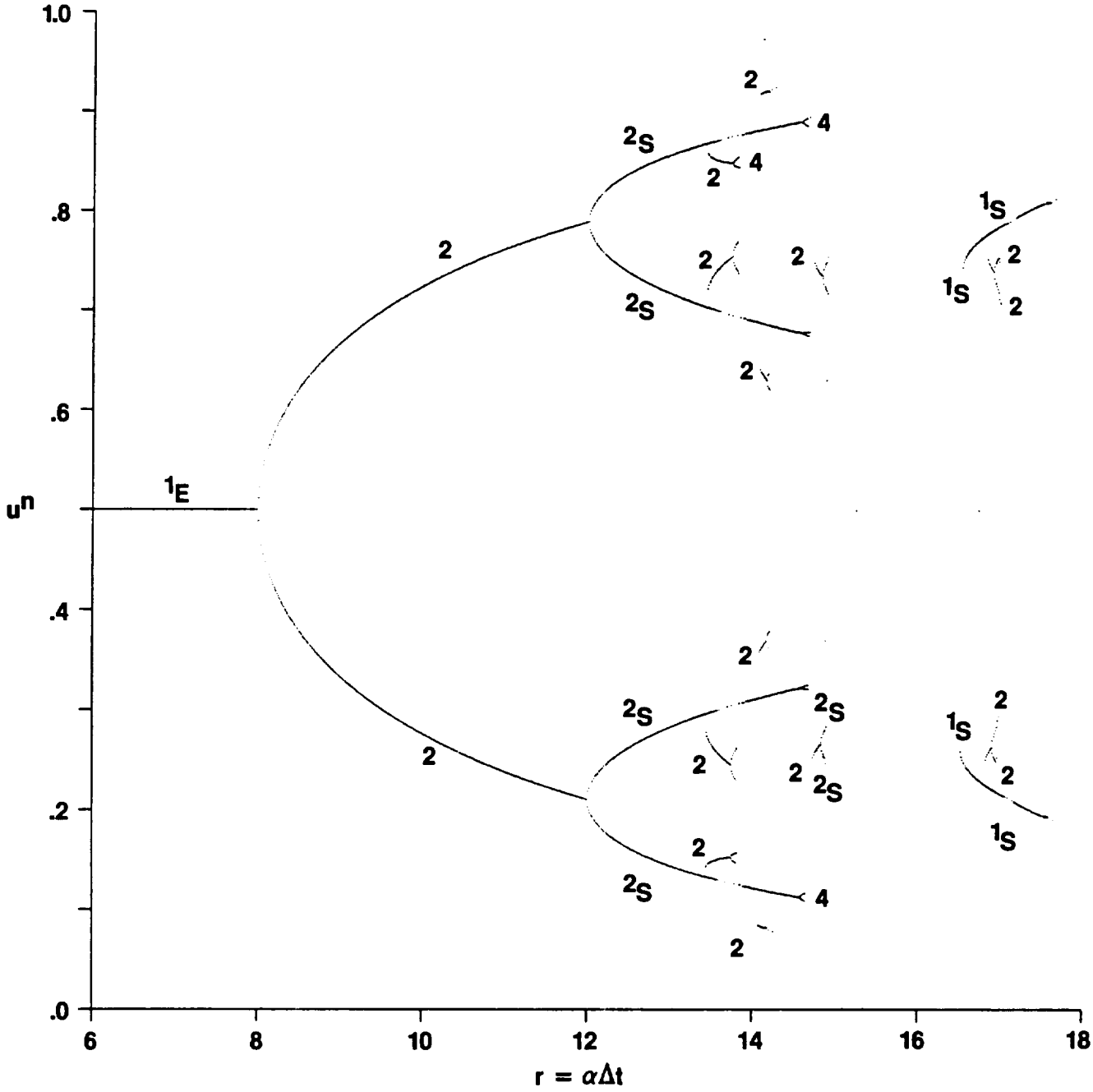

Fig. 3.12 Stable fixed points of periods 1,2,4,8 of the predictor-corrector scheme of order 2 for the ODE $du/dt = \alpha u(1-u)(0.5-u)$.

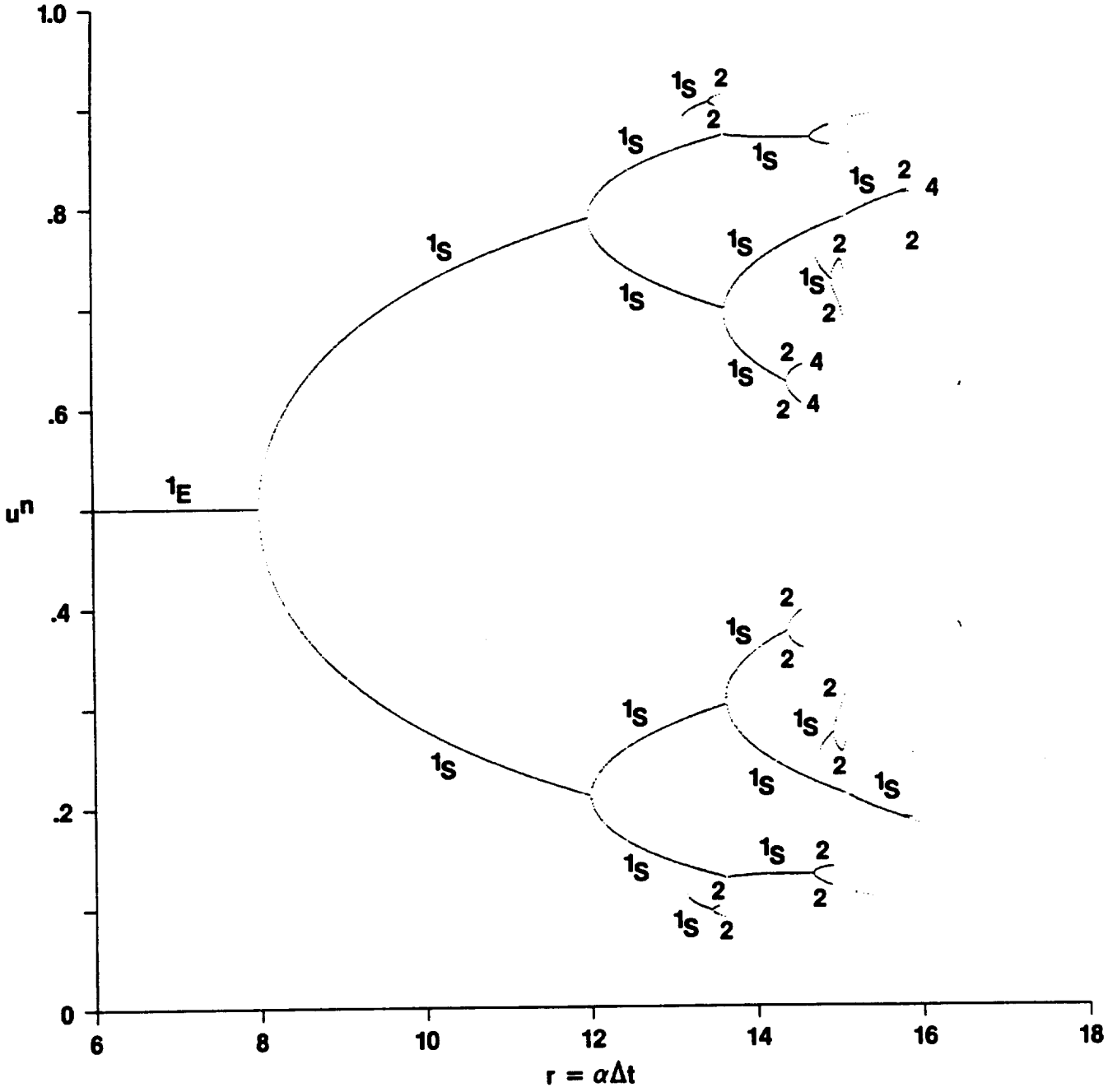

Fig. 3.13 Stable fixed points of periods 1,2,4,8 of the predictor-corrector scheme of order 3 for the ODE $du/dt = \alpha u(1-u)(0.5-u)$.

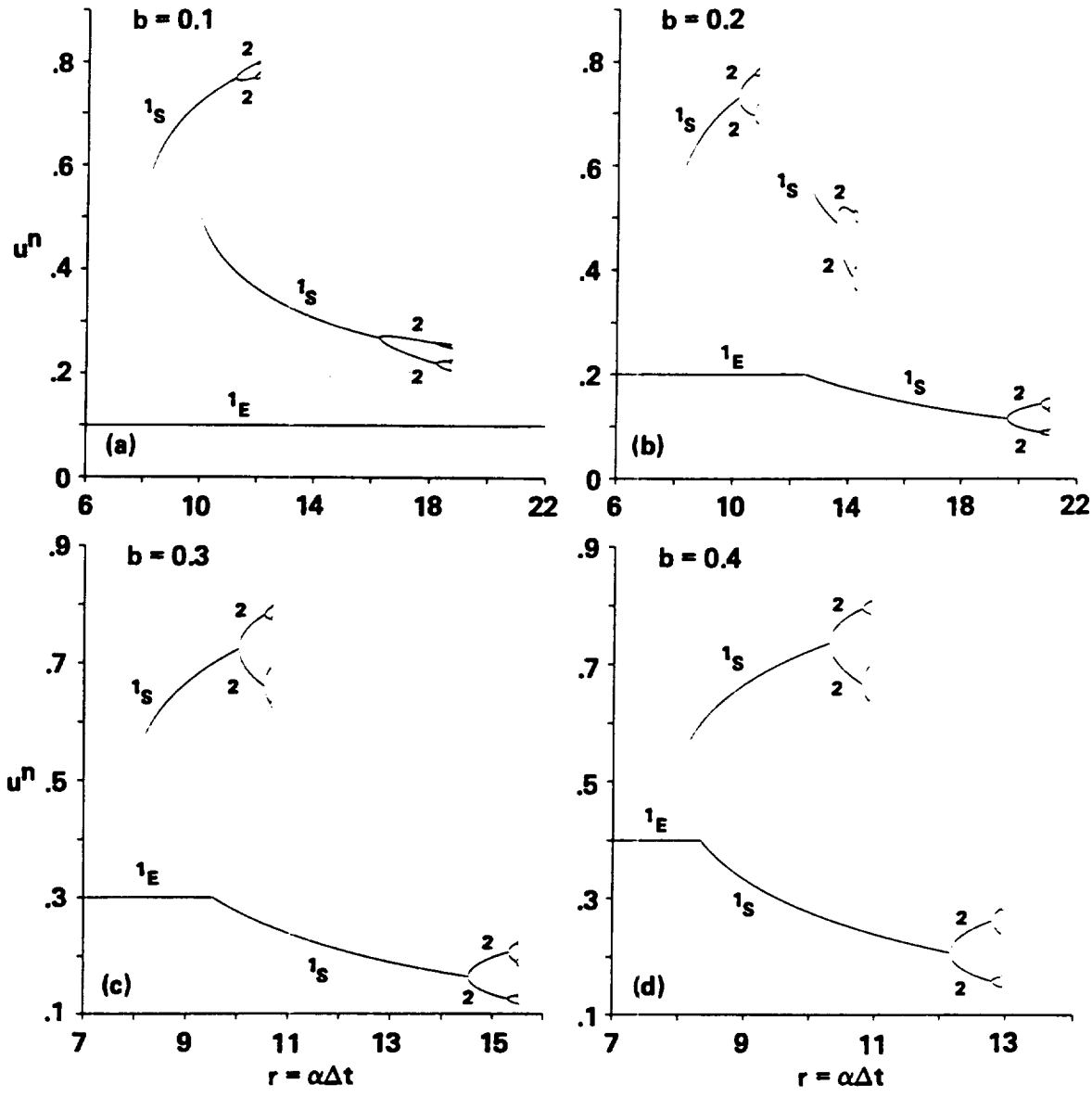

Fig. 3.14 Stable fixed points of periods 1,2,4,8 of the modified Euler (R-K 2) scheme for the ODE $du/dt = \alpha u(1-u)(b-u)$, $b = 0.1,\ 0.2,\ 0.3,\ 0.4$.

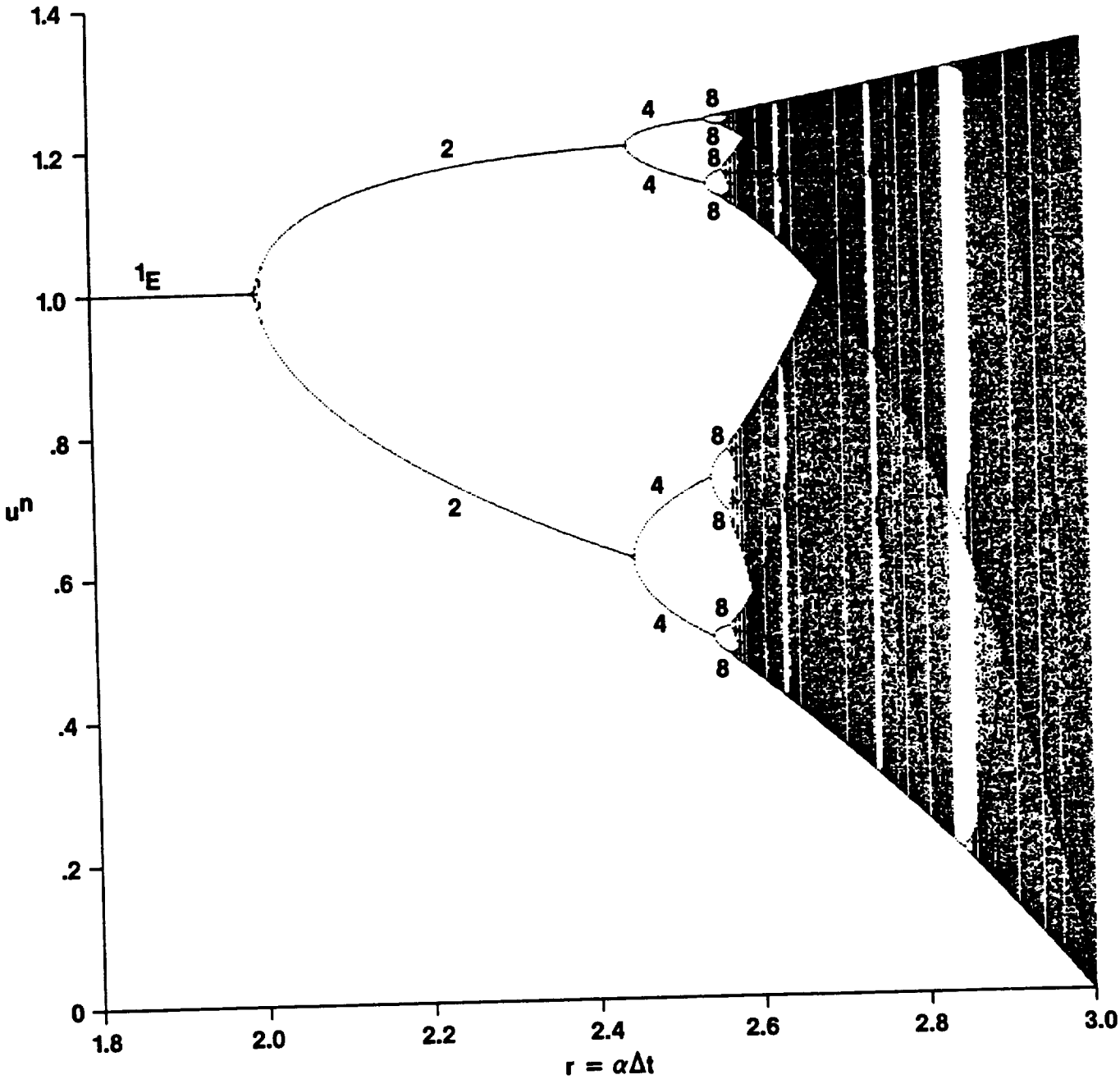

Fig. 3.15 Bifurcation diagram of the explicit Euler scheme for the logistic ODE $du/dt = \alpha u(1-u)$.

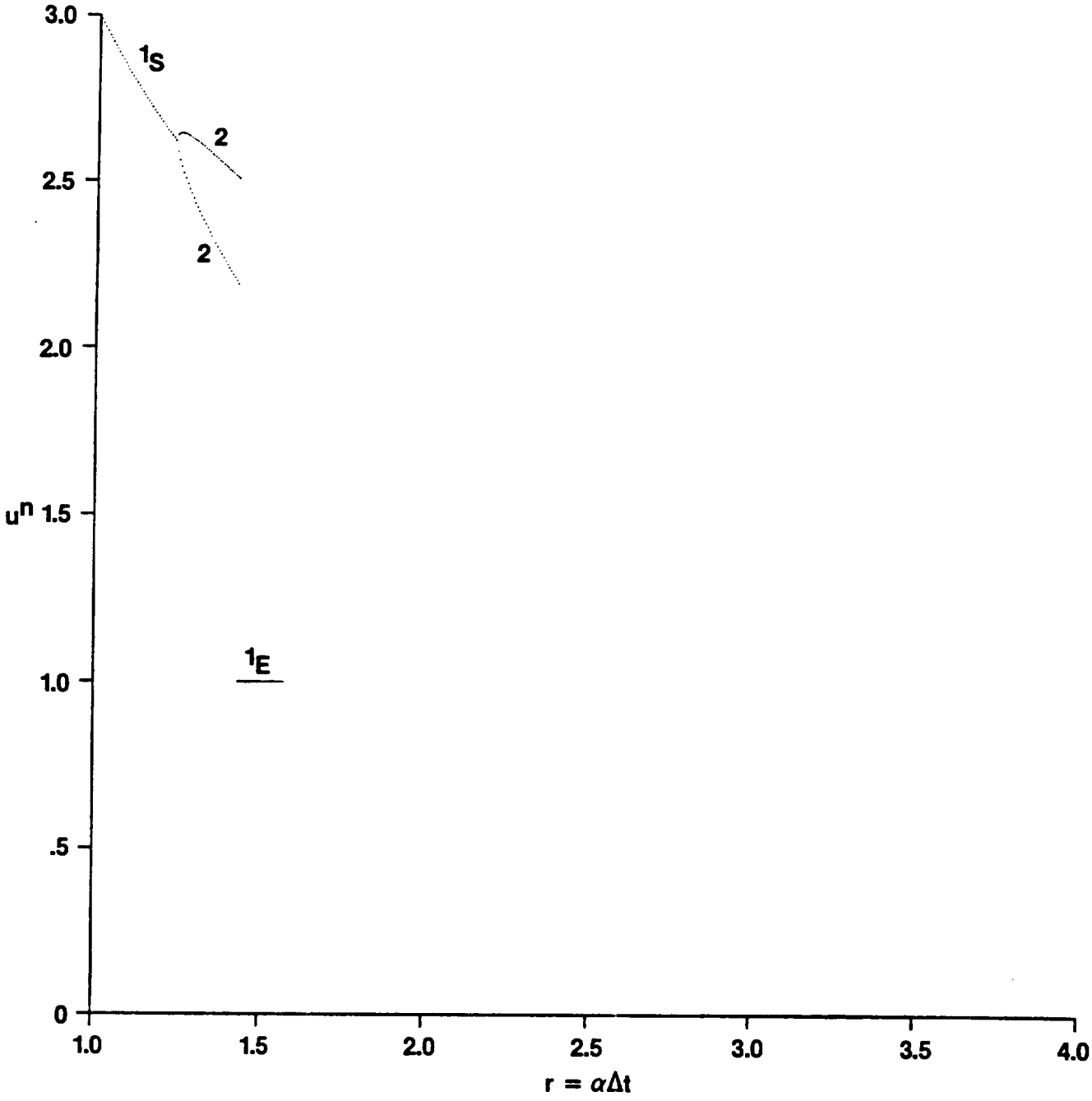

Fig. 3.16 Bifurcation diagram of the modified Euler (R-K 2) scheme for the logistic ODE $du/dt = \alpha u(1-u)$ with $u^0 = 2.7$.

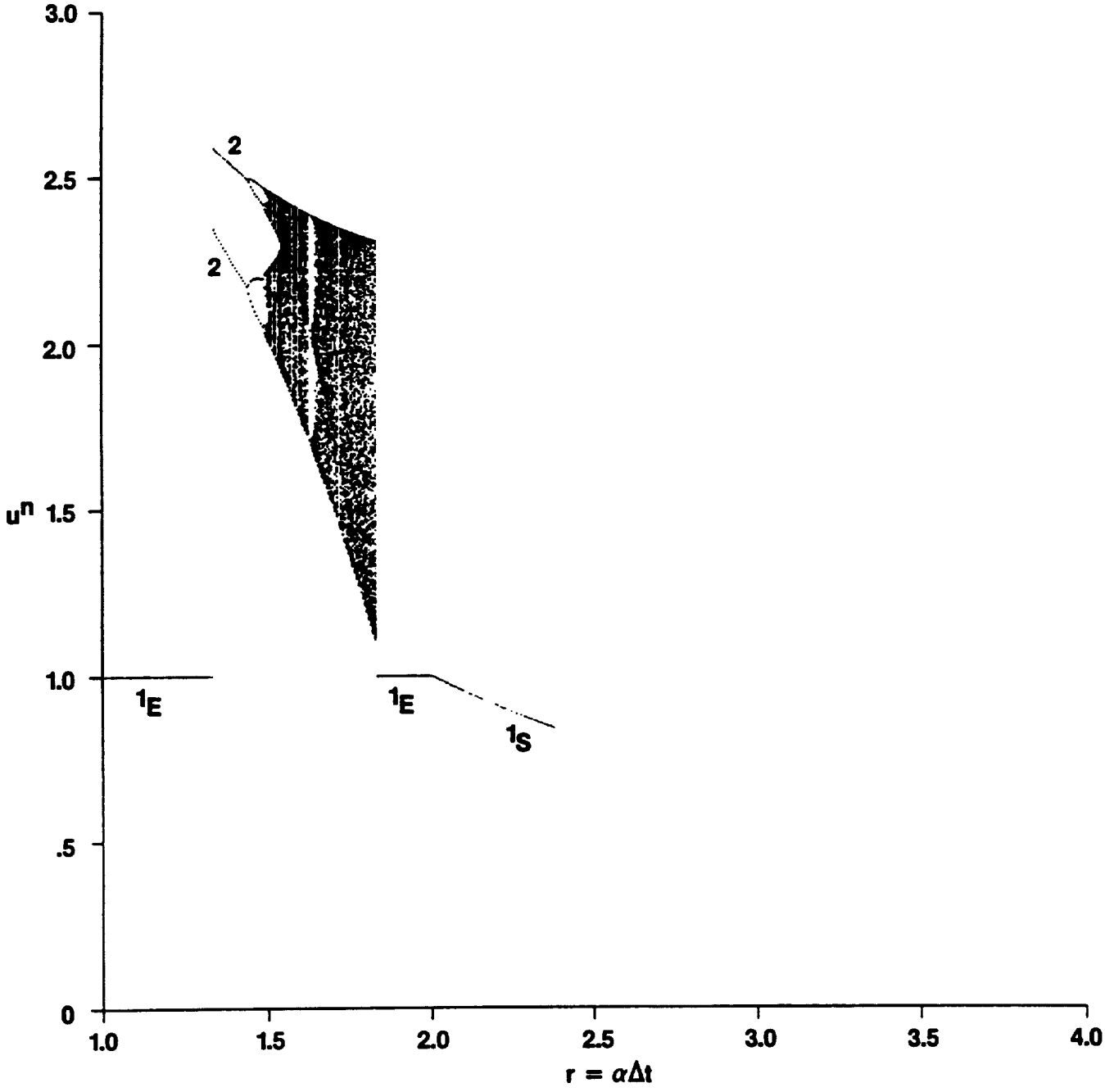

Fig. 3.17 Bifurcation diagram of the modified Euler (R-K 2) scheme for the logistic ODE $du/dt = \alpha u(1-u)$ with $u^0 = 1.5$.

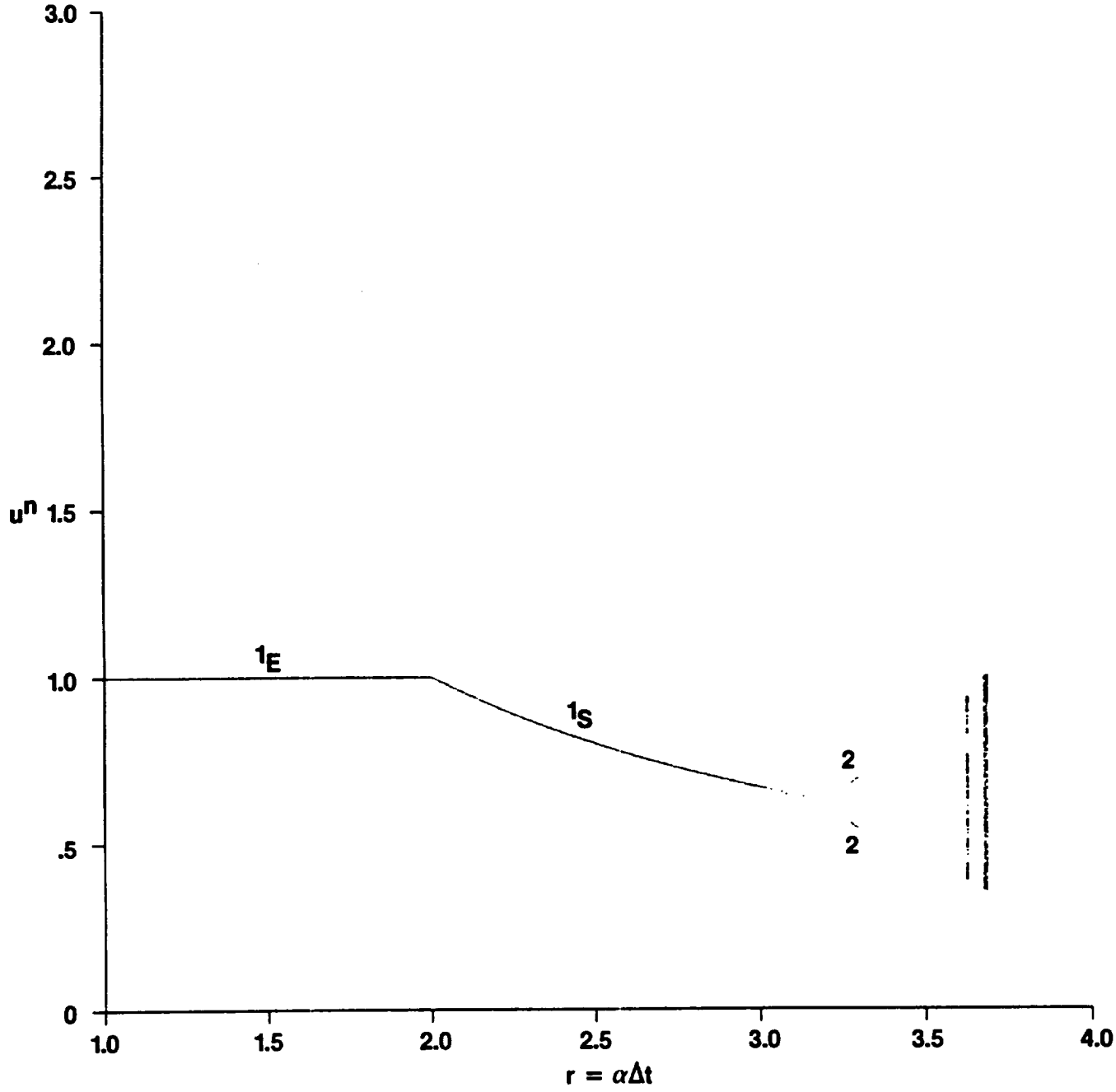

Fig. 3.18 Bifurcation diagram of the modified Euler (R-K 2) scheme for the logistic ODE $du/dt = \alpha u(1-u)$ with $u^0 = 0.25$.

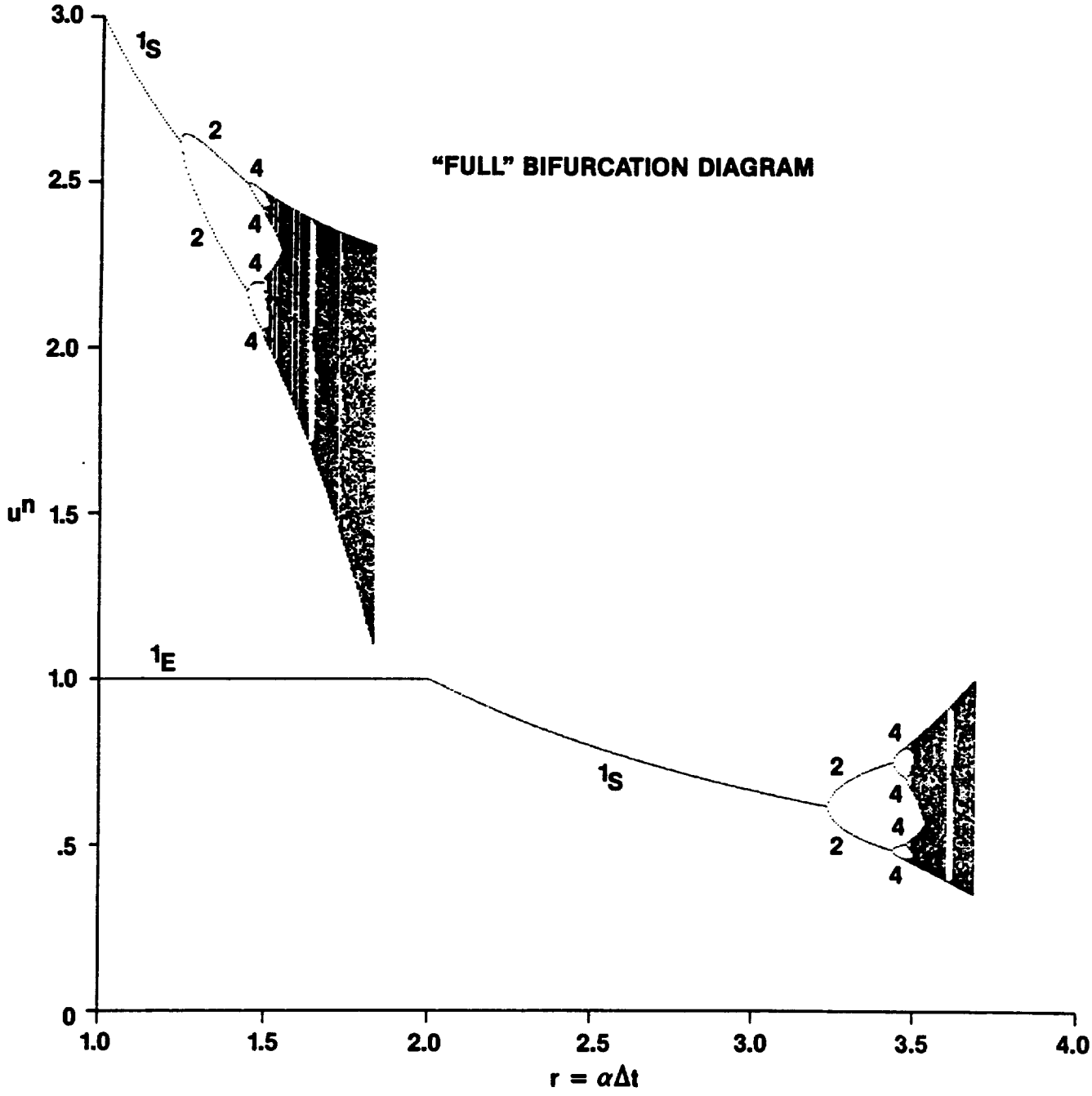

Fig. 3.19 "Full" bifurcation diagram of the modified Euler (R-K 2) scheme for the logistic ODE $du/dt = \alpha u(1-u)$.

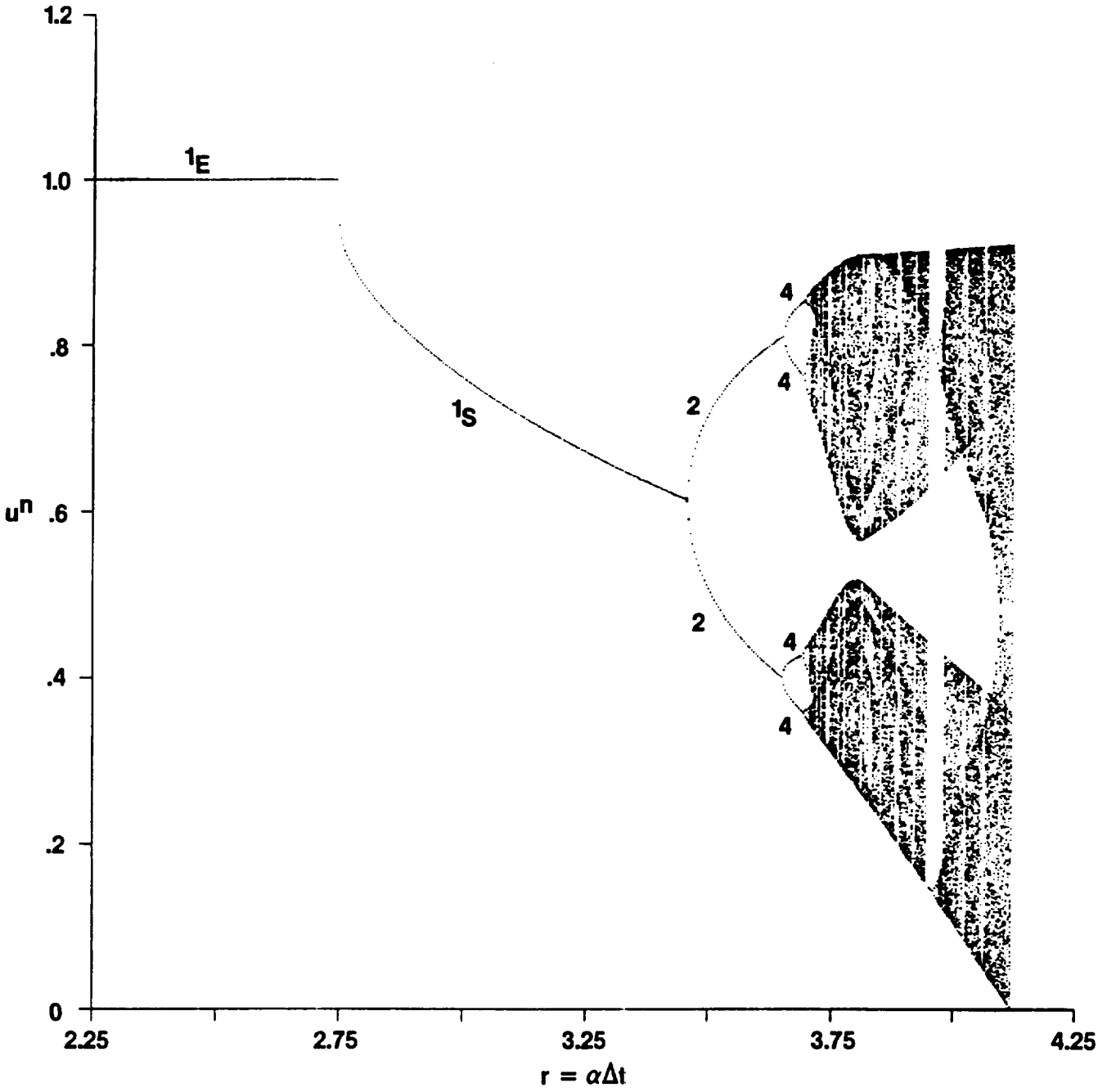

Fig. 3.20 Bifurcation diagram of the Runge-Kutta 4th-order (R-K 4) scheme for the logistic ODE $du/dt = \alpha u(1-u)$ with $u^0 = 0.5$.

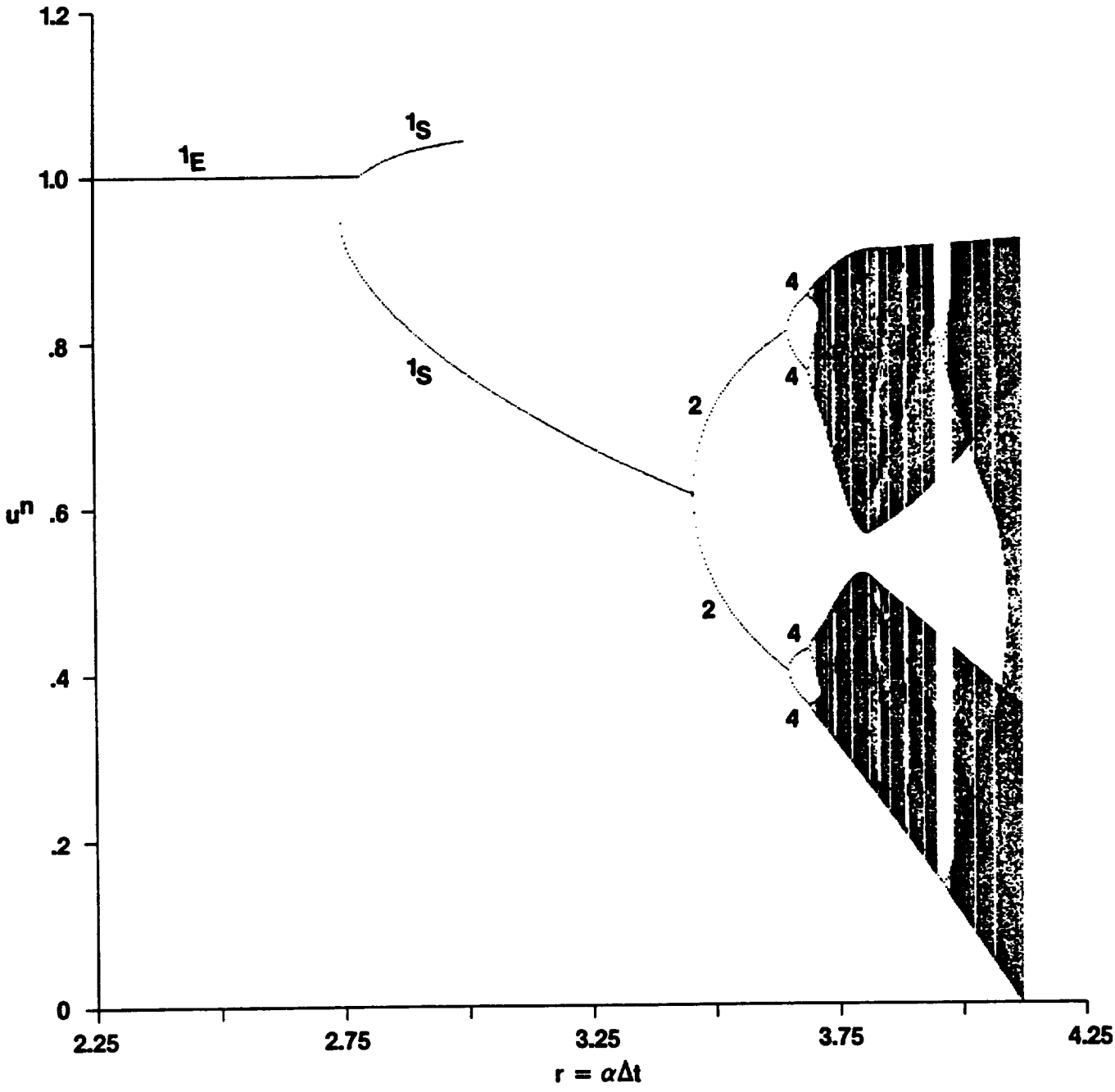

Fig. 3.21 Bifurcation diagram of the Runge-Kutta 4th-order (R-K 4) scheme for the logistic ODE $du/dt = \alpha u(1-u)$ with multiple initial data.

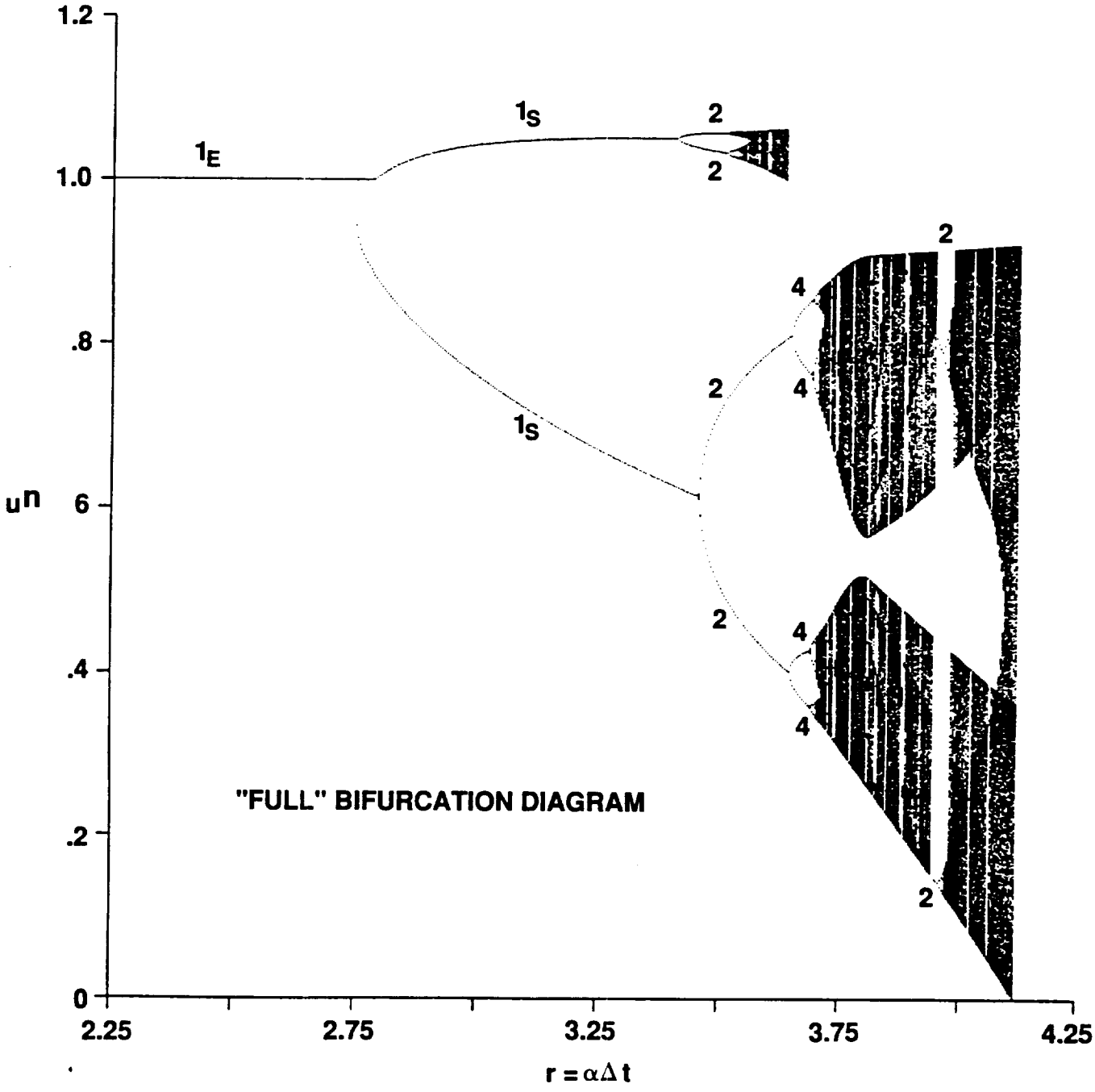

Fig. 3.22 "Full" bifurcation diagram of the Runge-Kutta 4th-order (R-K 4) scheme for the logistic ODE $du/dt = \alpha u(1-u)$.

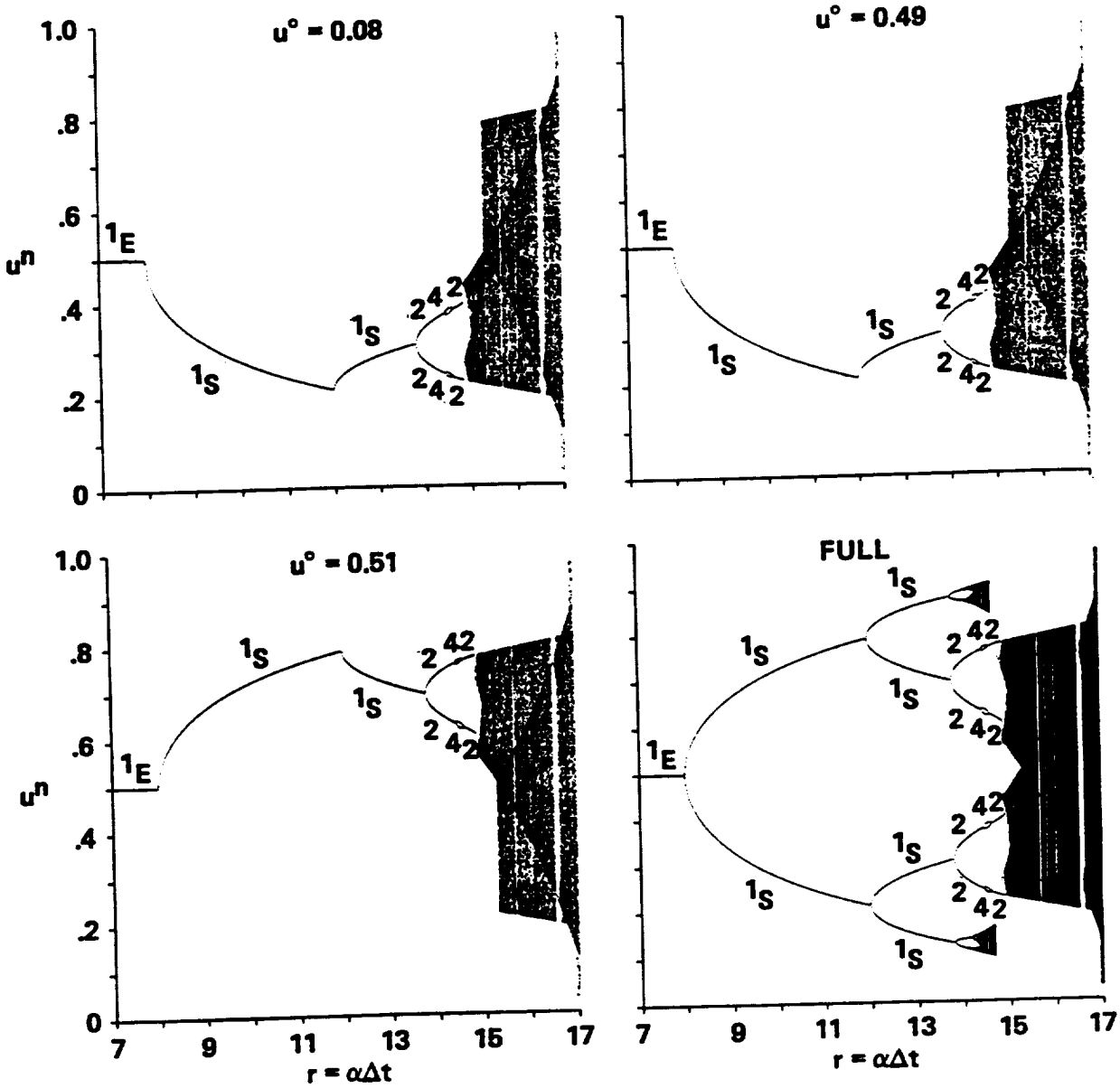

Fig. 3.23 Bifurcation diagrams of the improved Euler (R-K 2) scheme for the ODE $du/dt = \alpha u(1-u)(0.5-u)$ for four different sets of initial input data.

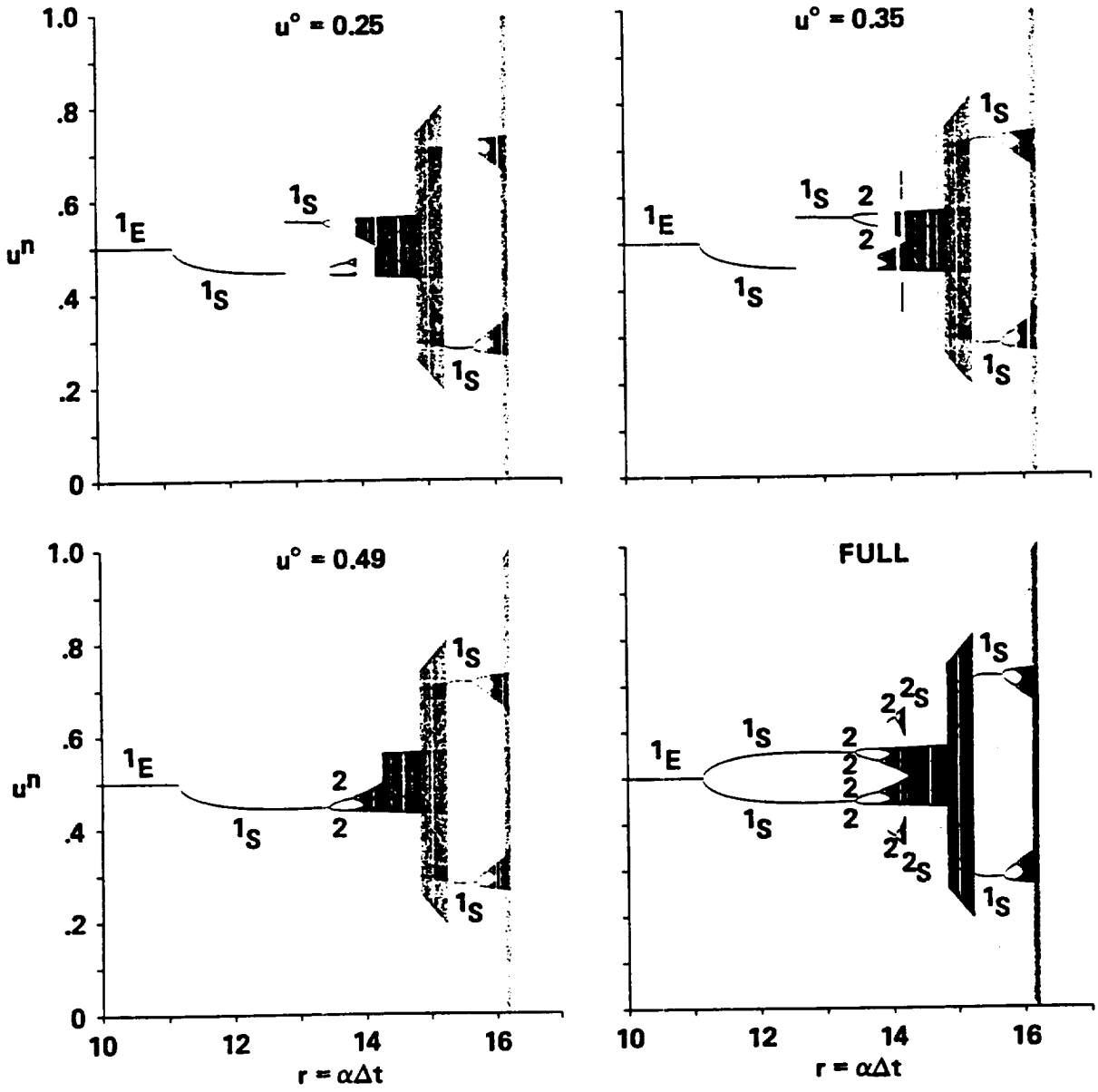

Fig. 3.24 Bifurcation diagrams of the Runge-Kutta 4th-order (R-K 4) scheme for the ODE $du/dt = \alpha u(1-u)(0.5-u)$ for four different sets of initial input data.

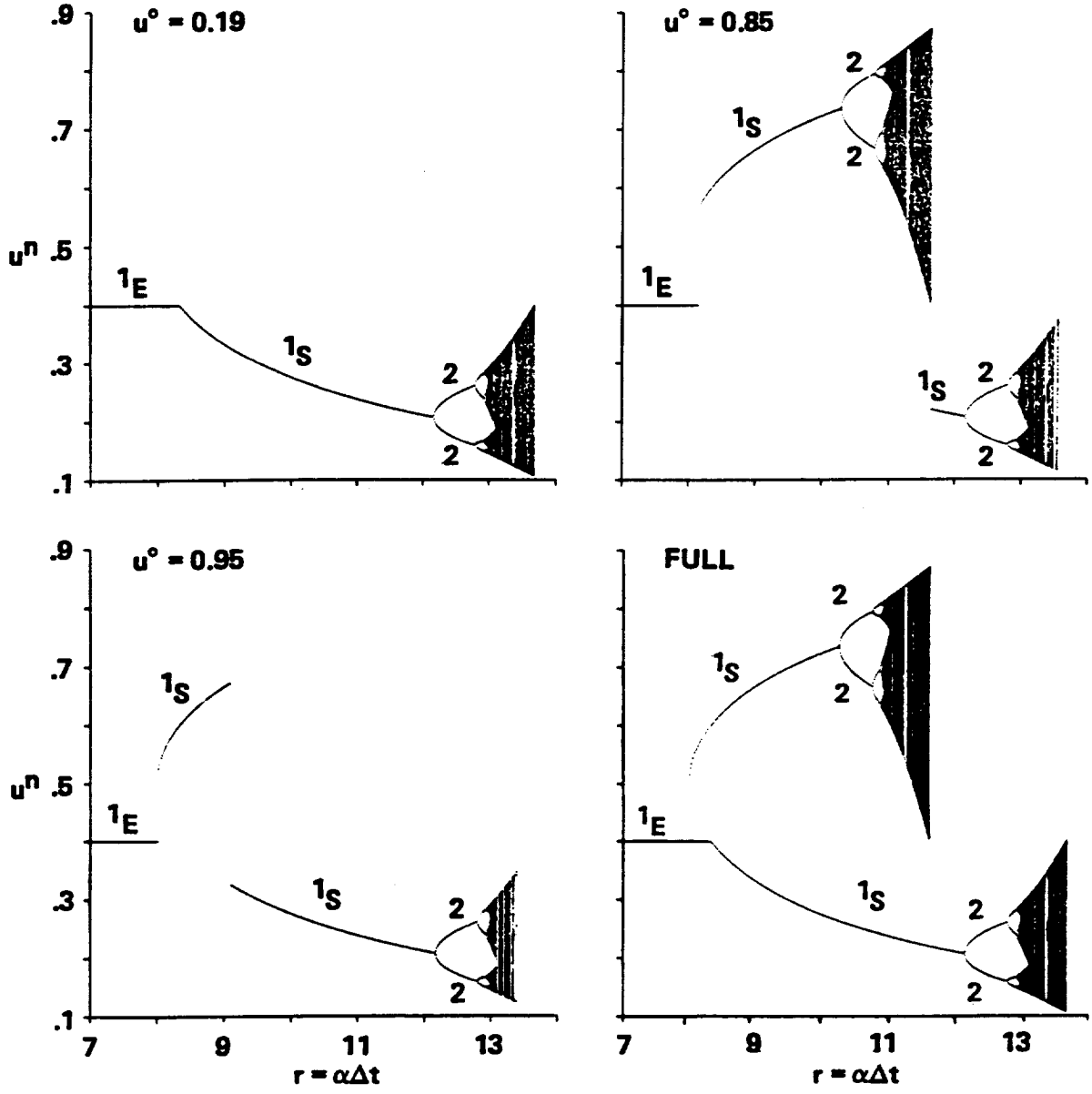

Fig. 3.25 Bifurcation diagrams of the modified Euler (R-K 2) scheme for the ODE $du/dt = \alpha u(1-u)(0.4-u)$ for four different sets of initial input data.

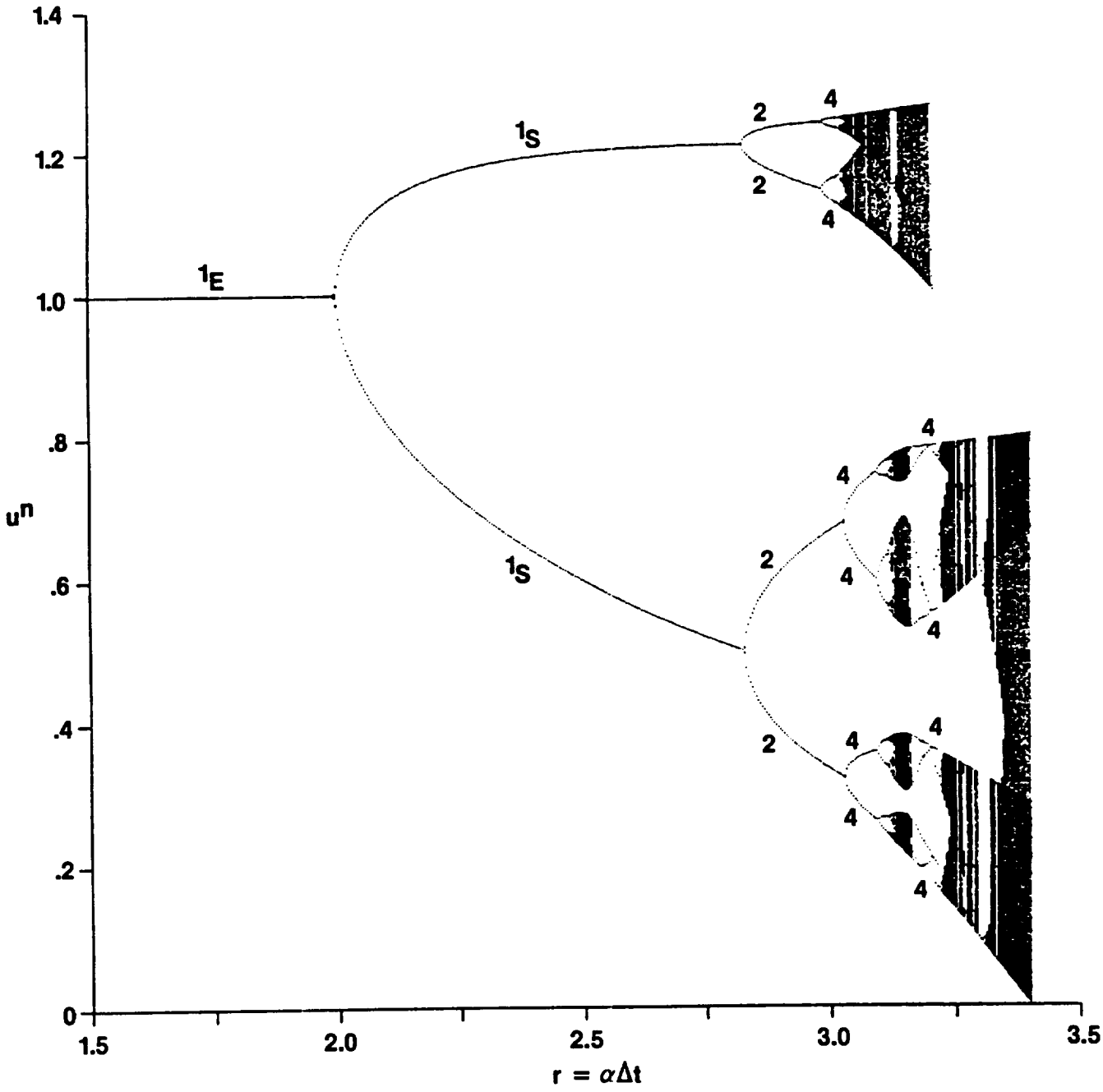

Fig. 3.26 "Full" bifurcation diagram of the improved Euler (R-K 2) scheme for the logistic ODE $du/dt = \alpha u(1-u)$.

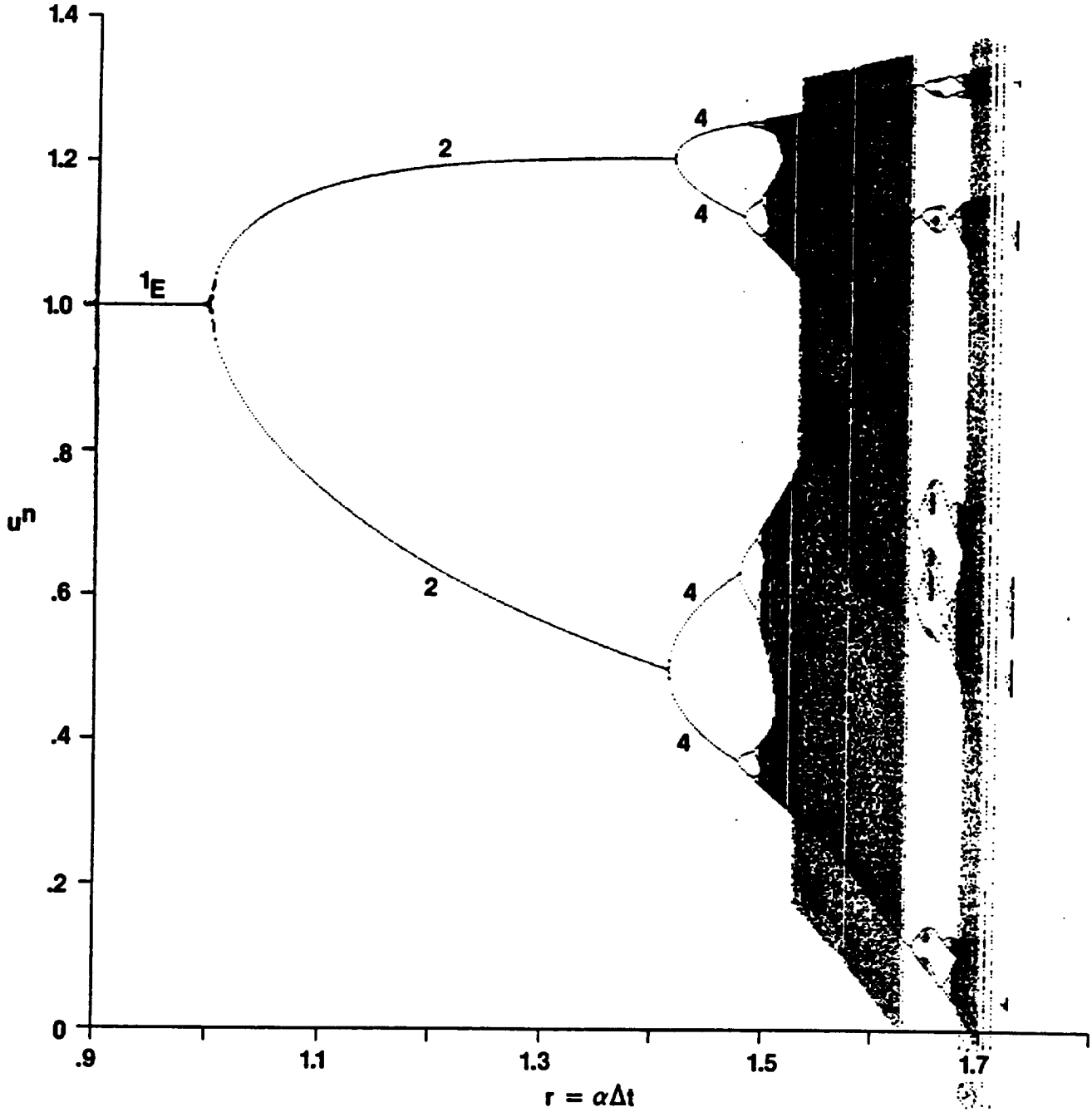

Fig. 3.27 "Full" bifurcation diagram of the Adam-Bashforth scheme for the logistic ODE $du/dt = \alpha u(1-u)$.

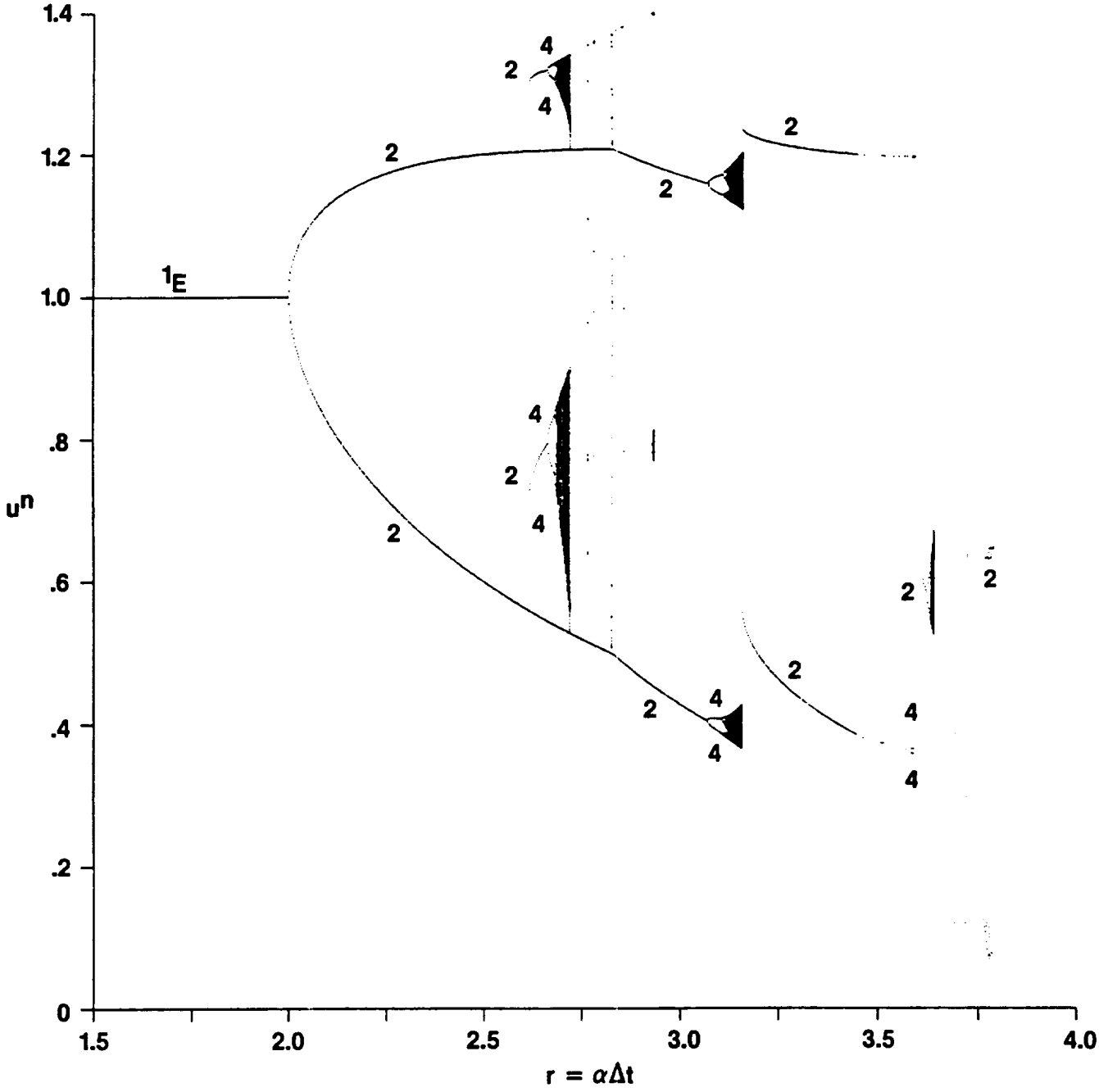

Fig. 3.28 "Full" bifurcation diagram of the predictor-corrector scheme of order 2 for the logistic ODE $du/dt = \alpha u(1-u)$.

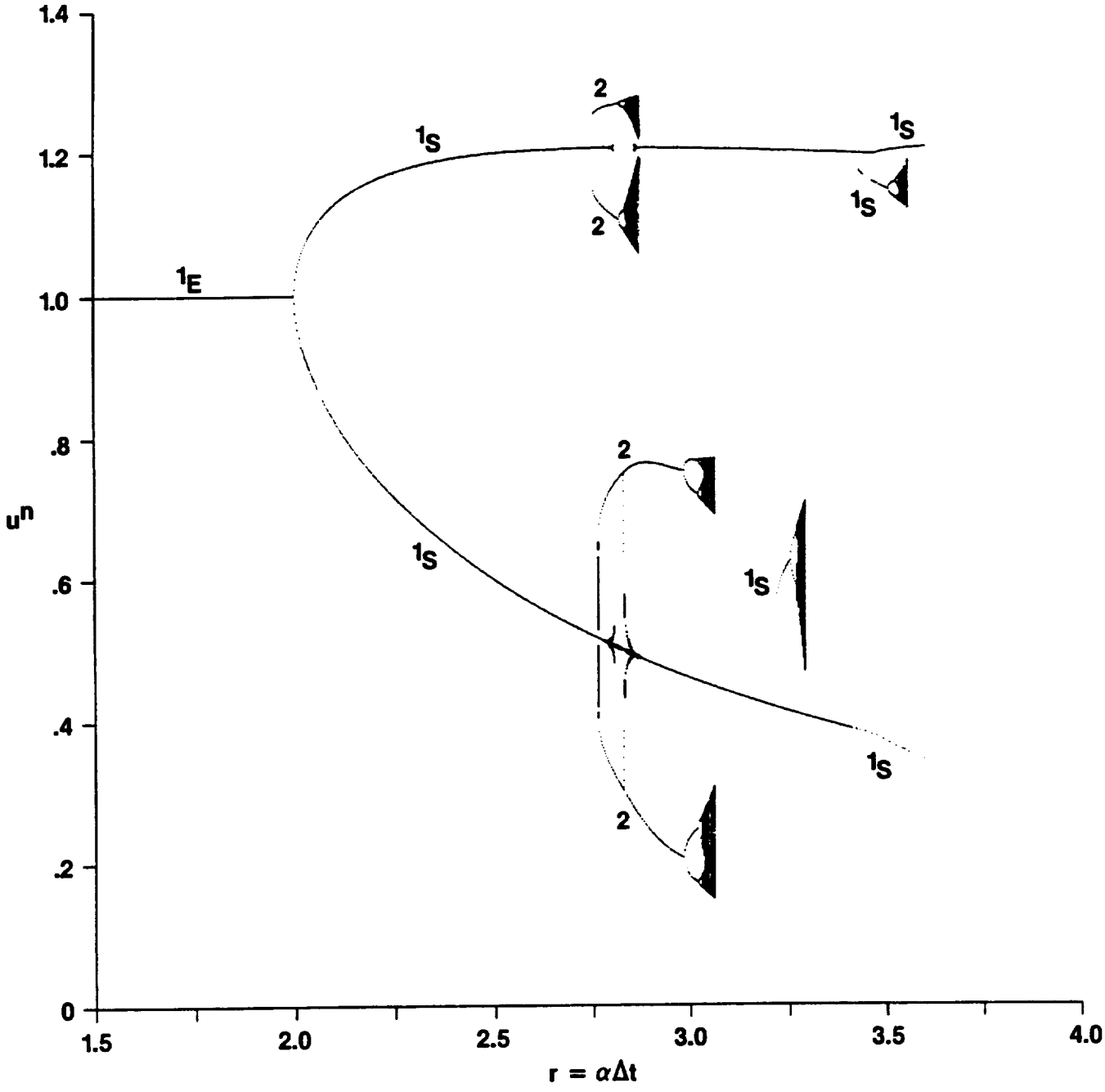

Fig. 3.29 "Full" bifurcation diagram of the predictor-corrector scheme of order 3 for the logistic ODE $du/dt = \alpha u(1-u)$.

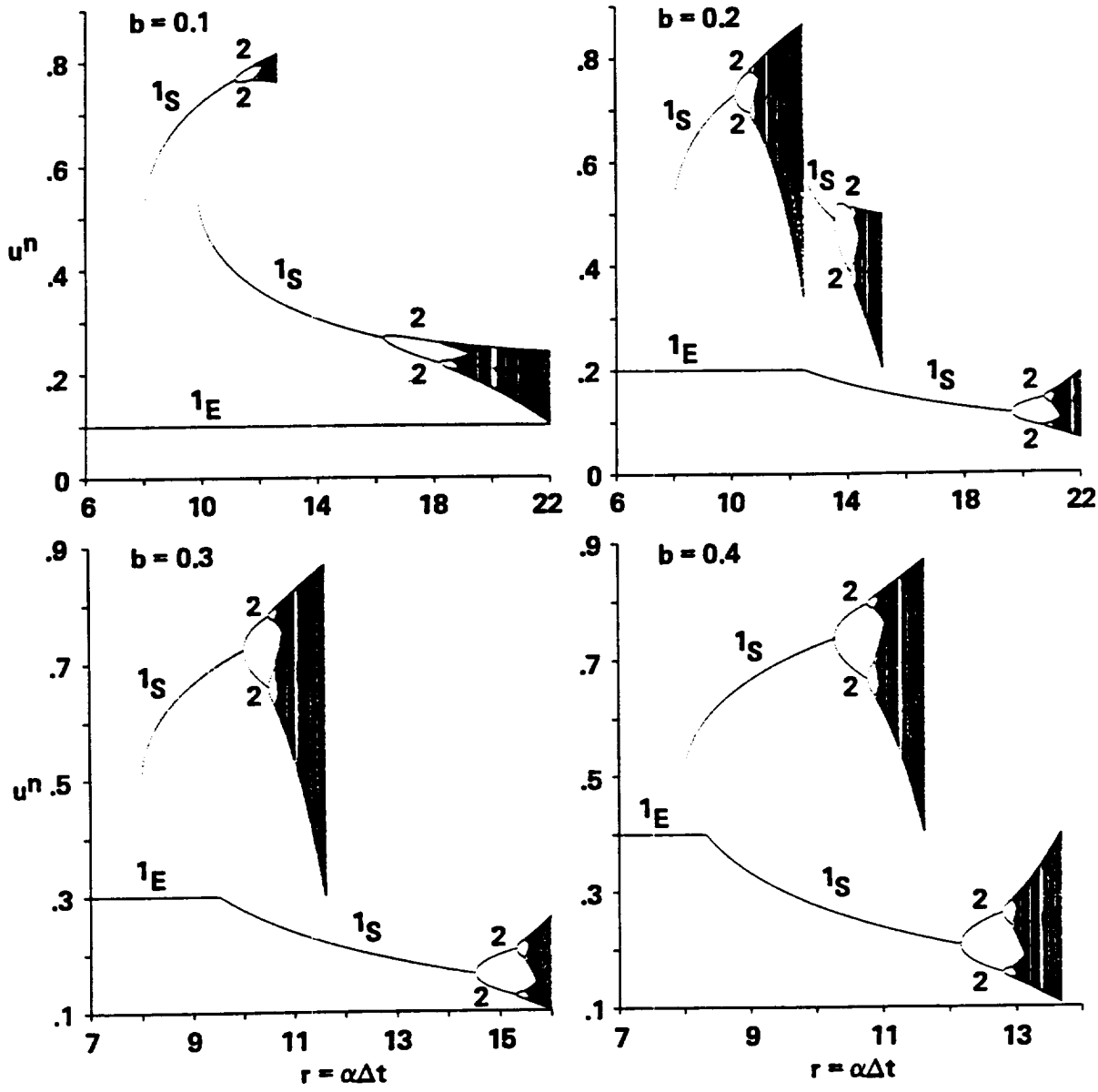

Fig. 3.30 "Full" bifurcation diagrams of the modified Euler (R-K 2) scheme for the ODE $du/dt = \alpha u(1-u)(b-u)$, $b = 0.1,\ 0.2,\ 0.3,\ 0.4$.

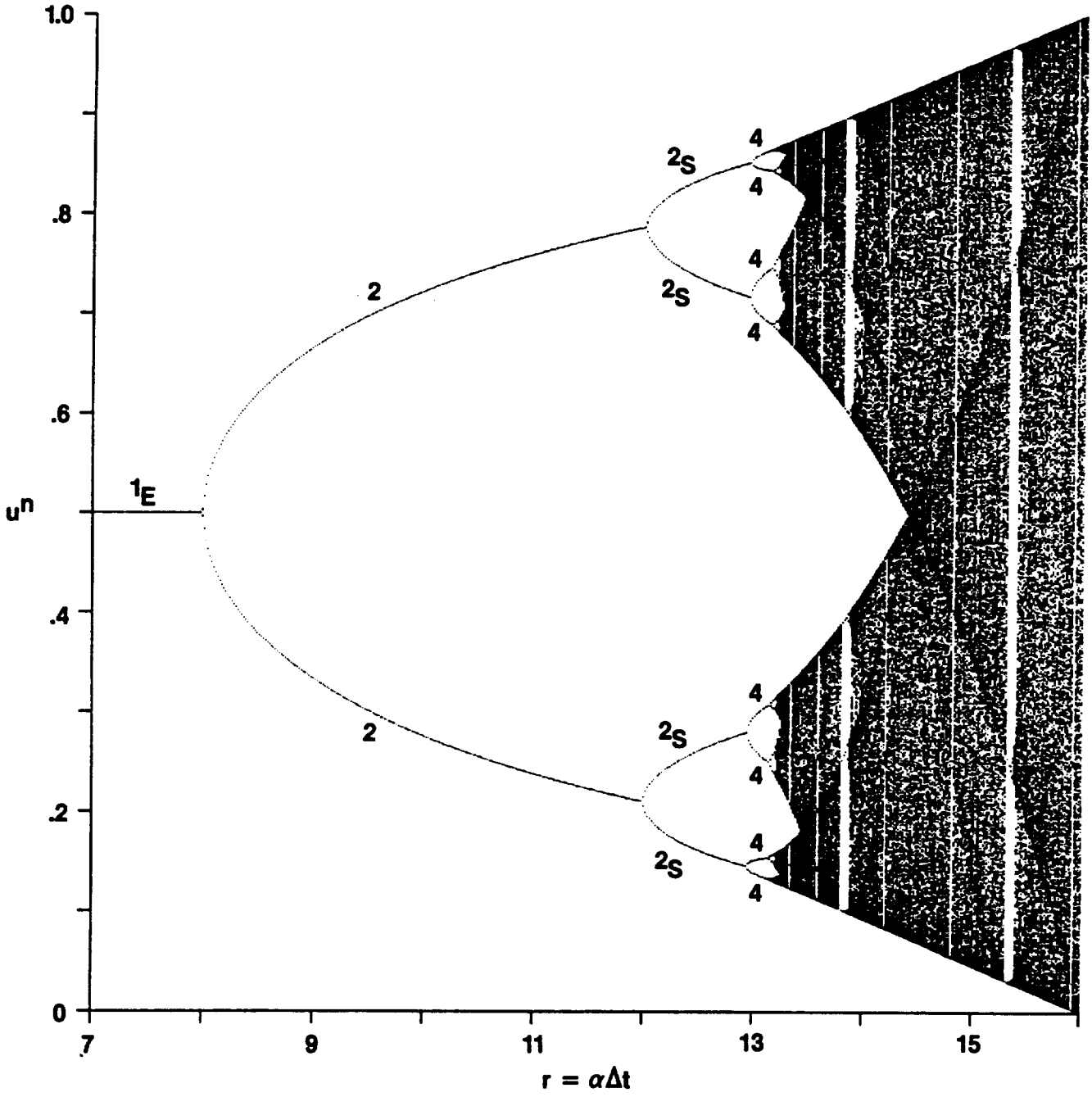

Fig. 3.31 "Full" bifurcation diagrams of the explict Euler scheme for the ODE $du/dt = \alpha u(1-u)(0.5-u)$.

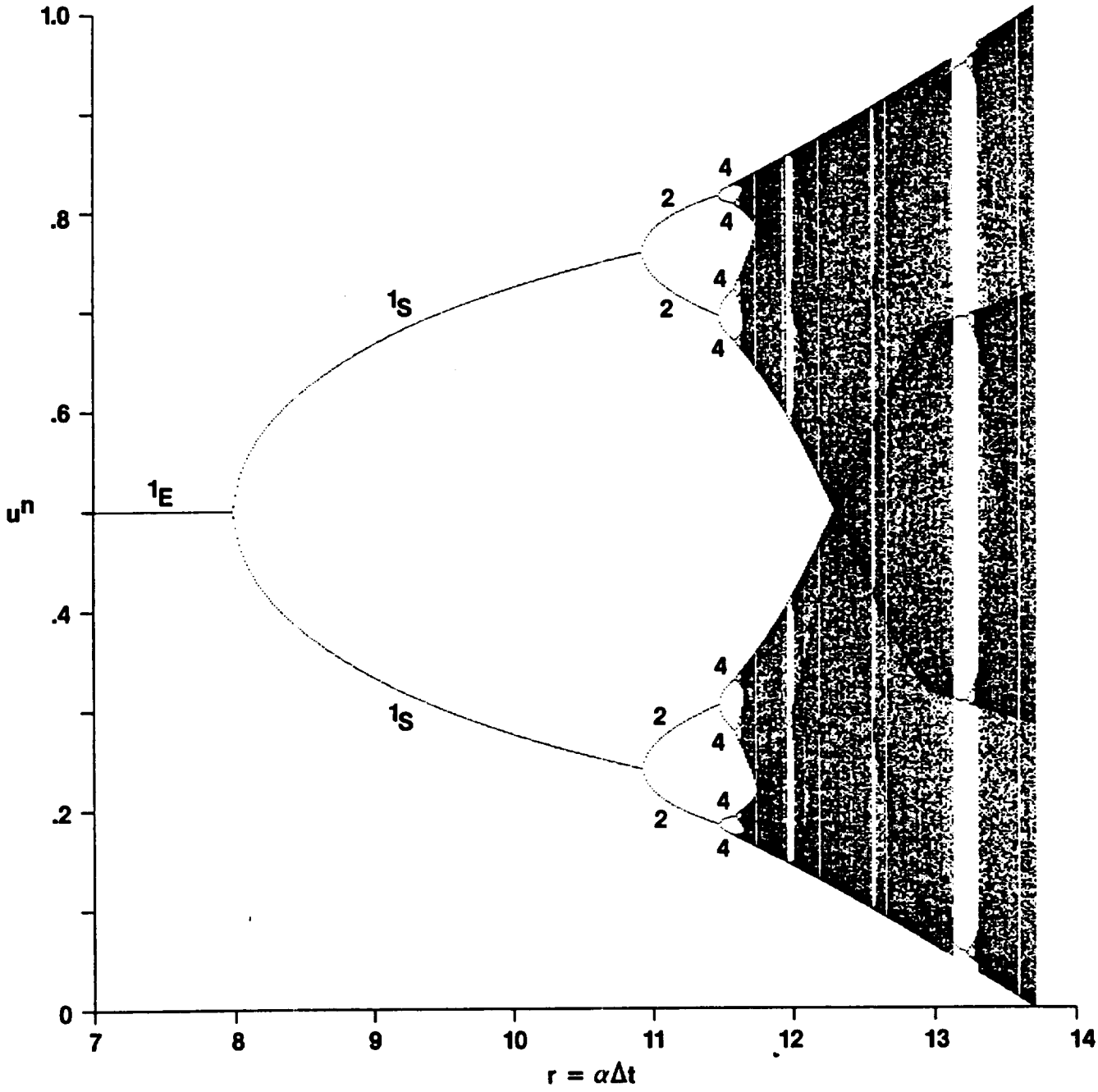

Fig. 3.32 "Full" bifurcation diagram of the modified Euler (R-K 2) scheme for the ODE $du/dt = \alpha u(1-u)(0.5-u)$.

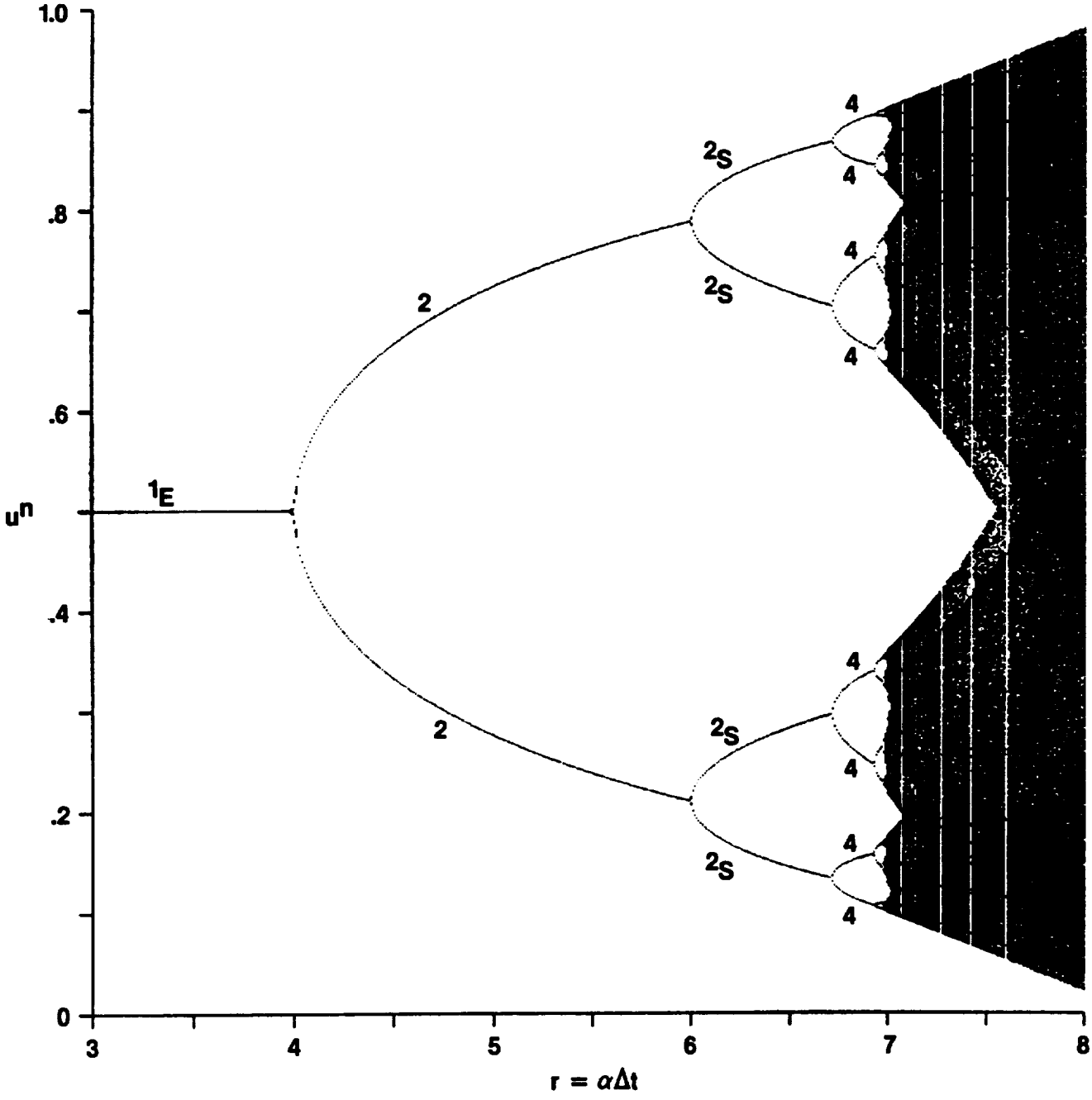

Fig. 3.33 "Full" bifurcation diagram of the Adam-Bashforth scheme for the ODE $du/dt = \alpha u(1-u)(0.5-u)$.

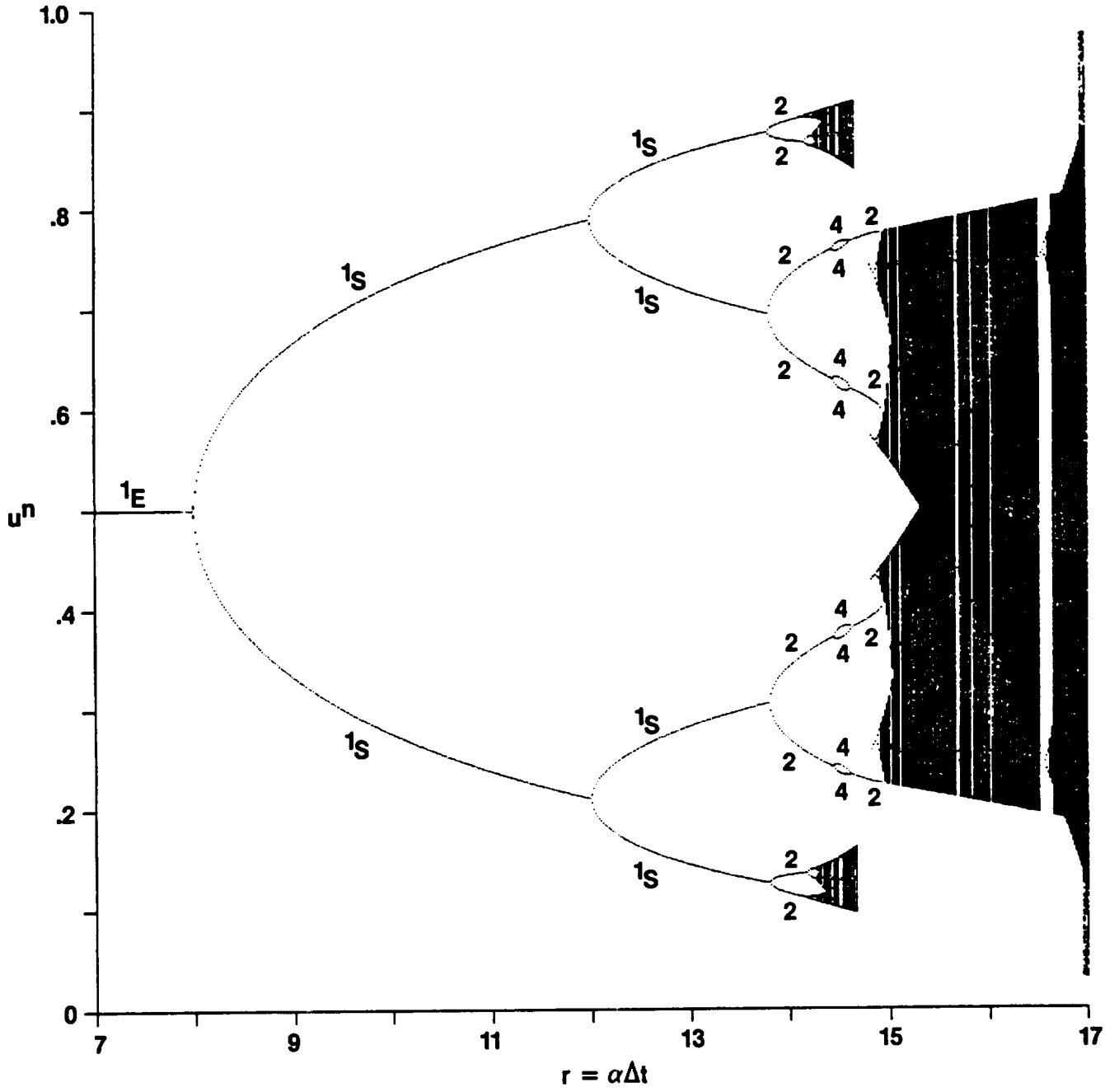

Fig. 3.34 "Full" bifurcation diagram of the improved Euler (R-K 2) scheme for the ODE $du/dt = \alpha u(1-u)(0.5-u)$.

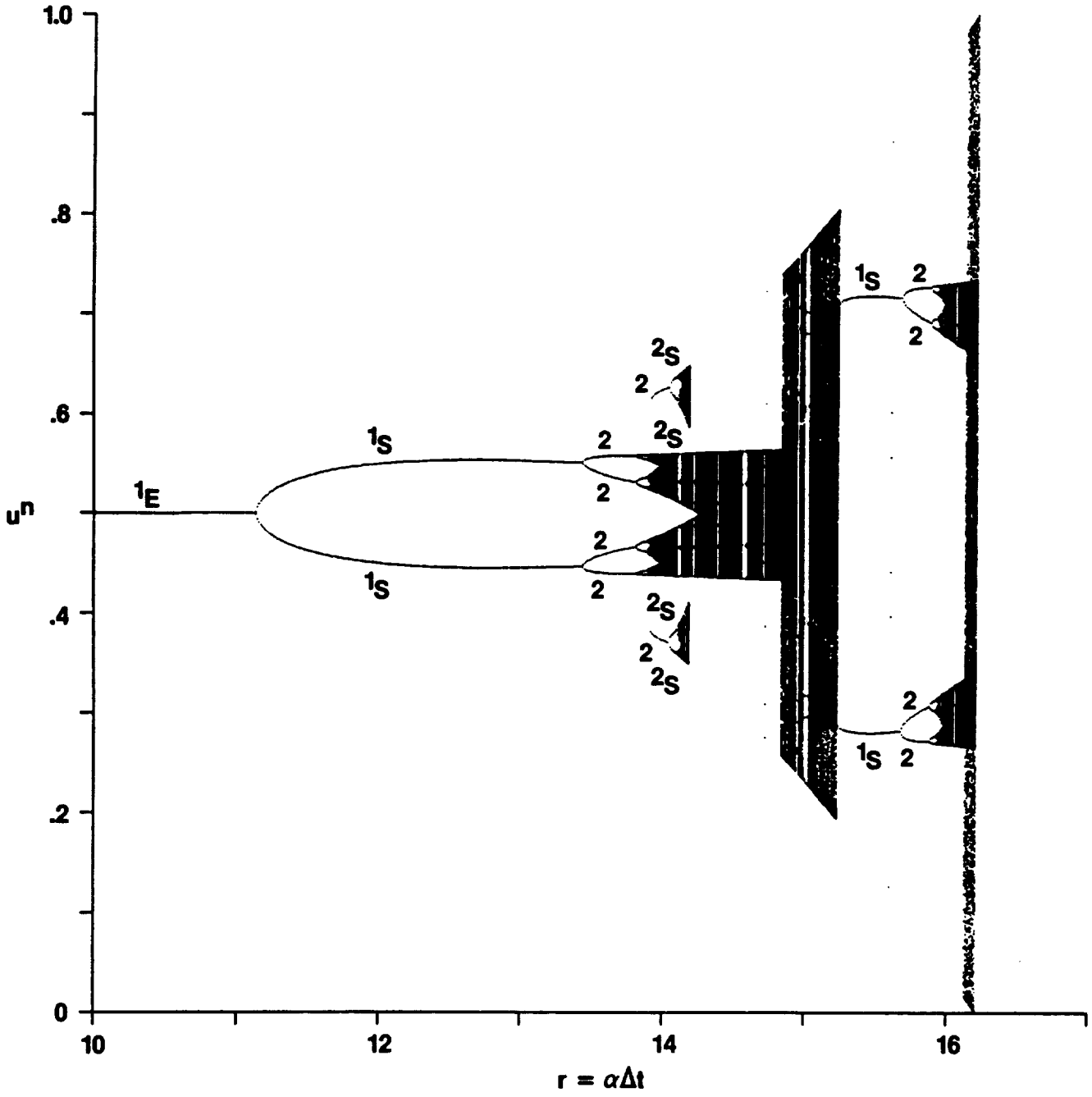

Fig. 3.35 "Full" bifurcation diagram of the Runge-Kutta 4th-order (R-K 4) scheme for the ODE $du/dt = \alpha u(1-u)(0.5-u)$.

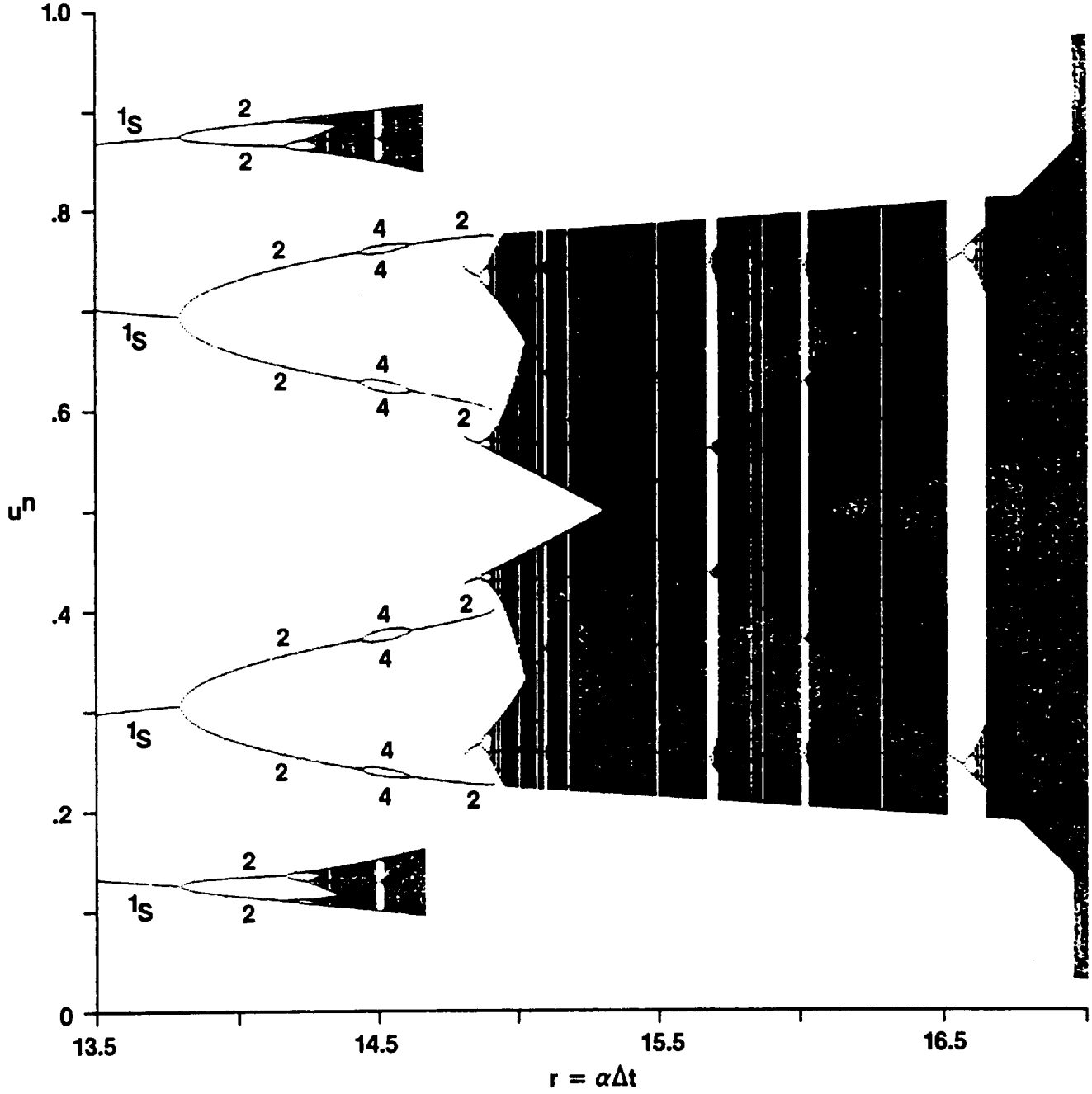

Fig. 3.36 "Full" bifurcation diagram of the improved Euler (R-K 2) scheme for the ODE $du/dt = \alpha u(1-u)(0.5-u)$ (enlarged).

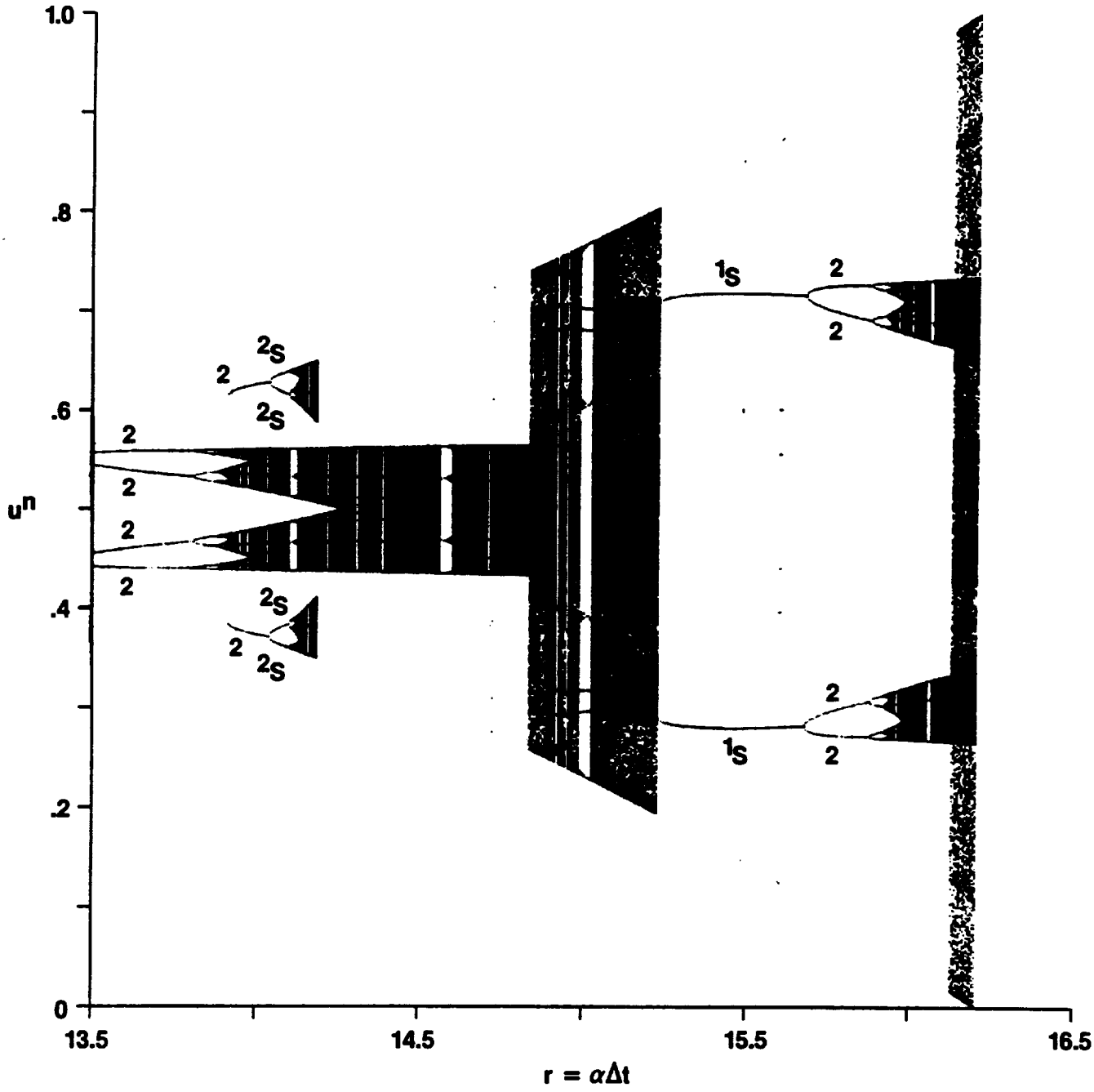

Fig. 3.37 "Full" bifurcation diagram of the Runge-Kutta 4th-order (R-K 4) scheme for the ODE $du/dt = \alpha u(1-u)(0.5-u)$ (enlarged).

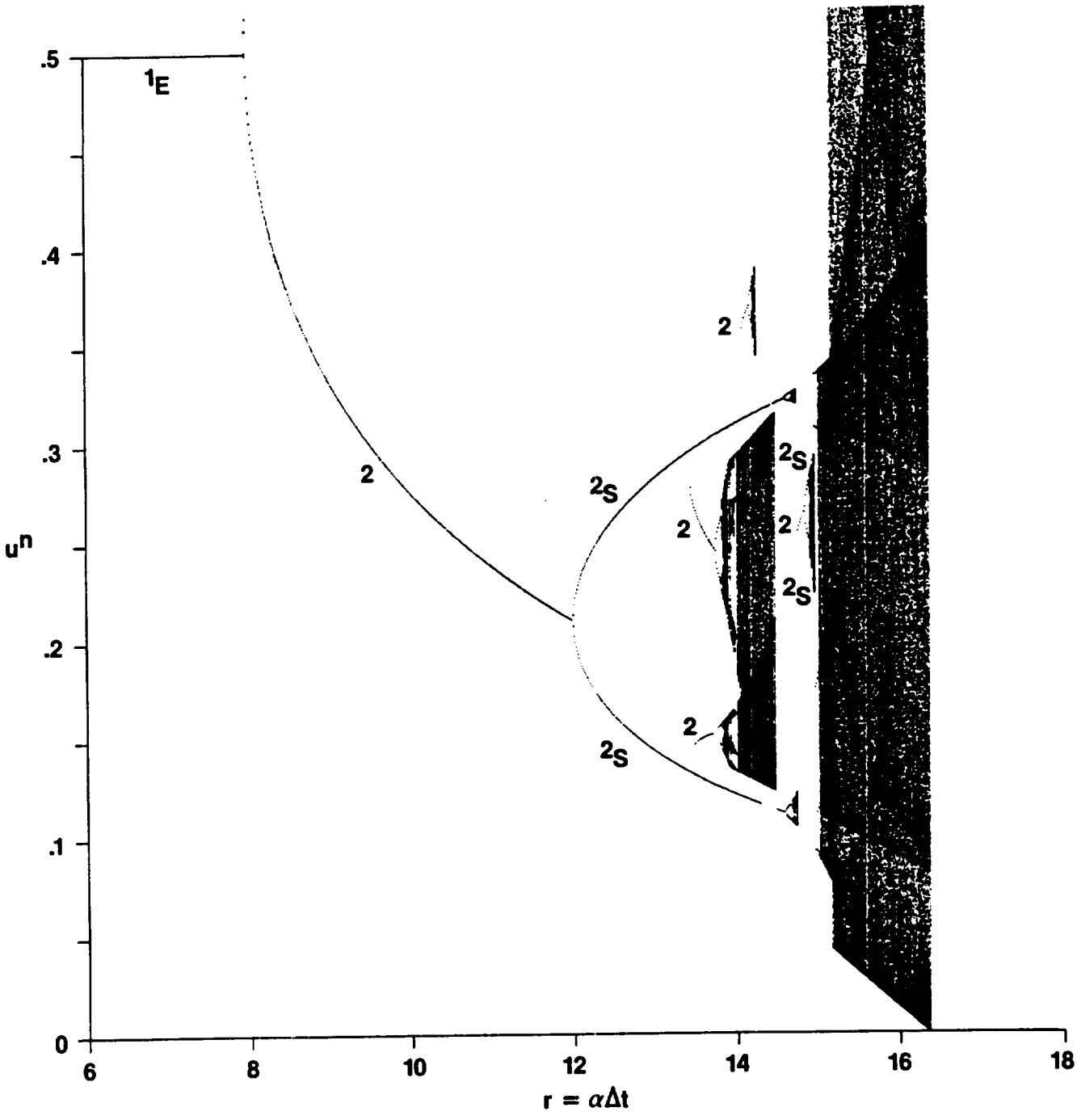

Fig. 3.38 "Full" bifurcation diagram of the predictor-corrector scheme of order 2 for the ODE $du/dt = \alpha u(1-u)(0.5-u)$.

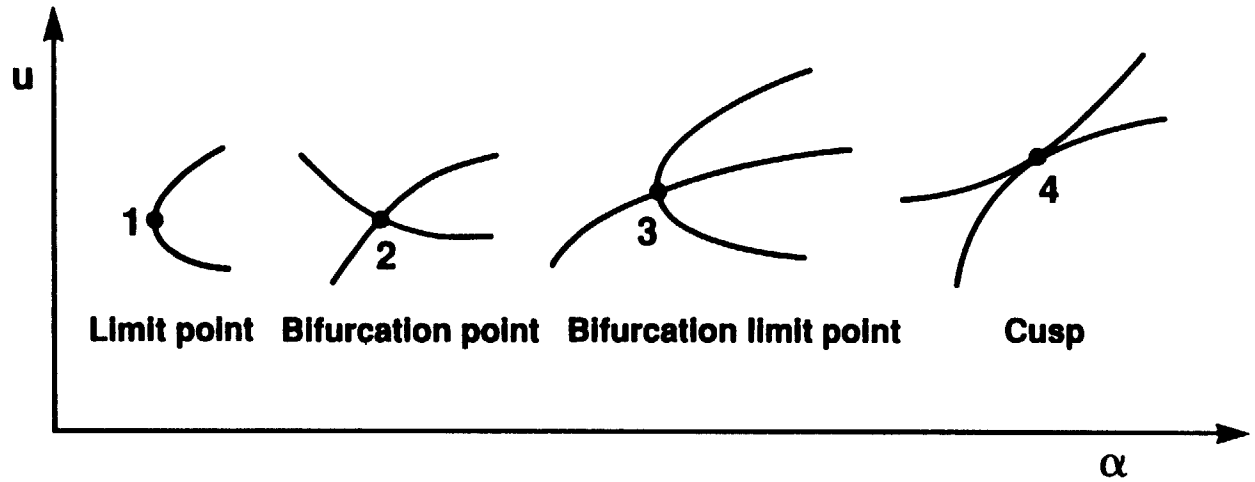

Fig. 3.39 Types of branching points.

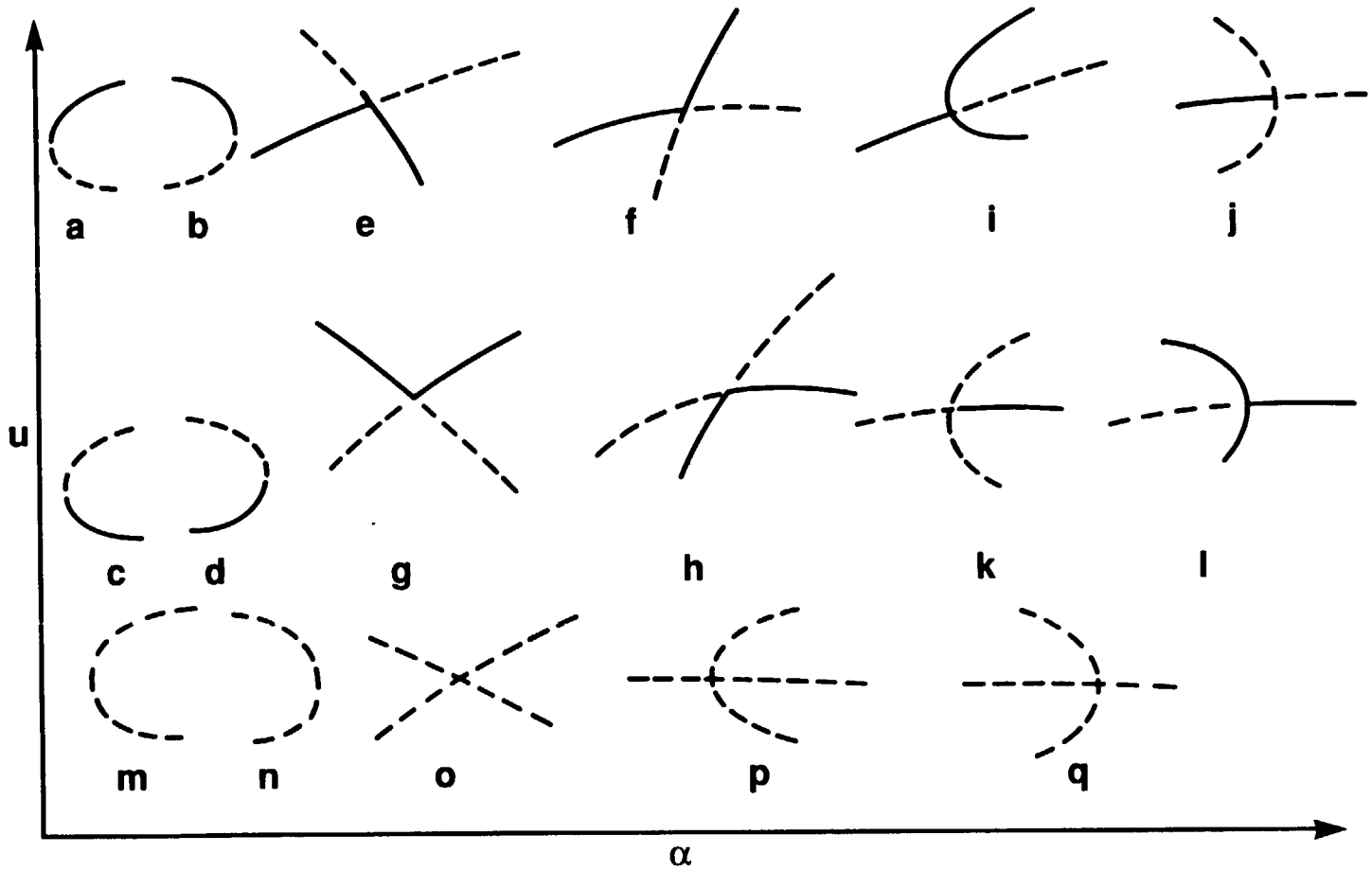

Fig. 3.40 Stability of solutions in the neighborhood of branch points, one-dimensional case. — stable, - - - unstable a,b,c,d: limit (regular turning) point; e,f,g,h: bifurcation (double) points; i,j,k,l: bifurcation-limit (singular turning) points; m,n,o,p,q: additional possible cases when the dimension of u is greater than one (this figure is taken from reference [7]).

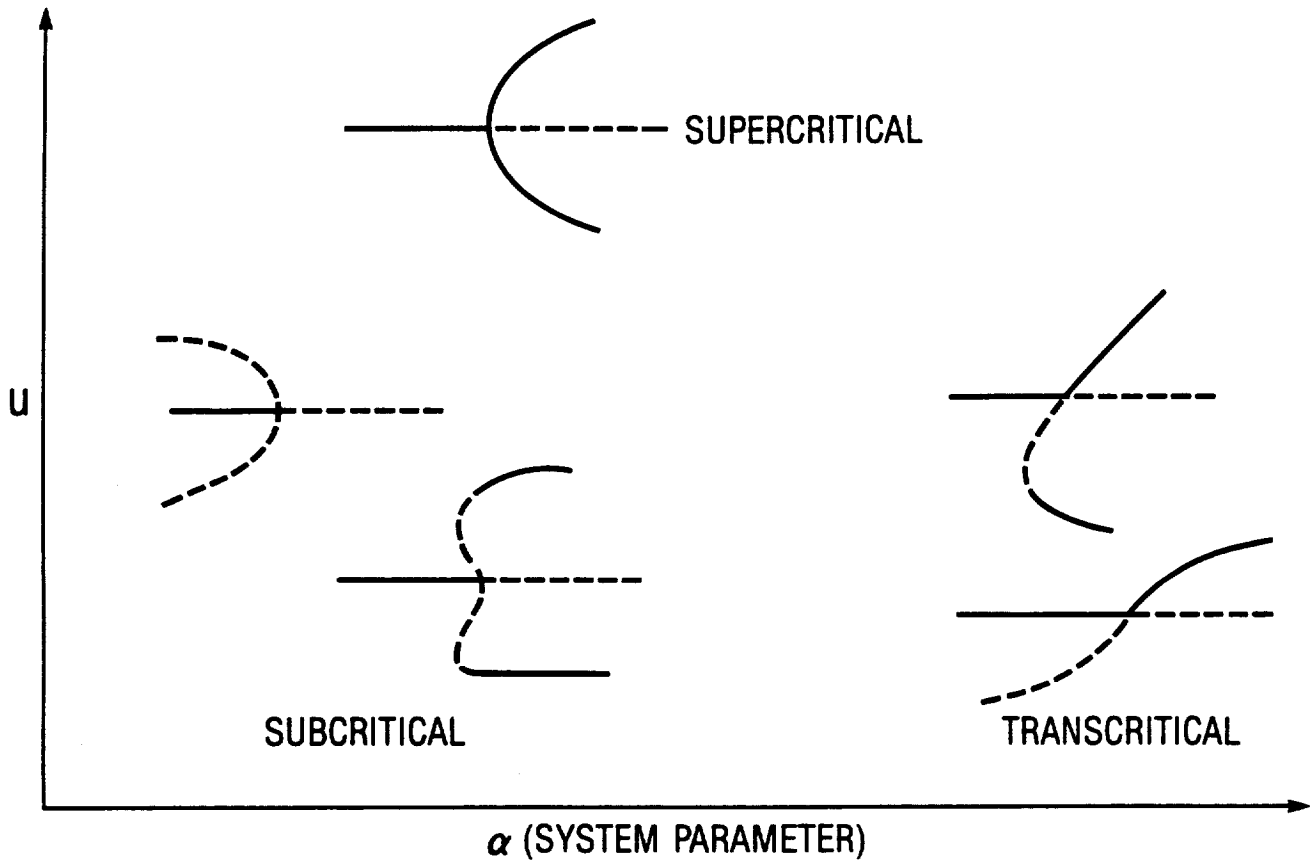

Fig. 3.41 Stability of steady-state solutions arising through three types of bifurcation phenomena (— stable, - - - unstable).

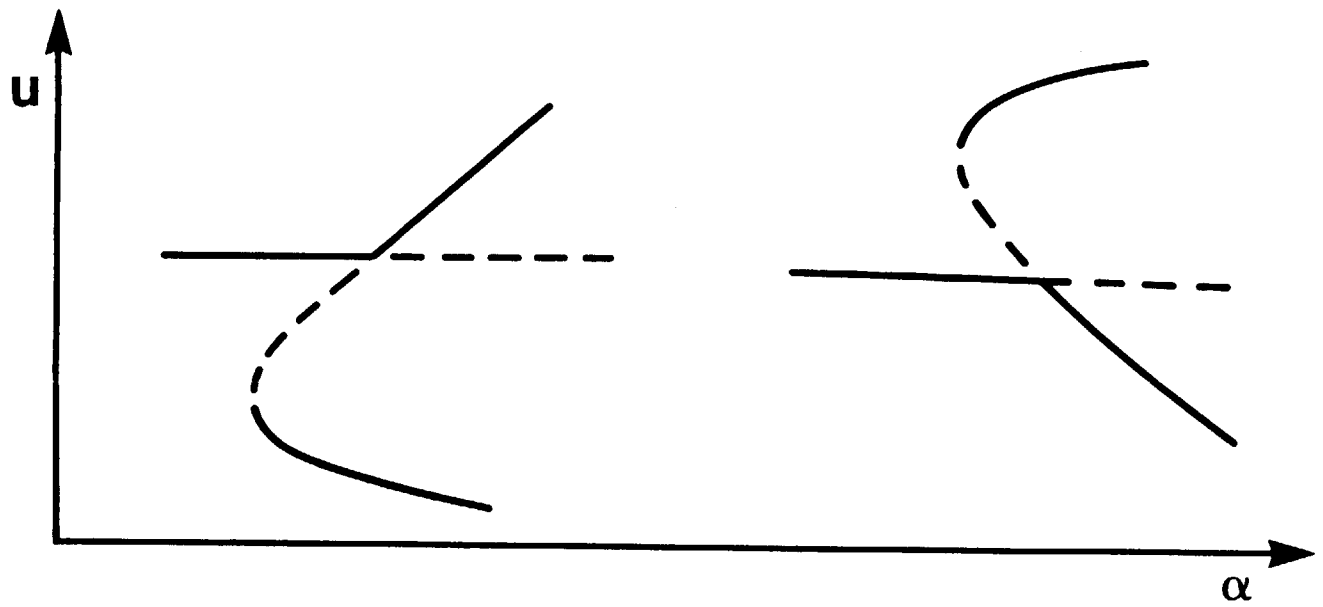

Fig. 3.42 Spurious fixed points arising from transcritical bifurcations.

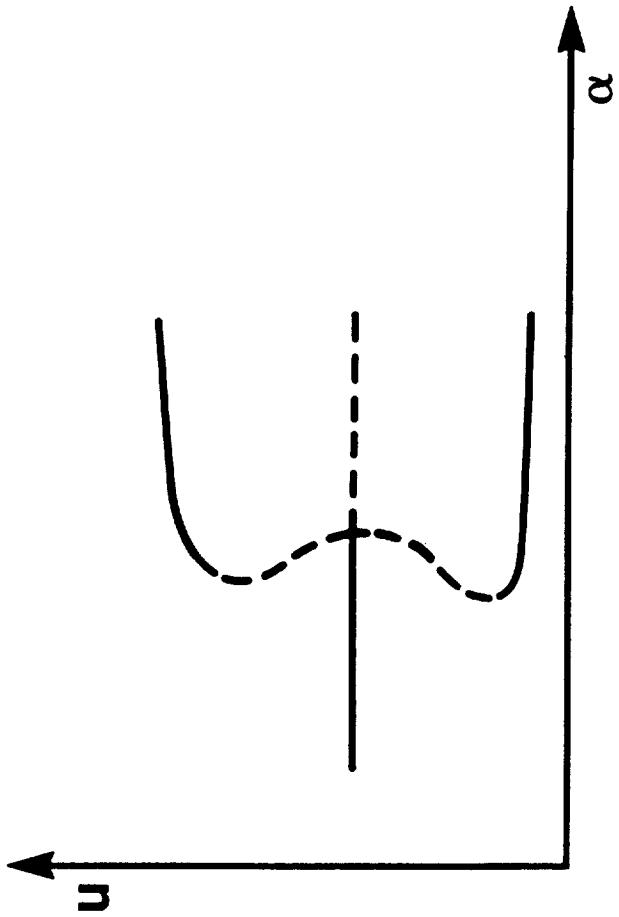

Fig. 3.43 Spurious fixed points arising from subcritical bifurcation.

C-2

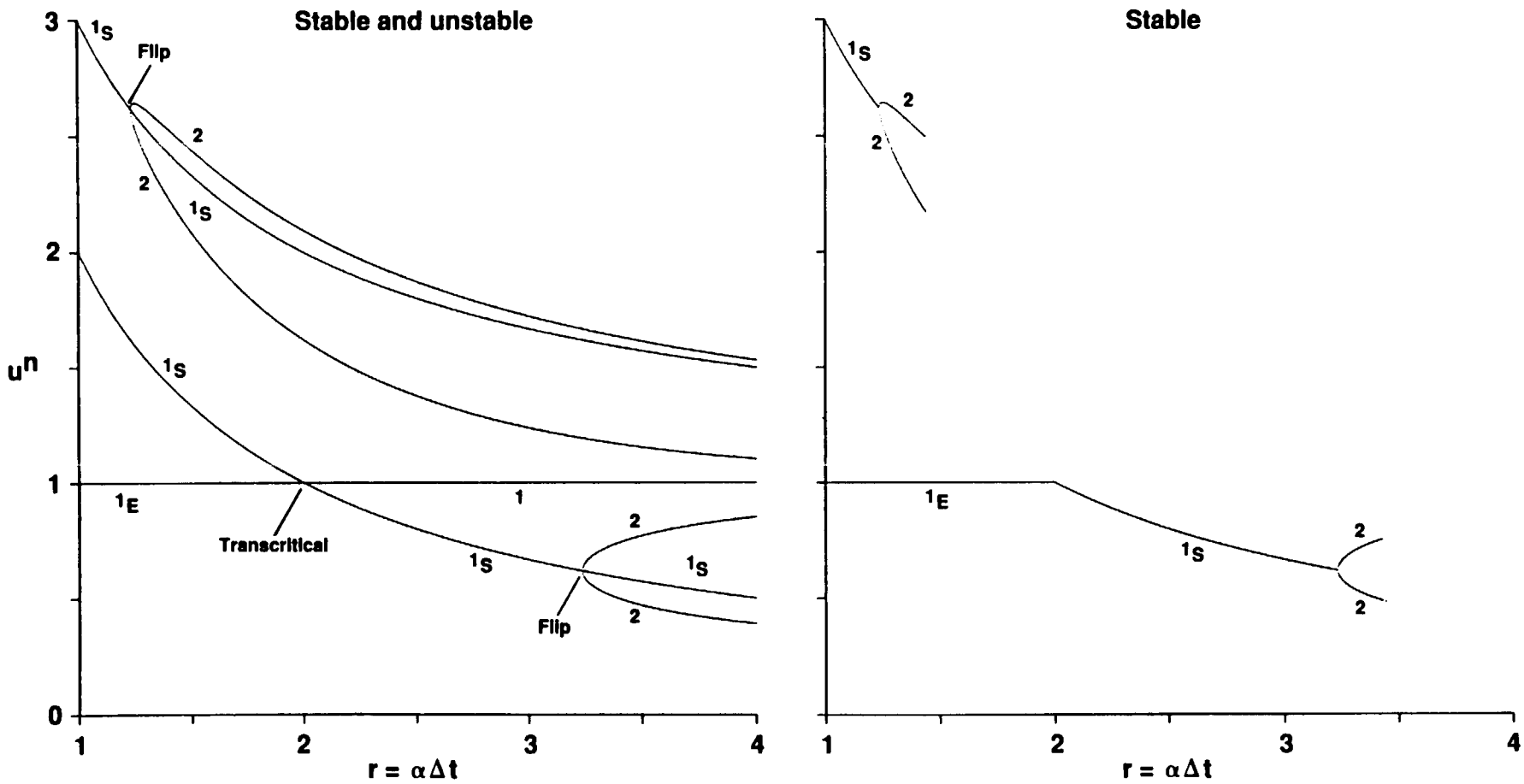

Fig. 3.44 Stable and unstable fixed points of periods 1,2 of the modified Euler (R-K 2) scheme for the logistic ODE $du/dt = \alpha u(1-u)$.

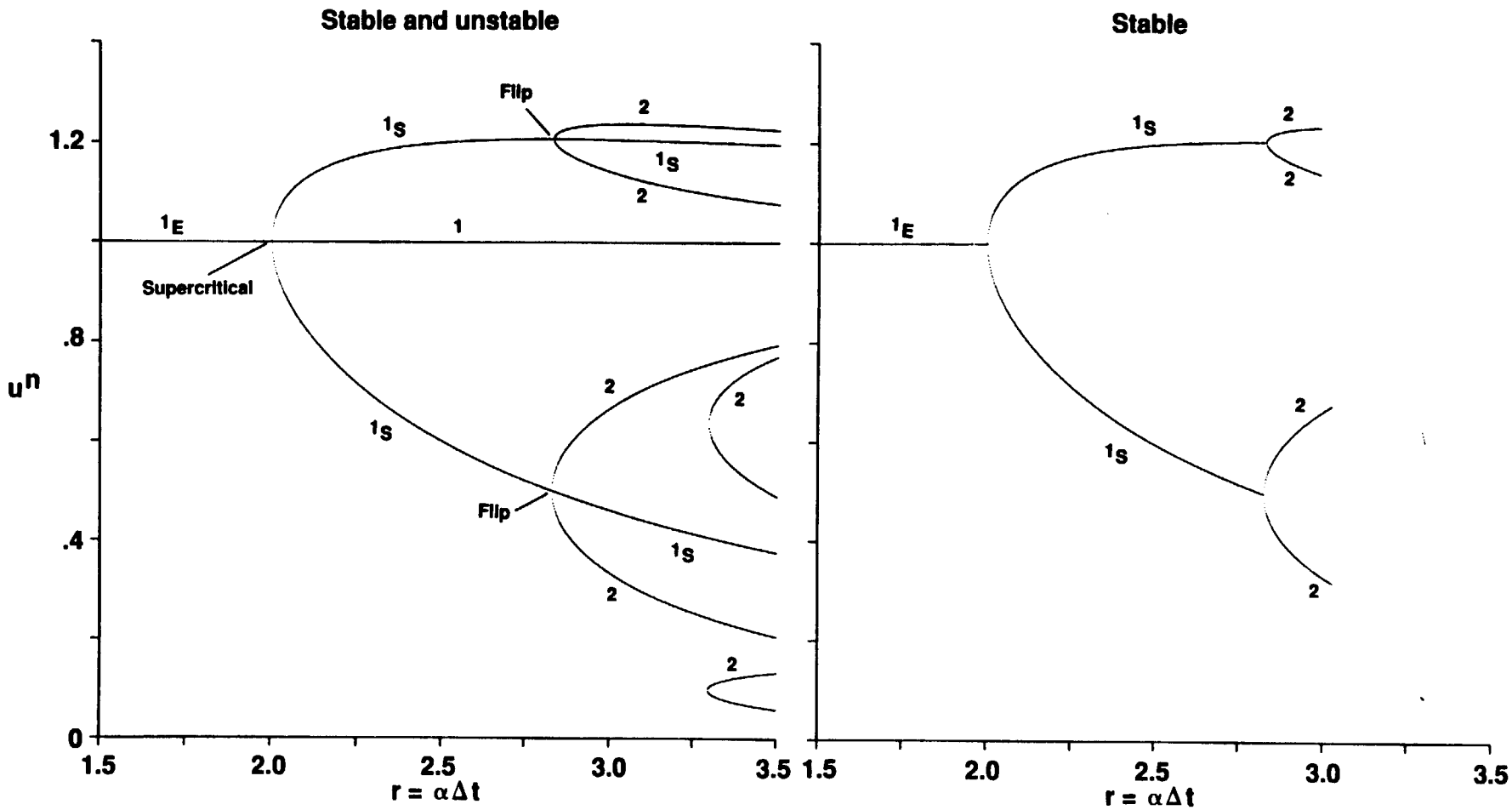

Fig. 3.45 Stable and unstable fixed points of periods 1,2 of the improved Euler (R-K 2) scheme for the logistic ODE $du/dt = \alpha u(1-u)$.

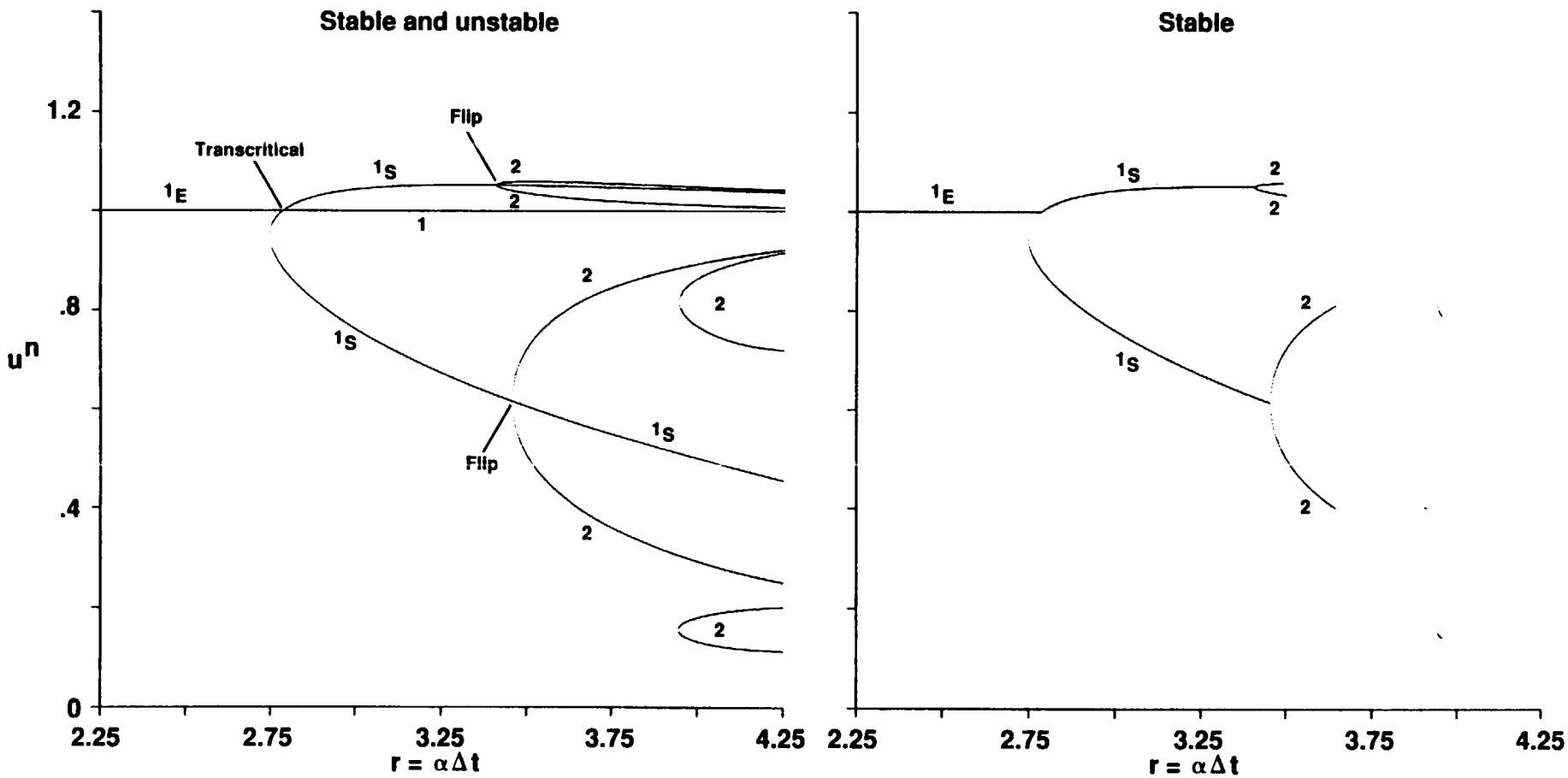

Fig. 3.46 Stable and unstable fixed points of periods 1,2 of the Runge-Kutta 4th-order (R-K 4) scheme for the logistic ODE $du/dt = \alpha u(1-u)$.

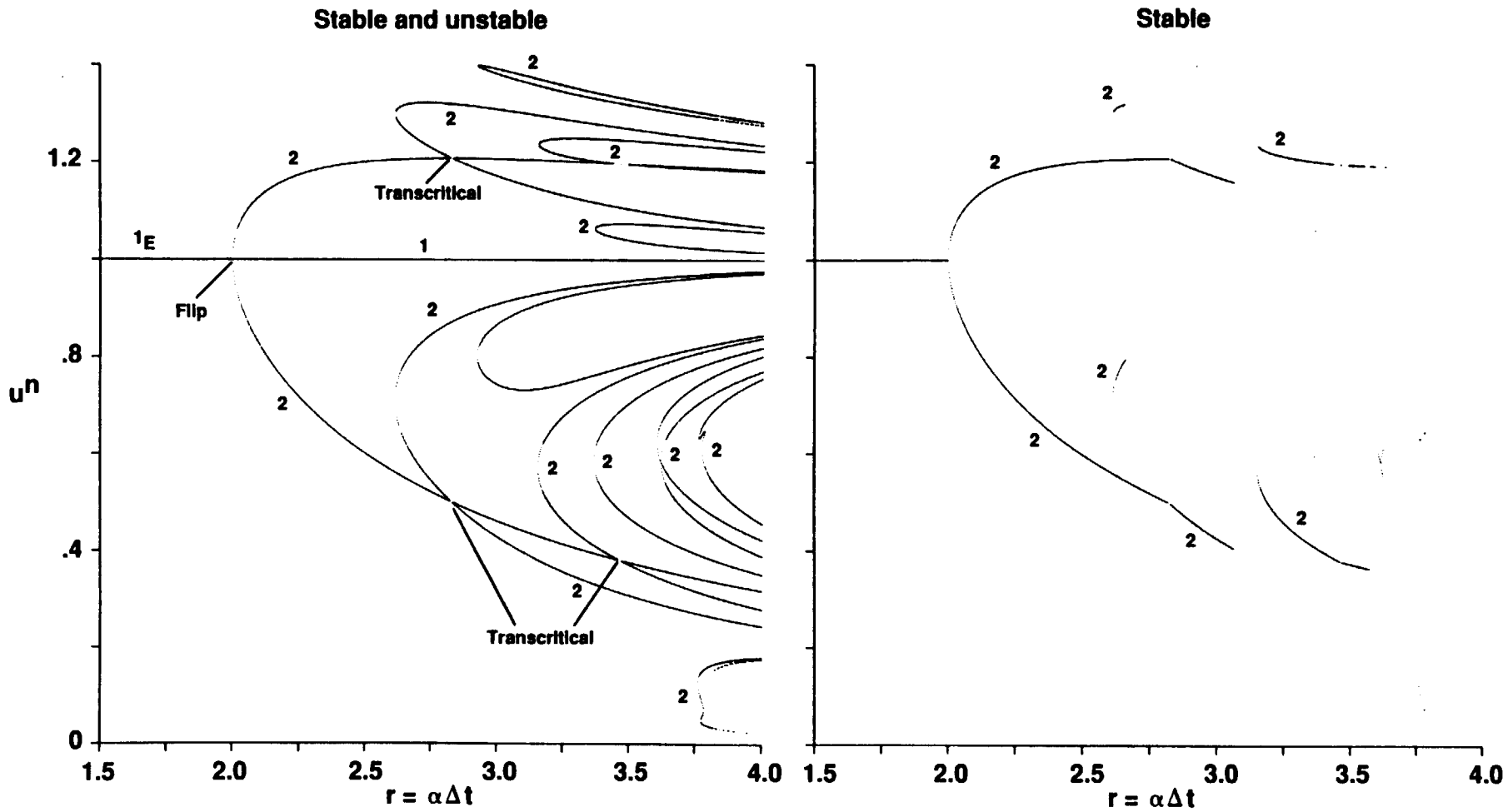

Fig. 3.47 Stable and unstable fixed points of periods 1,2 of the predictor-corrector scheme of order 2 for the logistic ODE $du/dt = \alpha u(1-u)$.

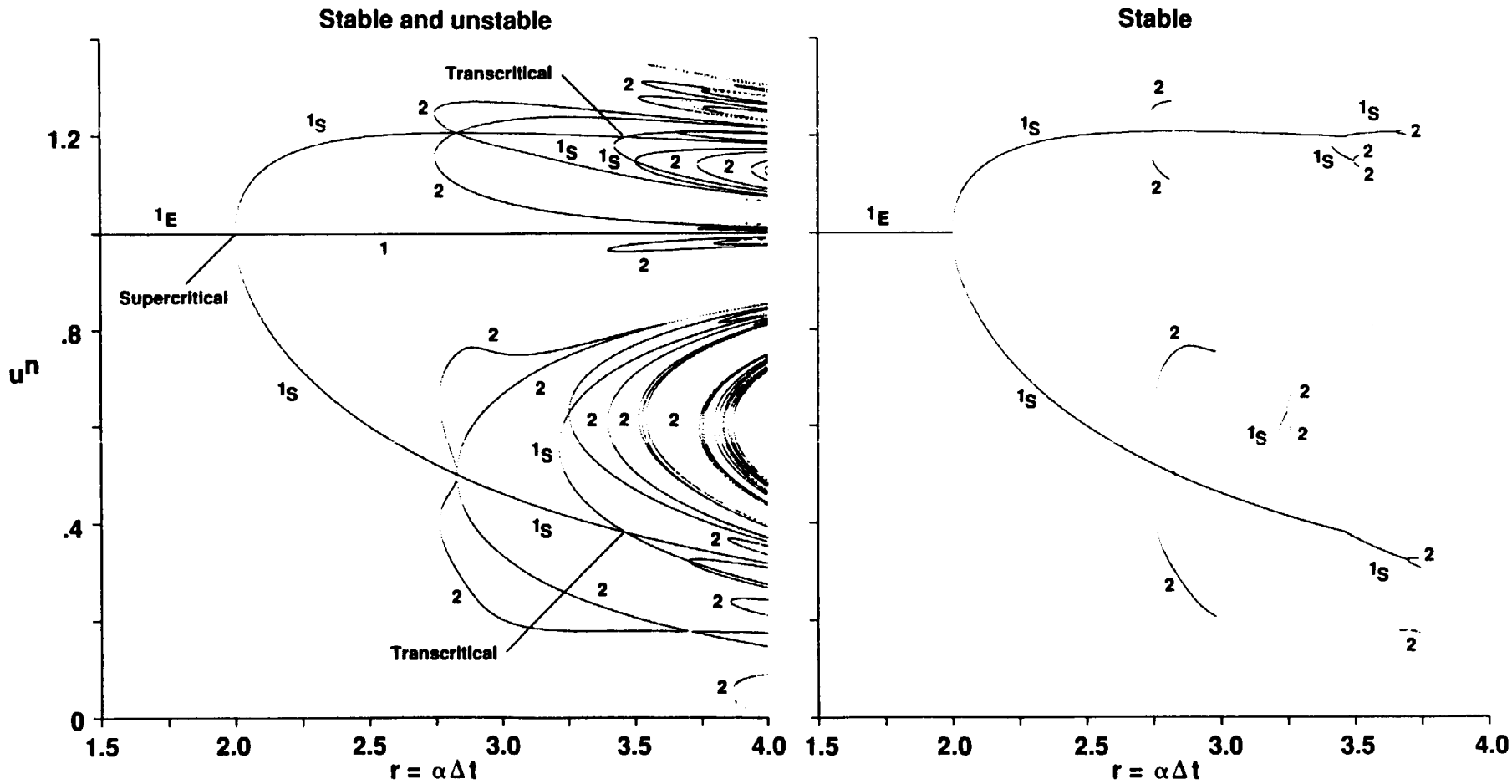

Fig. 3.48 Stable and unstable fixed points of periods 1,2 of the predictor-corrector scheme of order 3 for the logistic ODE $du/dt = \alpha u(1-u)$.

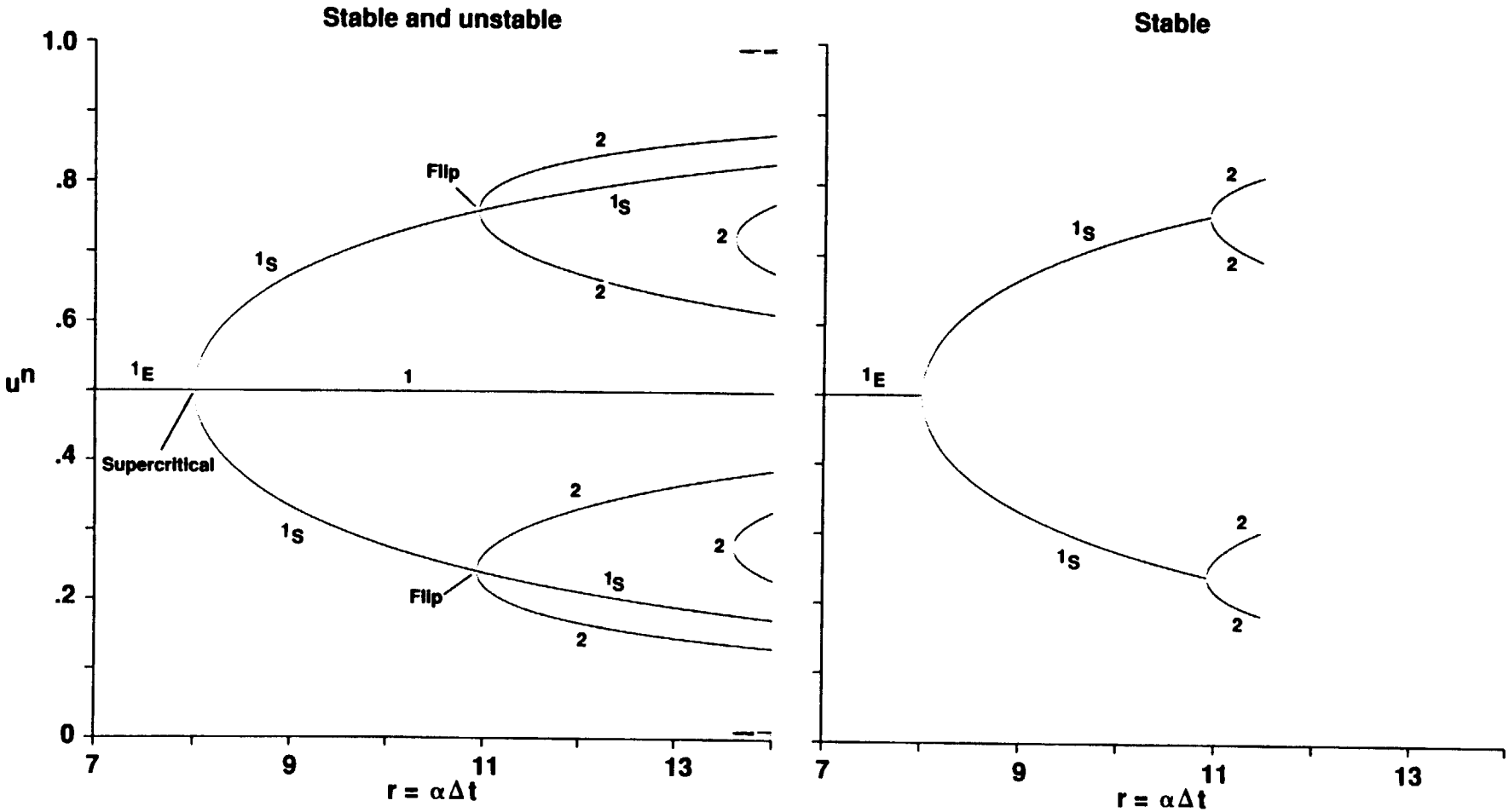

Fig. 3.49 Stable and unstable fixed points of periods 1,2 of the modified Euler (R-K 2) scheme for the ODE $du/dt = \alpha u(1-u)(0.5-u)$.

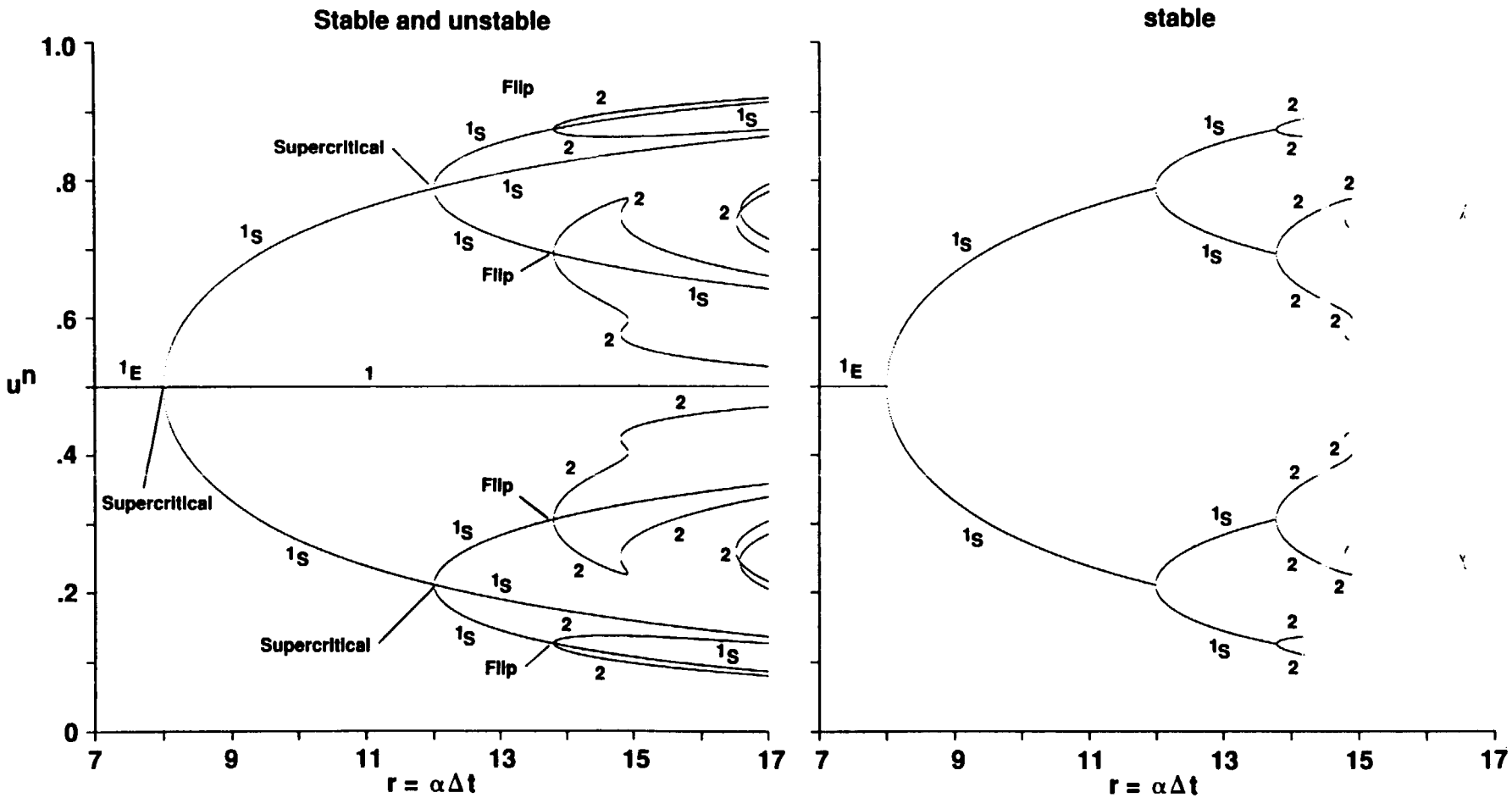

Fig. 3.50 Stable and unstable fixed points of periods 1,2 of the improved Euler (R-K 2) scheme for the ODE $du/dt = \alpha u(1-u)(0.5-u)$.

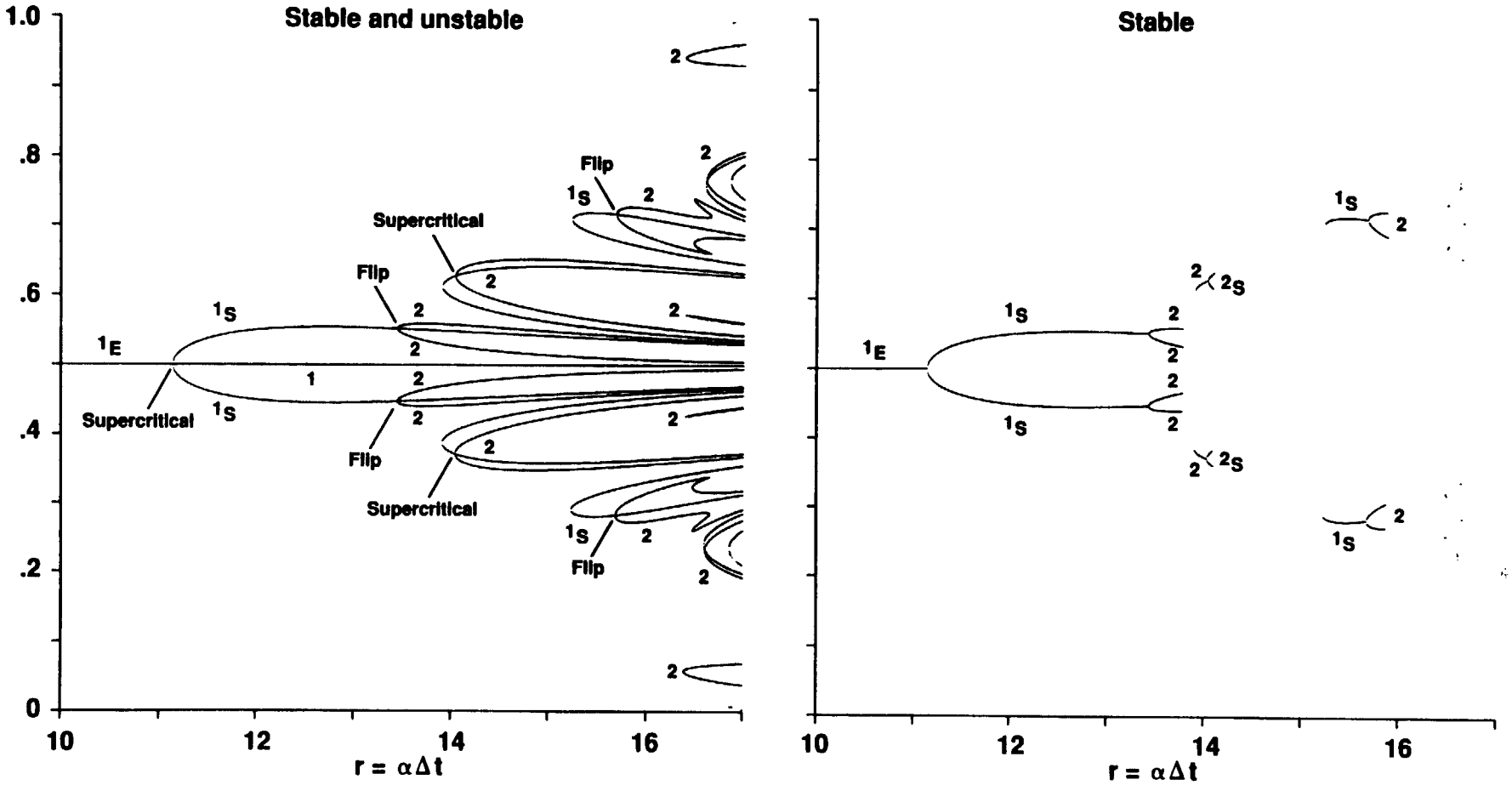

Fig. 3.51 Stable and unstable fixed points of periods 1,2 of the Runge-Kutta 4th-order (R-K 4) scheme for the ODE $du/dt = \alpha u(1-u)(0.5-u)$.

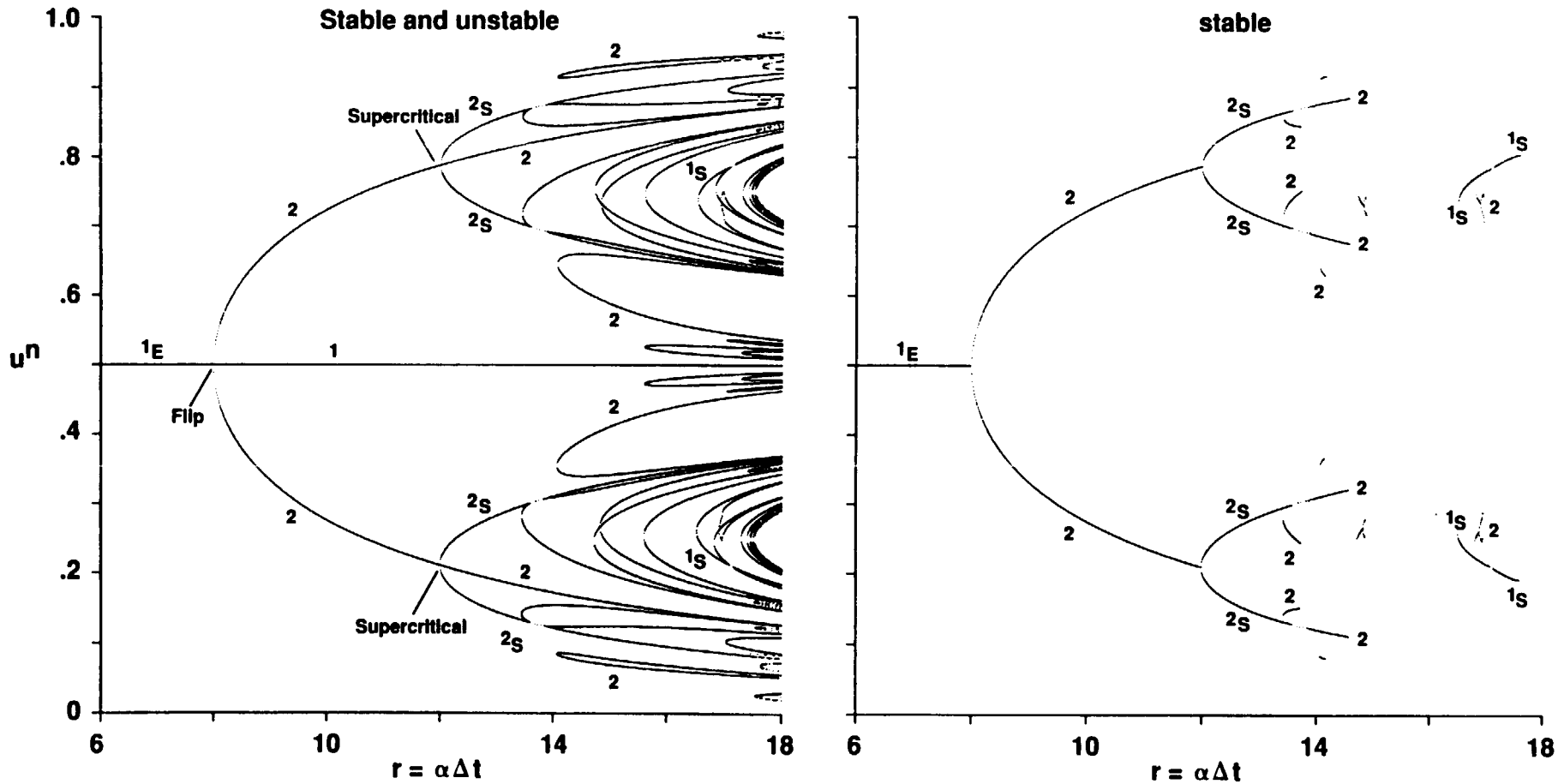

Fig. 3.52 Stable and unstable fixed points of periods 1,2 of the predictor-corrector scheme of order 2 for the ODE $du/dt = \alpha u(1-u)(0.5-u)$.

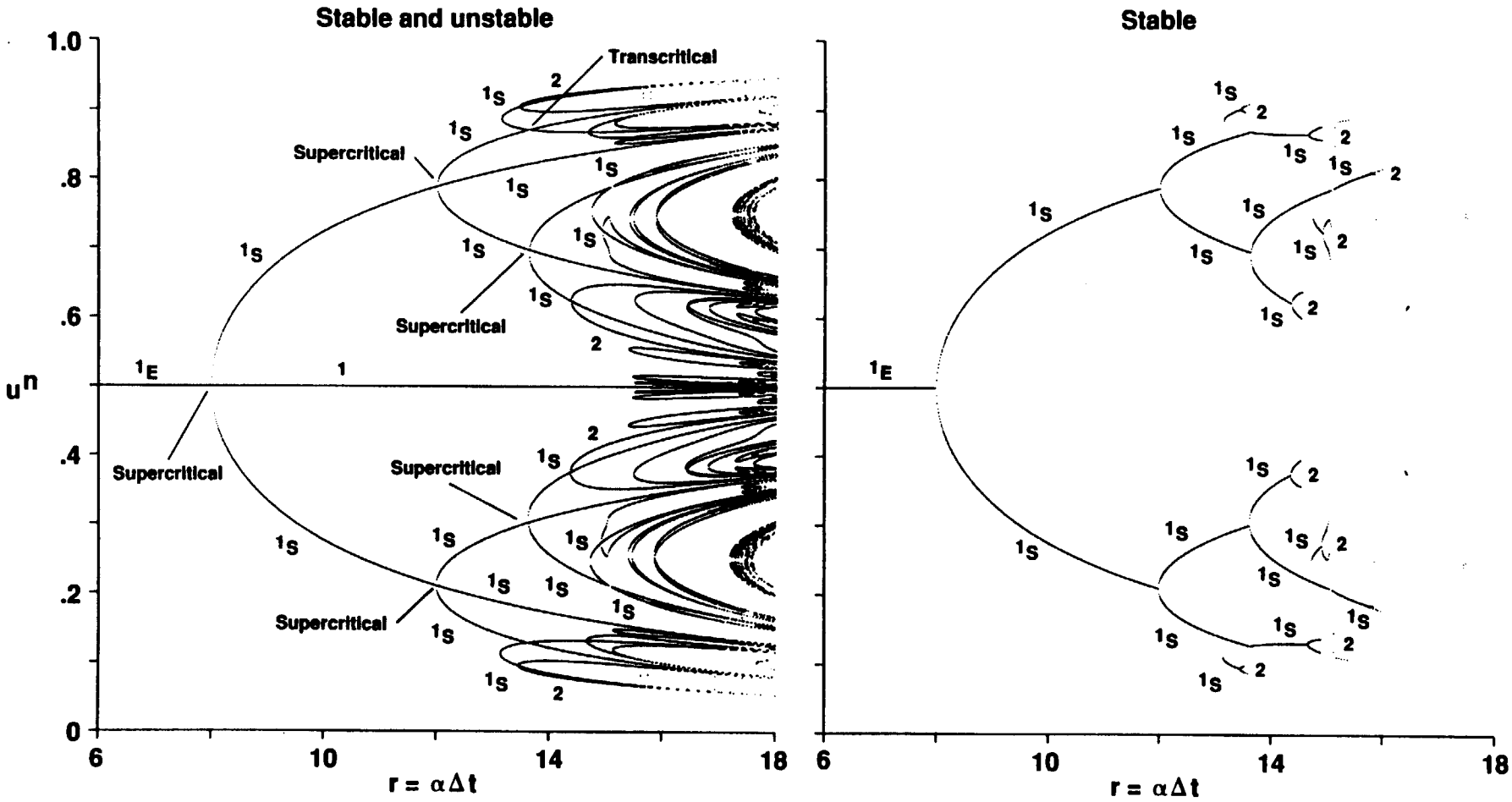

Fig. 3.53 Stable and unstable fixed points of periods 1,2 of the predictor-corrector scheme of order 3 for the ODE $du/dt = \alpha u(1-u)(0.5-u)$.

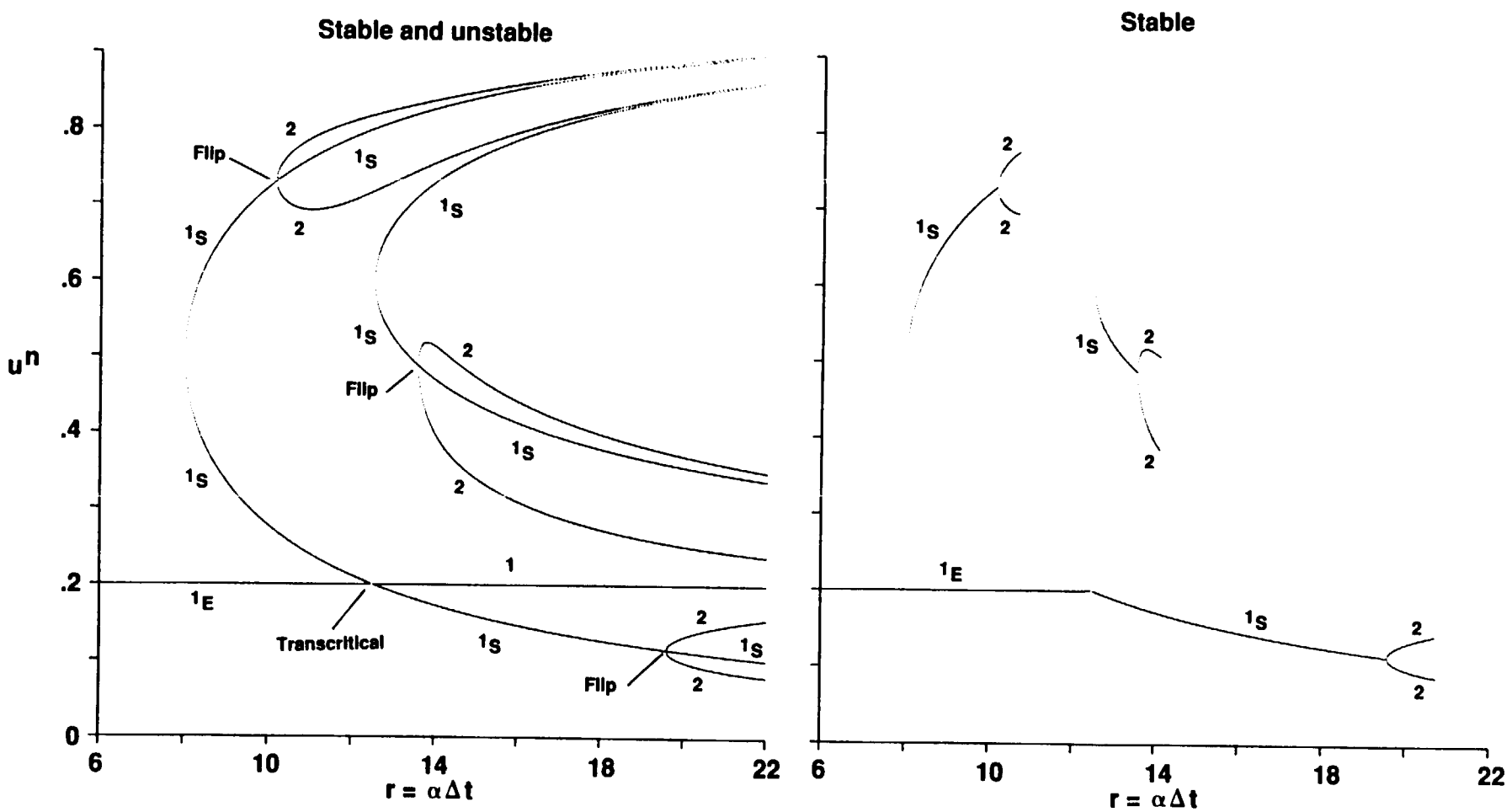

Fig. 3.54 Stable and unstable fixed points of periods 1,2 of the modified Euler (R-K 2) scheme for the ODE $du/dt = \alpha u(1-u)(0.2-u)$.

NASA
National Aeronautics and Space Administration

Report Documentation Page

1. Report No.	2. Government Accession No.	3. Recipient's Catalog No.
NASA TM-102820		

4. Title and Subtitle
Dynamical Approach Study of Spurious Steady-State Numerical Solutions of Nonlinear Differential Equations
Part 1 – The ODE Connection and Its Implications for Algorithm Development in Computational Fluid Dynamics

5. Report Date
April 1990

6. Performing Organization Code

7. Author(s)
H. C. Yee, P. K. Sweby (University of Reading, Whiteknights, and), and D. F. Griffiths (University of Dundee, and)

8. Performing Organization Report No.
A-90149

10. Work Unit No.
505-60

zation Name and Address
:h Center
, CA 94035-1000

11. Contract or Grant No.

13. Type of Report and Period Covered
Technical Memorandum

cy Name and Address
)nautics and Space Administration
DC 20546-0001

14. Sponsoring Agency Code

lotes
tact: H. C. Yee, Ames Research Center, MS 202A-1, Moffett Field, CA 94035-1000
(415) 604-4769 or FTS 464-4769
ted at 12th International Conference on Numerical Methods in Fluid Dynamics, Oxford, y 9-13, 1990.

stable as well as unstable steady-state numerical solutions, spurious asymptotic numerical solutions of higher en stable chaotic behavior can occur when finite-difference methods are used to solve nonlinear differential) numerically. The occurrence of spurious asymptotes is independent of whether the DE possesses a unique steady ditional periodic solutions and/or exhibits chaotic phenomena. The form of the nonlinear DEs and the type of emes are the determining factor. In addition, the occurrence of spurious steady states is not restricted to the time eyond the linearized stability limit of the scheme. In many instances, it can occur below the linearized stability re, it is essential for practitioners in computational sciences to be knowledgeable about the dynamical behavior ence methods for nonlinear scalar DEs before the actual application of these methods to practical computations. rtant to change the traditional way of thinking and practices when dealing with genuinely nonlinear problems. t, spurious asymptotes were observed in numerical computations but tended to be ignored because they all were beyond the linearized stability limits of the time step parameter Δt. As can be seen from our study, bifurcations purious asymptotic solutions and transitions to computational instability not only are highly scheme dependent lependent, but also initial data and boundary condition dependent, and not limited to time steps that are beyond stability limit.

ggested by Author(s))	18. Distribution Statement
Nonlinear dynamics, Chaotic dynamics, Dynamics of numerics, Computational fluid dynamics, Hypersonic reacting flows, Nonlinear ordinary differential equations, Nonlinear dynamical systems	Unclassified-Unlimited Subject Category – 64

19. Security Classif. (of this report)	20. Security Classif. (of this page)	21. No. of Pages	22. Price
Unclassified	Unclassified	110	A06